



US 20220056535A1

(19) **United States**

(12) **Patent Application Publication**  
**Hendricks et al.**

(10) **Pub. No.: US 2022/0056535 A1**

(43) **Pub. Date: Feb. 24, 2022**

(54) **IDENTIFICATION OF HER2 MUTATIONS IN LUNG CANCER AND METHODS OF TREATMENT**

**Publication Classification**

(71) Applicants: **THE TRANSLATIONAL GENOMICS RESEARCH INSTITUTE**, Phoenix, AZ (US); **OHIO STATE UNIVERSITY**, Columbus, OH (US)

(51) **Int. Cl.**  
*C12Q 1/6886* (2006.01)  
*A61K 45/06* (2006.01)  
(52) **U.S. Cl.**  
CPC ..... *C12Q 1/6886* (2013.01); *C12Q 2600/158* (2013.01); *A61K 45/06* (2013.01)

(72) Inventors: **William Hendricks**, Phoenix, AZ (US); **Muhammed Murtaza**, Phoenix, AZ (US); **Gwendolen Lorch**, Columbus, OH (US)

(57) **ABSTRACT**

Methods are provided for treating lung cancer, and more particularly for treating pulmonary adenocarcinoma in a canine subject. The method may comprise assaying a biological sample from the canine subject, such as a tumor sample or a plasma sample, for a mutation in the HER2 gene. The mutation may include HER2 V659E, HER2 A664T, or HER2 K676E. If one or more of the mutations is present in the biological sample, the methods further include treating the canine subject by administering a therapeutically effective amount of an inhibitor of HER2. For example, a HER2 V659E may indicate increase sensitivity to a HER2 inhibitor. The HER2 inhibitor may include a small molecule HER2 inhibitor, such as trastuzumab, neratinib, lapatinib, erlotinib, and pertuzumab.

(21) Appl. No.: **17/413,488**

(22) PCT Filed: **Dec. 11, 2019**

(86) PCT No.: **PCT/US19/65715**

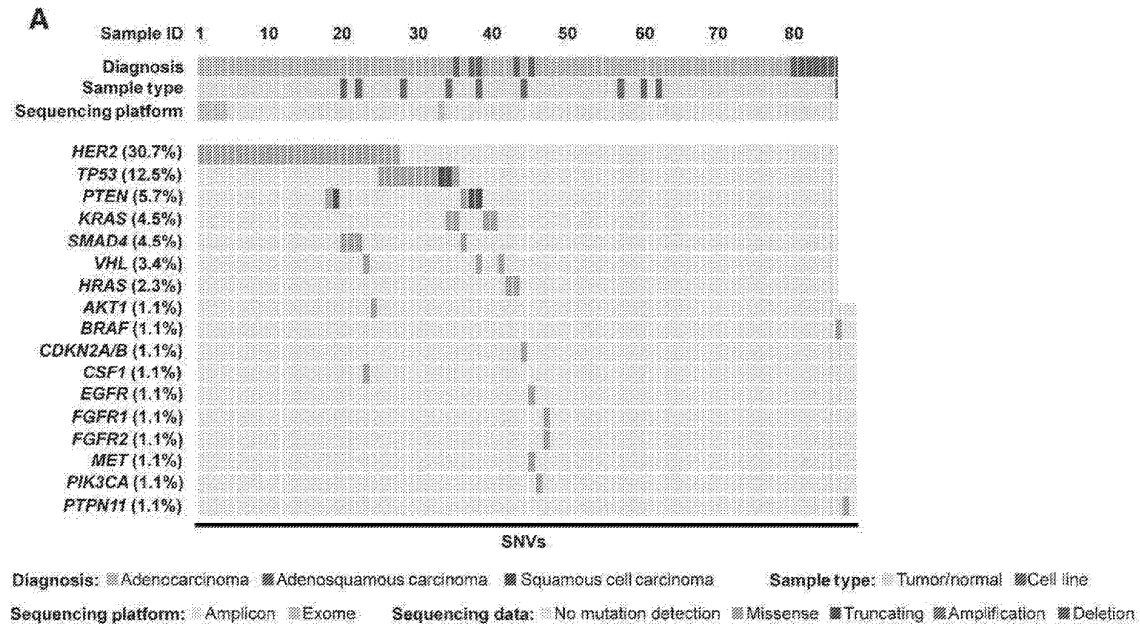
§ 371 (c)(1),

(2) Date: **Jun. 11, 2021**

**Related U.S. Application Data**

(60) Provisional application No. 62/778,282, filed on Dec. 11, 2018.

**Specification includes a Sequence Listing.**



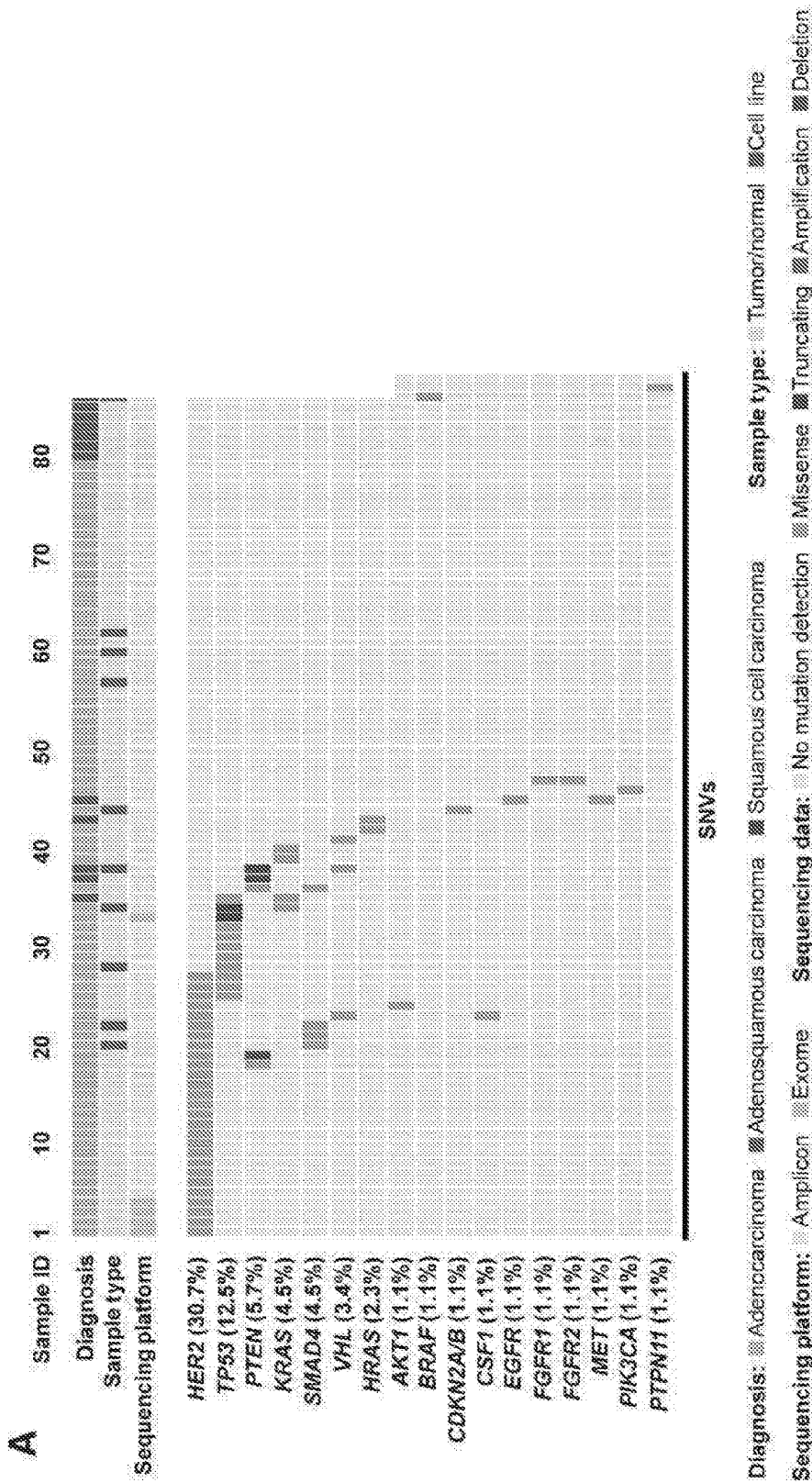


**FIG. 1A**

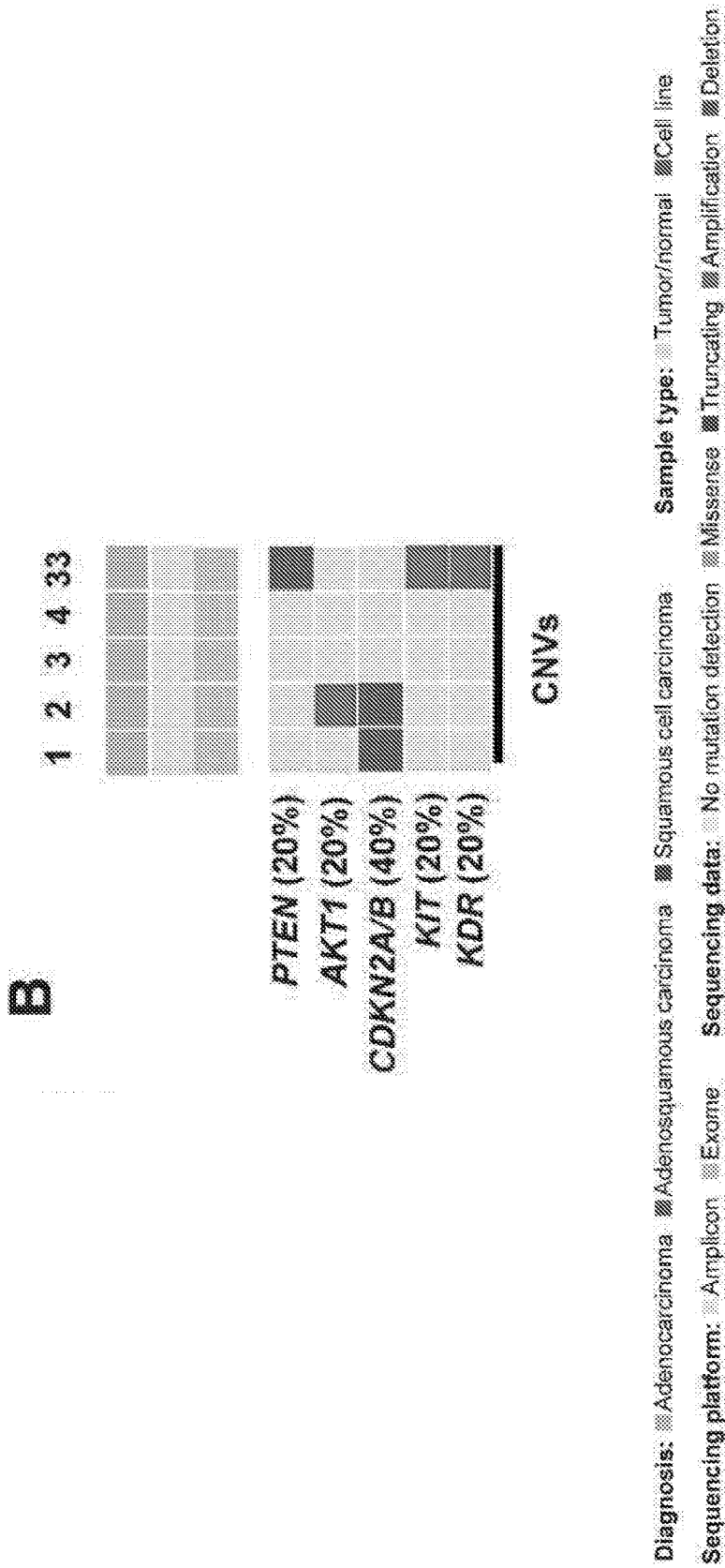


FIG. 1B

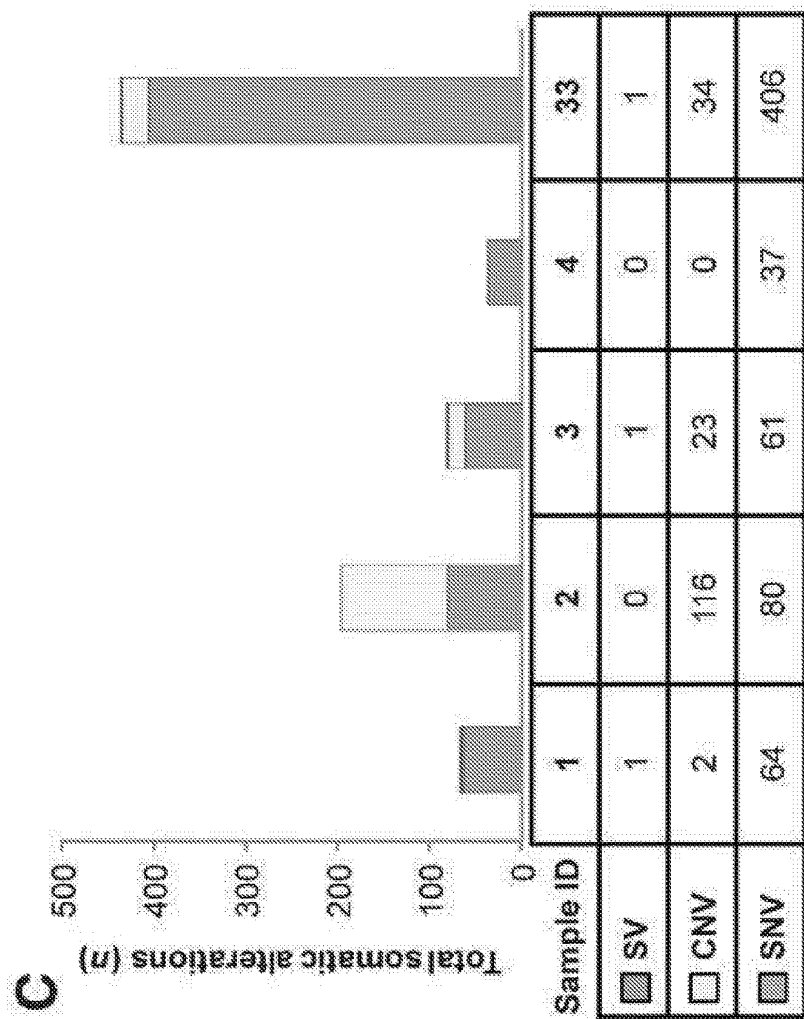


FIG. 1C

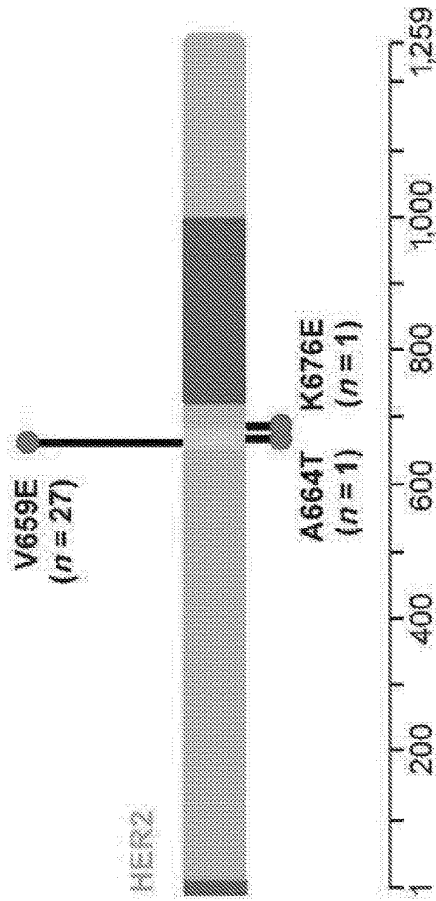


FIG. 1D

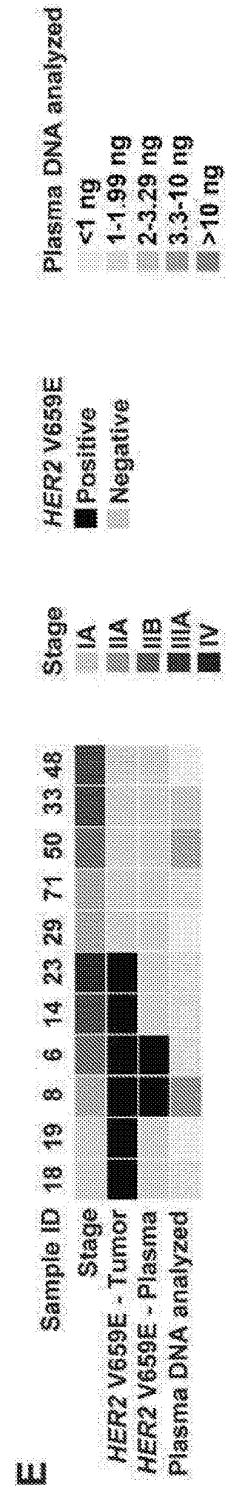
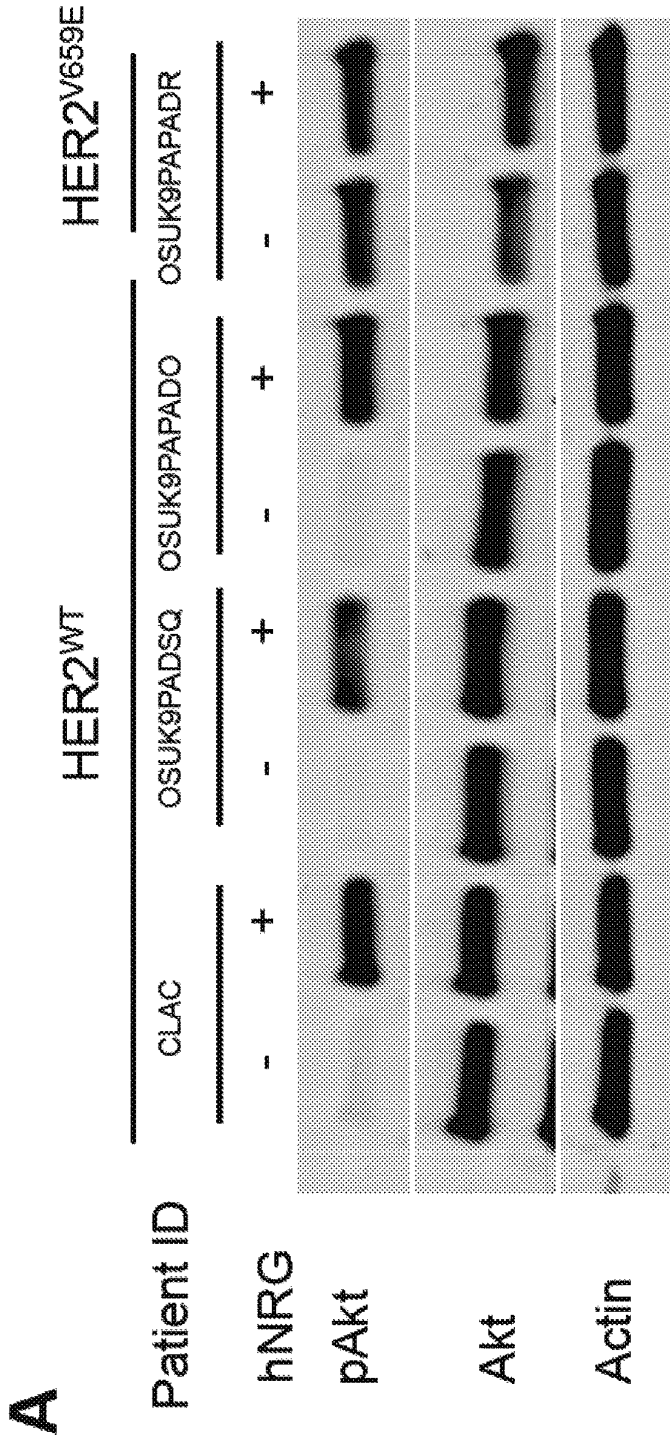


FIG. 1E



**FIG. 2A**

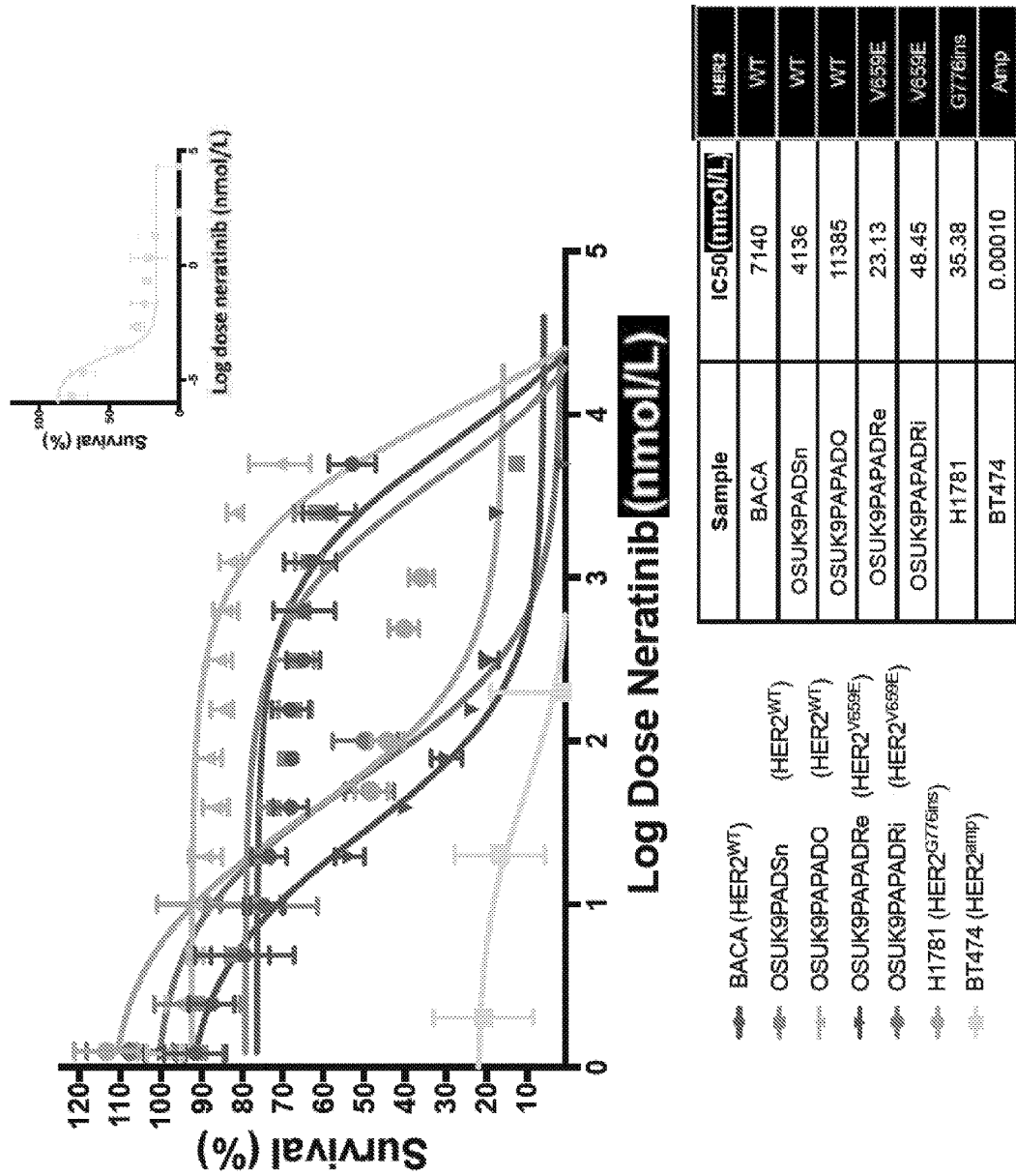


FIG. 2B

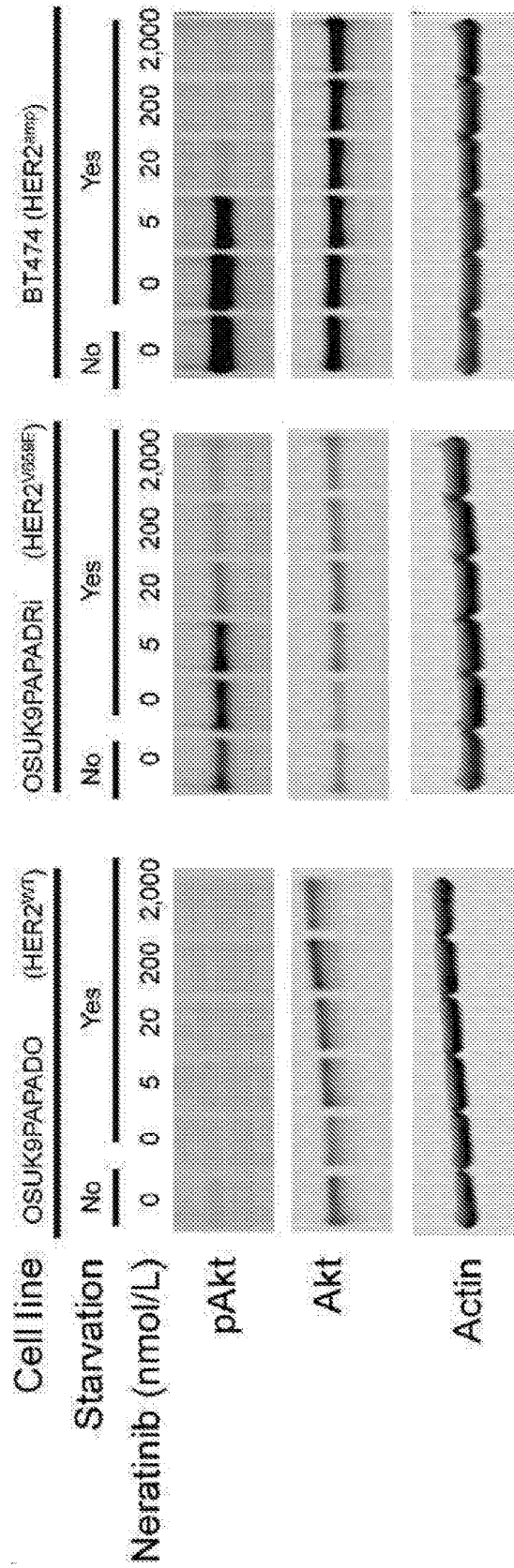


FIG. 2C



# Affected Breeds

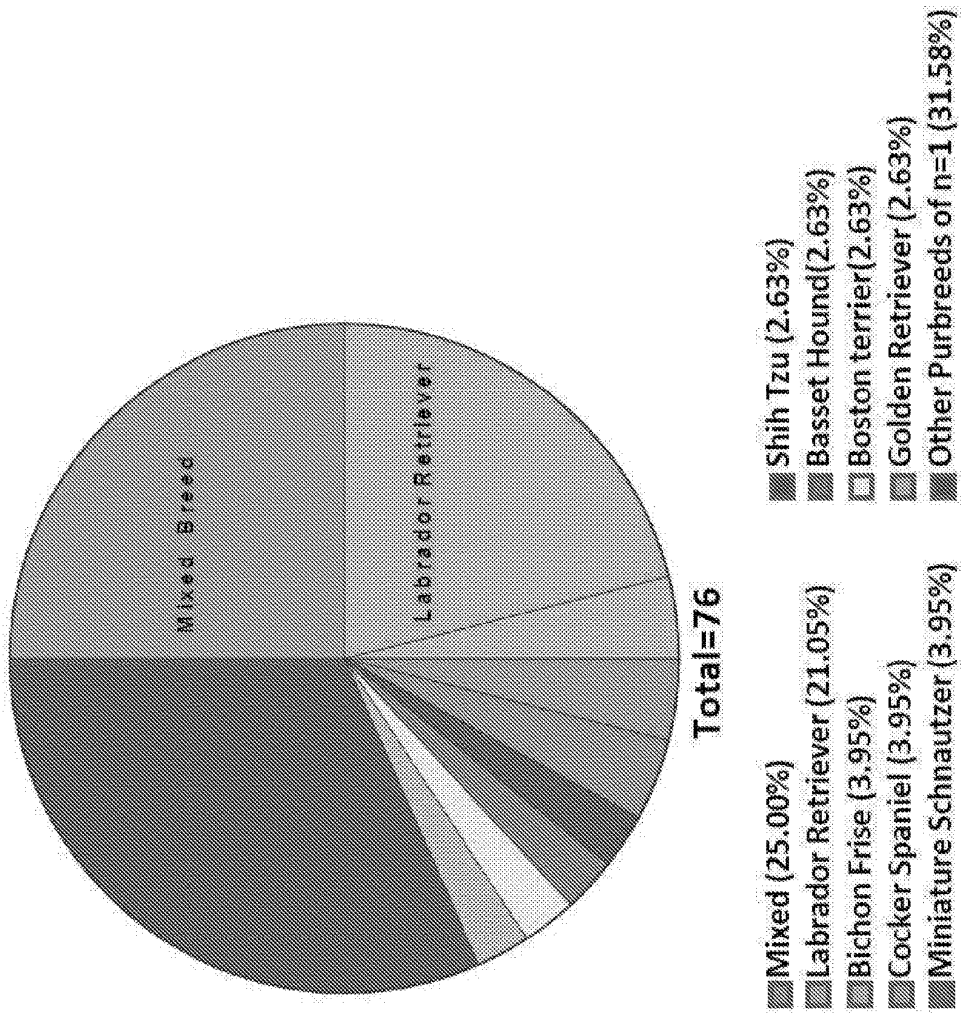


FIG. 3A

# Age at Diagnosis

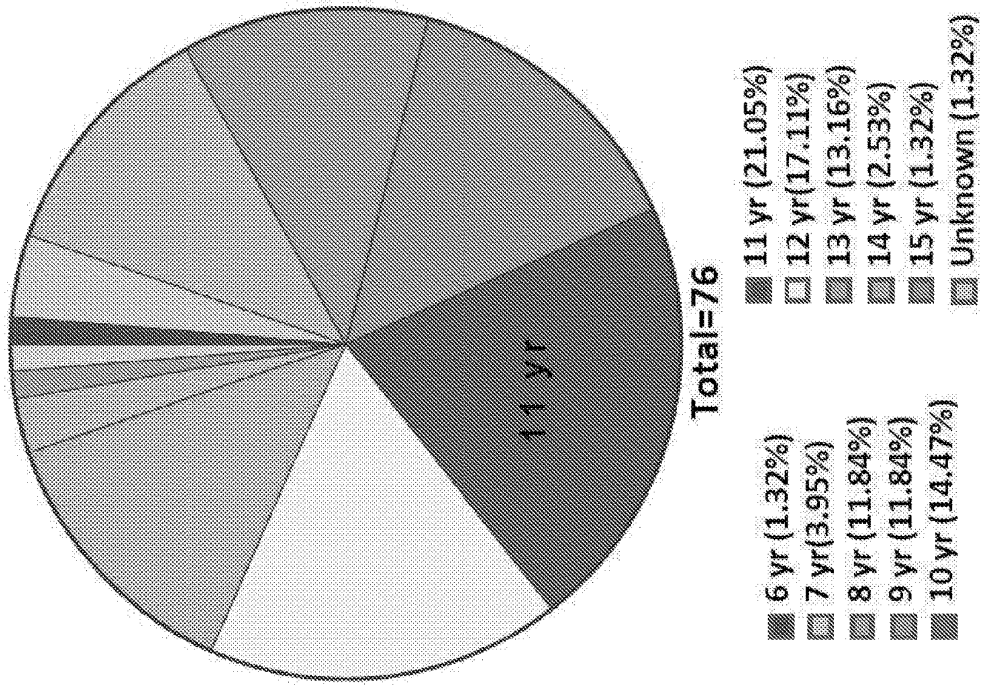


FIG. 3B

# Primary Tumor location

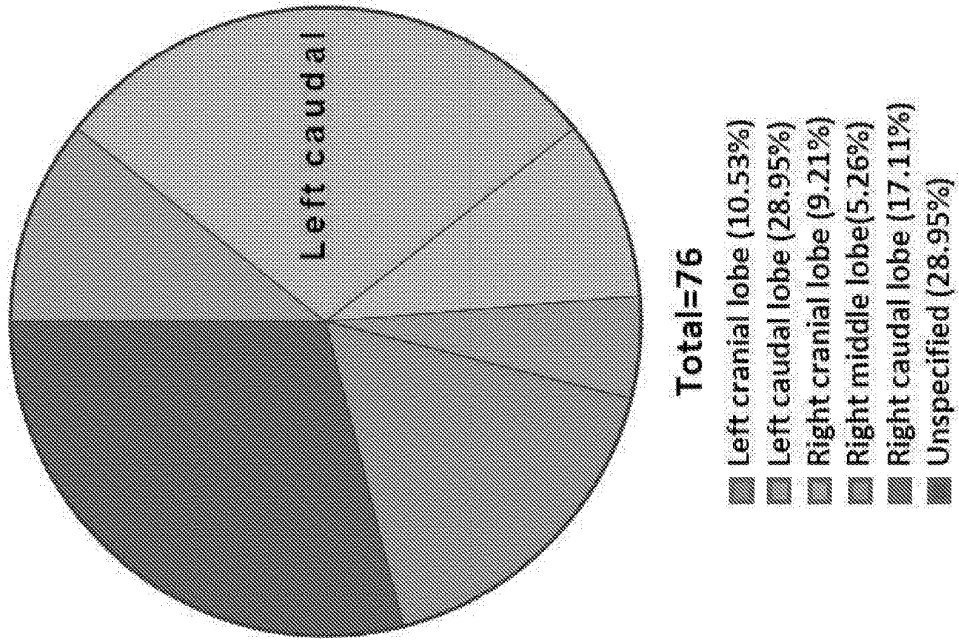
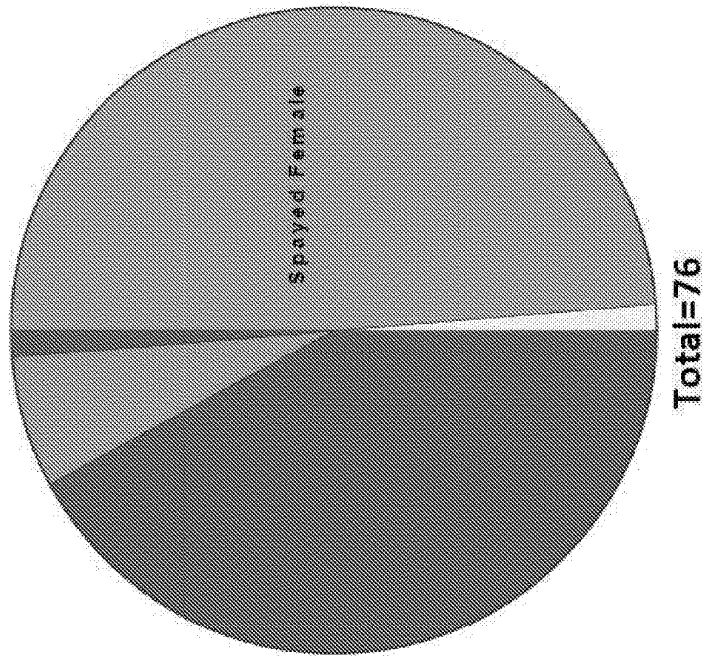


FIG. 3C

# Sex Distribution



- Spayed Female (48.68%)
- Unknown Female (1.32%)
- Castrated Male (42.11%)
- Intact Male (6.58%)
- Unknown (1.32%)

FIG. 3D

# Adenocarcinoma Subtype

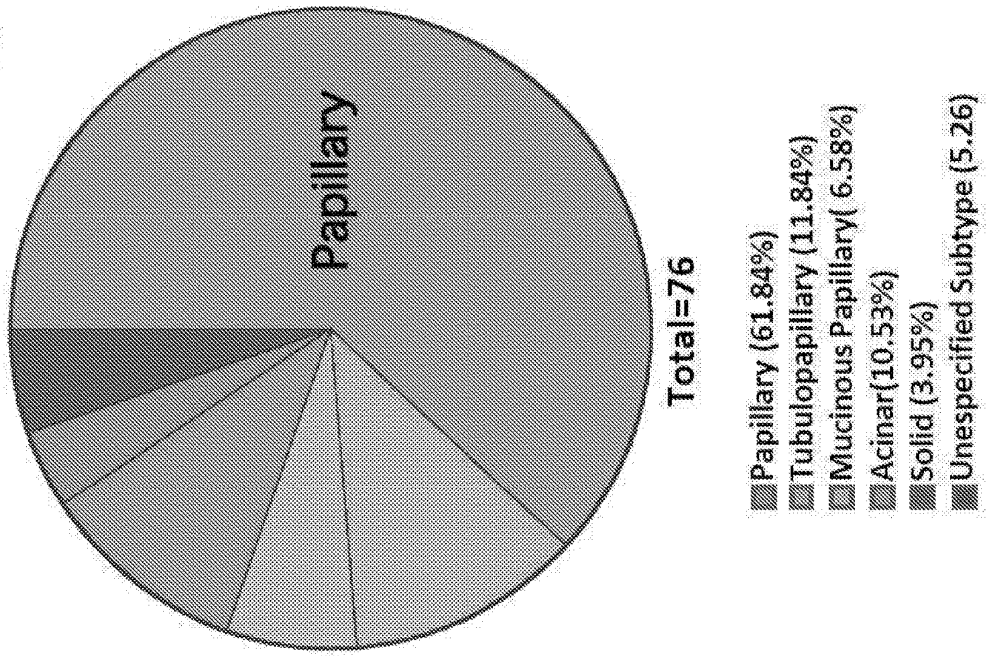


FIG. 3E

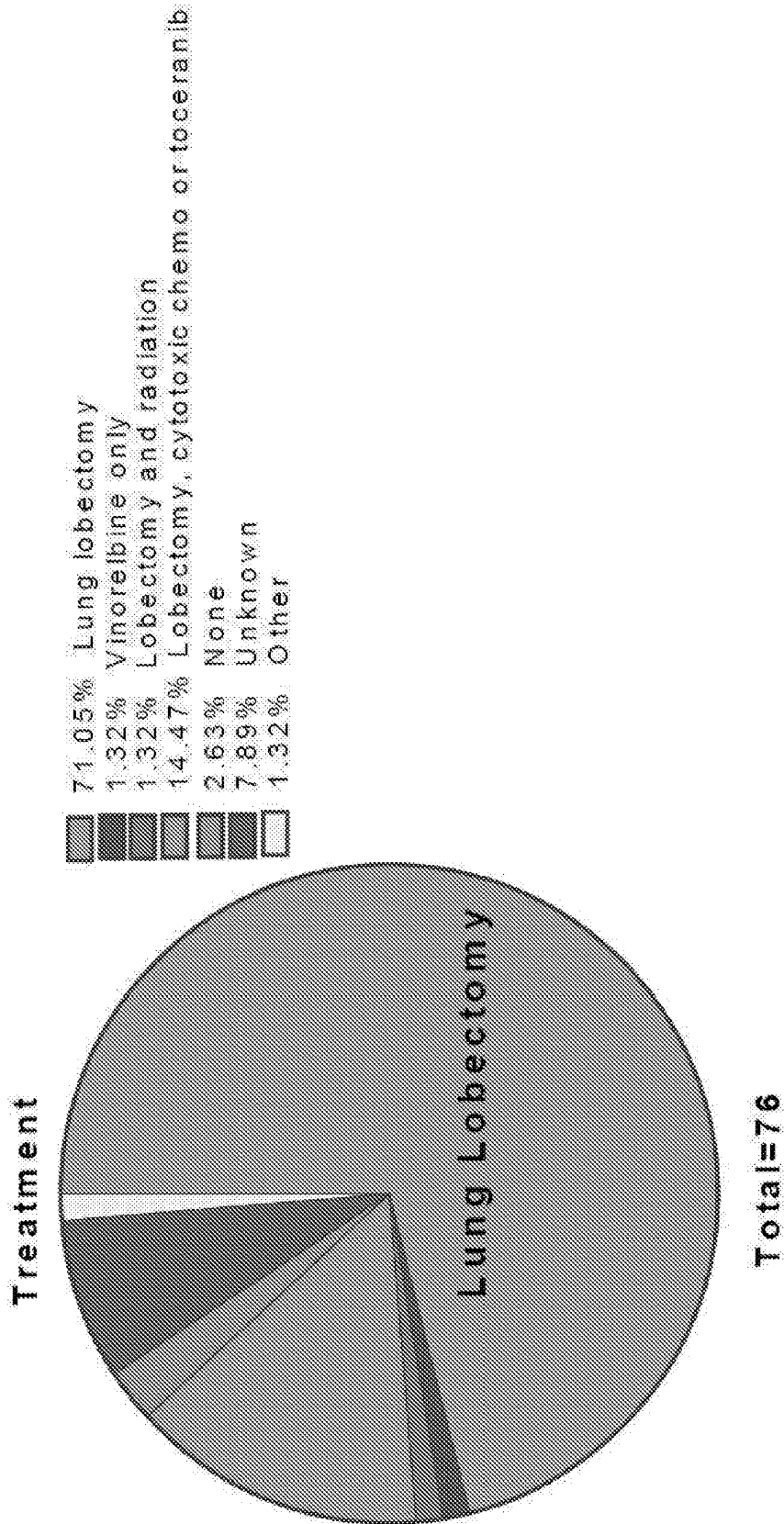


FIG. 3F



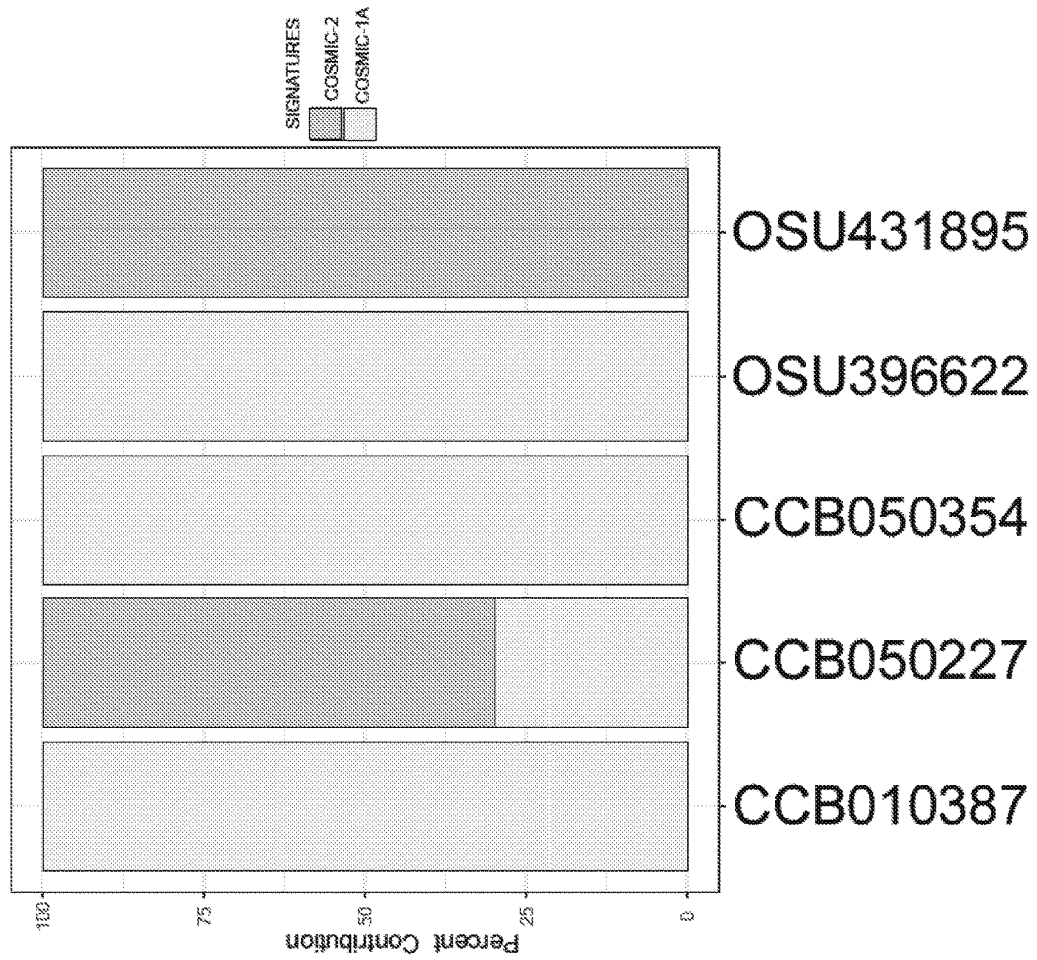
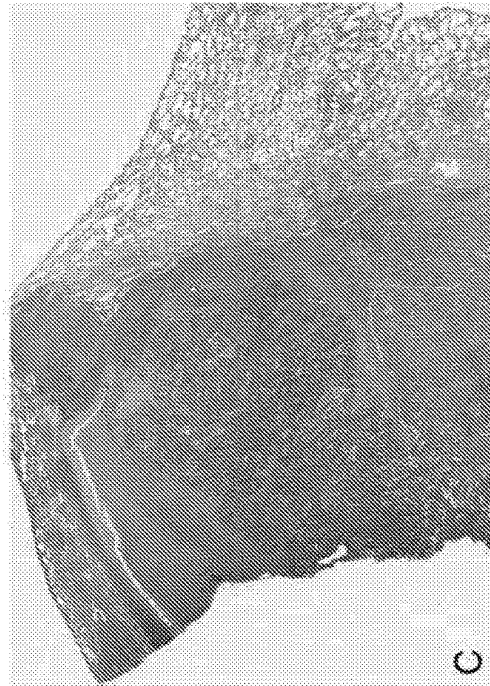
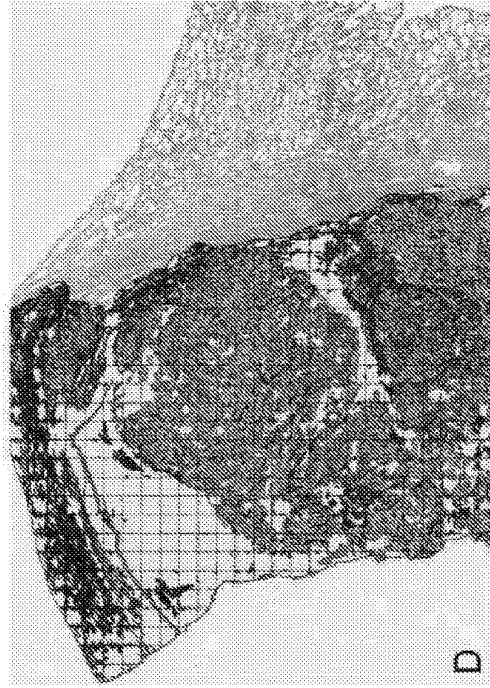
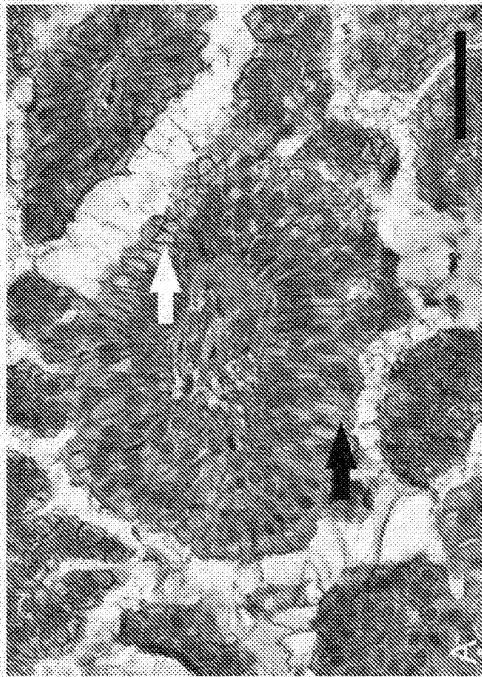
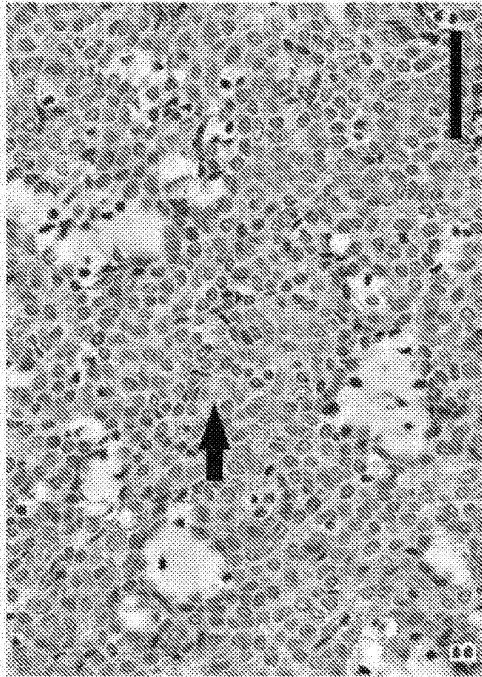
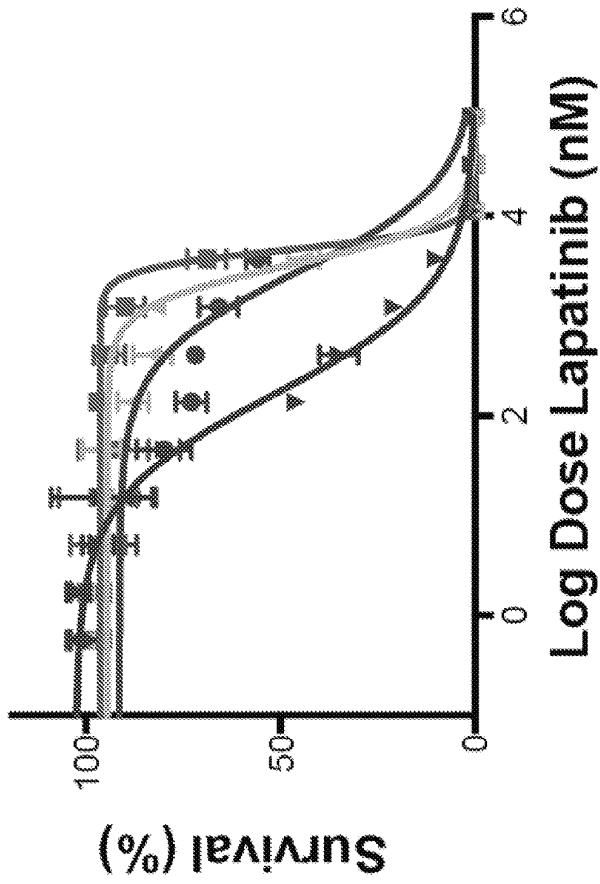


FIG. 4B







Sample	IC50 (nM)
BACA (HER2 <sup>WT</sup> )	2743
OSUK9PADSn (HER2 <sup>WT</sup> )	4592
OSUK9PAPADO (HER2 <sup>WT</sup> )	3259
OSUK9PAPADRE (HER2 <sup>V659E</sup> )	167.6

FIG. 6

Supplementary Table 1. Informatic tools utilized in primary canine lung cancer analysis

Sequencing Platform	Tool	Version	Flags	Flag Purpose and/or Parameters where Applicable
Exome	BWA	0.7.6	-R "\${RGTAG}"	RGTAGs consists of the flowcell ID, lane number and the library tag ID specific for every library prep and assay type
			-M -l	8
	GATK- Recalibrate	3.3.0	-nct --disable_indel_qual -knownsites -cov -cov -cov -cov	8  Known SNPs from dbSNP QualityScoreCovariate ReadGroupCovariate CycleCovariate ContextCovariate
	GATK- MarkDups	3.3.0	ASSUME_SORTED REMOVE_DUPLICATES MAX_RECORDS_IN_RAM CREATE_INDEX VALIDATION_STRINGENCY	TRUE FALSE 18000000 TRUE SILENT
	GATK - RealignerTargetCreator	3.3.0	-nt --maxIntervalSize -DBQ	16 350 1
	GATK-indelRealigner	3.3.0	-DBQ --maxReadsInMemory --maxConsensus --maxReadsForConsensus --maxReadsForRealignment -model -known	1 5000000 24 80 12000 KNOWNS_ONLY Known INDELS from dbSNP
	GATK -HaplotypeCaller	3.3.0	-nct -D	8 KNOWN

FIG. 7A

Sequencing Platform	Tool	Version	Flags	Flag Purpose and/or Parameters where Applicable
			-mbq	10
	Samtools-mpileup	1.2	-DSS0G -C -F -vmC	50 0.01 V
	Freebayes		--ploidy --min-repeat-entropy	2 1
	Seurat	2.6	--both_strands --metrics --indels --allele-metrics	
	MuTect	1.1.4	--cosmic --dbsnp --fraction_contamination --minimum_mutation_cell_fraction --minimum_normal_allele_fraction --min_qscore --gap_events_threshold --heavily_clipped_read_fraction -- required_maximum_alt_allele_mapping_qualit y_score --max_alt_alleles_in_normal_count --max_alt_alleles_in_normal_qscore_sum --max_alt_alleles_in_normal_fraction	cosmicVCF dbSNP variants 0.02 0 0 5 3 0.3
	Picard - MultiMetrics	1.128	PROGRAM PROGRAM PROGRAM PROGRAM ASSUME_SORTED	CollectInsertSizeMetrics CollectAlignmentSummaryMetrics QualityScoreDistribution MeanQualityByCycle TRUE

FIG. 7B

Sequencing Platform	Tool	Version	Flags	Flag Purpose and/or Parameters where Applicable
STAR		2.4	--limitOutSAMoneReadBytes --readFilesCommand --outFilterType --outFilterMultimapNmax --outFilterMismatchNmax --outFilterMismatchNoverLmax --alignIntronMin --alignIntronMax --alignMatesGapMax --alignSJoverhangMin --alignSJDBoverhangMin --seedSearchStartLmax --chimSegmentMin --chimJunctionOverhangMin --runThreadn --genomeLoad --outSAMstrandField --outSAMunmapped --outSAMmapUnique --outSAMattrRGline --outSAMmode	90000000 zcat BySJout 10 10 0.1 20 1000000 1000000 8 8 30 15 15 14 NoSharedMemory intronMotif Within 255 \$RGtags Full
1Conut			Default	
delly-0.7.6			-q	20
Amplicon	picardtools	2.10.3		
	FastQC	v0.11.5		
	EA utils	1.1.2		
	samtools - view, index, sort, mpileup	1.2		

FIG. 7C

Supplementary Table 2. Extended clinical and multiplatform annotation of primary canine lung cancer cases.

Patient ID	Breed	Sex	Neutered/		Age at diagnosis (yr)	Clinical finding
			Spayed	Neutered		
CCB010381	Labrador Retriever mix	Female	Yes		10	ND
CCB040231	Poodle	Female	Yes		13	ND
CCB050342	Flat-Coated Retriever	Female	Yes		11	Decreased energy level
OSU396622	Schnauzer (Miniature)	Male	Yes		12	Incidental
CCB010109	Labrador Retriever	Male	Yes		11	Cough
OSU361939	Cocker Spaniel	Female	Yes		13	Cough, shaking, anorexia
CCB030383	Labrador Retriever	Female	Yes		10	Incidental
CCB050097	Schipperke	Female	Yes		12	Cough
CCB060156	Great Dane	Male	No		7	ND
OSU428073	Boston Terrier	Male	Yes		11	Cough
CCB050345	Mixed Breed	Female	Yes		11	Seizures
CCB050350	Norwegian Elkhound	Female	Yes		15	Incidental
OSU388285	Basset Hound	Female	Yes		9	Lethargy, pyrexia, cough
CCB040245	Mixed Breed	Male	Yes		13	ND
CCB040385	Australian Shepherd	Male	Yes		9	ND
OSU424354	West Highland White Terrier	Male	Yes		8	Cough, respiratory effort, no appetite
CCB010387	Labrador Retriever	female	Yes		13	ND
OSU389339	Basset Hound	Female	Yes		9	Cough
OSUK9PAPADO	Schnauzer (Miniature)	Male	Yes		10	Dyspnea
CCB050354	Labrador Retriever	Male	No		9	Cough, exercise intolerance
OSUK9PAPADRe	Mixed Breed	Male	Yes		9	Hemoptysis
OSU419040	Pomeranian	Female	Yes		13	Wheezing, collapse after exercise
CCB030381	Labrador Retriever	Female	Yes		12	Cough
CCB060143	Mixed Breed	Male	Yes		11	ND

FIG. 8A

Signalment and history				Neutered/ Spayed		Age at diagnosis (yr)		Clinical finding
Patient ID	Breed	Sex		Yes	No			
CCB070294	Mixed Breed	Female		Yes		9	Lethargy	
CCB050356	Brittany Spaniel	Female		Yes		11	Cough	
CLAC	Pointer	Male		No		10	ND	
OSU429271	Wheaten Terrier	Female		Yes		9	Incidental	
CCB070214	Mixed Breed	Female		Yes		8	ND	
CCB070142	Mixed Breed	Female		Yes		12	ND	
CCB050081	Weimaraner	Female		Yes		12	Incidental	
OSU431895	Lhasa Apso	Female		Yes		13	Cough	
OSUK9PADSn	Shih Tzu	Male		Yes		12	Incidental	
CCB050363	Boxer	Male		Yes		7	Incidental	
CCB020198	Boxer	Male		Yes		8	Collapse, thoracic pain	
CCB040005	Labrador Retriever	Male		Yes		10	ND	
OSUK9PADSQ	Mixed Breed	Female		Yes		11	Hemoptysis	
CCB050243	Shih Tzu	Female		Yes		8	ND	
OSU381645	German Shepherd	Male		Yes		11	Incidental	
CCB050352	Mixed Breed	Female		Yes		12	ND	
OSU415281	Mixed Breed	Male		Yes		12	Incidental	
OSU422557	Mixed Breed	Male		Yes		14	Weight loss	
BACA	ND	ND		ND		ND	ND	
CCB030382	Bichon Frise	Female		Yes		12	Cough	
CCB070152	Mixed Breed	Male		Yes		10	ND	
CCB050346	Mixed Breed	Female		Yes		10	Cough after exercise	
CCB020070	Labrador Retriever	Female		Yes		12	Cough	
CCB050200	Mixed Breed	Male		Yes		10	ND	
CCB020203	Scottish Terrier	Male		Yes		8	Wheezing, cough, dyspnea	
CCB060040	Welsh Corgi, Pembroke	Male		Yes		14	ND	
CCB060056	Papillon	Female		Yes		12	ND	

FIG. 8B

Signalment and history						
Patient ID	Breed	Sex	Neutered/ Spayed	Age at diagnosis (yr)	Clinical finding	
CCB040149	Labrador Retriever	Male	Yes	13	ND	
CCB010227	Australian Shepherd	Female	Yes	11	Cough	
CCB070114	Bichon Frise	Female	Yes	14	ND	
CCB070295	Mixed Breed	Female	Yes	12	ND	
CCB060157	Golden Retriever	Male	Yes	9	ND	
OSUK9PAPADSh	Dachshund	Female	Yes	10	Cough	
CCB070006	Labrador Retriever	Female	Yes	13	ND	
CCB070296	Bichon Frise	Female	Yes	11	ND	
OSUK9PAPADI	Labrador Retriever mix	Female	Yes	6	Incidental	
OSU421496	American Bulldog	Male	No	7	Dyspnea	
OSUK9PADBa	Golden Retriever	Male	Yes	13	Cough	
CCB020251	Border Collie	Male	Yes	12	Cough, dyspnea	
CCB040011	Weimaraner	Female	Yes	12	ND	
CCB010336	Mixed Breed	Female	Yes	11	ND	
CCB050348	Rat Terrier	Male	Yes	10	ND	
CCB010105	Shih Tzu	Male	Yes	10	Cough	
CCB010131	Bichon frise	Female	Yes	11	ND	
CCB010262	Mixed Breed	Male	Yes	11	ND	
CCB010379	Keeshound	Male	Yes	13	ND	
CCB020051	Schnauzer (Miniature)	Male	Yes	12	Hemoptysis	
CCB020245	Labrador Retriever	Male	Yes	11	Incidental	
CCB020293	Cocker Spaniel	Male	Yes	9	Incidental, painful abdomen	
CCB040068	Samoyed	Male	Yes	11	ND	
CCB050181	Mixed Breed	Female	Yes	11	ND	
CCB050260	Doberman Pinscher	Female	Yes	11	Dyspnea	
CCB050349	Mixed Breed	Female	Yes	9	Cough	
OSU454408	Boston Terrier	Female	Yes	8	Incidental	

FIG. 8C



Signalment and history						
Patient ID	Breed	Sex	Neutered/ Spayed	Age at diagnosis (yr)	Clinical finding	
OSU452418	Mixed Breed	Male	Yes	10	Cough, restless, panting	
CCB070169	English Cocker Spaniel	Male	Yes	8	ND	
CCB050362	Mixed Breed	Male	Yes	11	Hemoptysis	
CCB010196	Labrador Retriever	Female	Yes	8	ND	
CCB010139	Labrador Retriever	Male	No	8	Lame	
CCB050227	Labrador Retriever	Female	Yes	11	Cough	
CCB010358	Greyhound	Female	Yes	12	Dyspnea	
OSULSCC1	Labrador Retriever	Female	Yes	10	Cough	
CCB010120	Labrador Retriever	Male	Yes	9	ND	
CCB050353	Bichon Frise	Female	Yes	8	Cough	
OSUK9PAPADRI	Labrador Retriever	Female	Yes	11	Cough	

\* Only tumor data  
 ND= no data

FIG. 8D

Supplementary Table 2 (cont1). Extended clinical and multiparameter annotation of primary canine lung cancer cases. Histopathological and imaging findings

Patient ID	Histopathological diagnosis	Anthraxosis	Side lung affected	Lung lobe affected	Treatment	
CCB010381	Adenocarcinoma-Tubulopapillary	Anthraxosis	Left	ND	ND	
CCB040231	Adenocarcinoma-Papillary	No	Left	Cranial	Left cranial lung lobectomy	
CCB050342	Adenocarcinoma-Tubulopapillary	No	Right	Caudal dorsal	Right caudal lung lobectomy	
OSU396622	Adenocarcinoma-Papillary	No	Left	Caudal	Left caudal lung lobectomy	
CCB010109	Adenocarcinoma-Papillary	No	ND	ND	Removal of mass only	
OSU361939	Adenocarcinoma-Papillary	No	Left	Cranial	Left cranial lung lobectomy and mediastinal mass removal + 5 FU intracavity chemotherapy followed by carboplatin infusion	
CCB030383	Adenocarcinoma-Papillary	No	Left	Cranial	Left cranial and caudal lung lobectomies	
CCB050097	Adenocarcinoma-Acinar	No	Left	Caudal	Left caudal lung lobectomy	
CCB060156	Adenocarcinoma-Tubulopapillary	No	Left	Caudal	Left caudal lung lobectomy	
OSU428073	Adenocarcinoma-Papillary	No	Right	Cranial and middle	Right cranial and middle lung lobectomy + carboplatin + vinblastine	
CCB050345	Adenocarcinoma-Papillary	Anthraxosis	Right	Caudal	Right caudal lung lobectomy	
CCB050350	Adenocarcinoma-Papillary	No	Right	Cranial	Right cranial lung lobectomy	
OSU388285	Adenocarcinoma-Papillary	No	Right	Caudal and middle	Right middle and caudal lung lobectomies	
CCB040245	Adenocarcinoma-Papillary	No	ND	ND	Lung lobectomy	
CCB040385	Adenosquamous carcinoma	No	ND	ND	ND	
OSU424354	Adenocarcinoma-Papillary	No	Left	Cranial	Left cranial lung lobectomy	
CCB010387	Adenocarcinoma-Acinar	Anthraxosis	Right	Cranial	Right cranial lung lobectomy	
OSU369339	Adenocarcinoma-Papillary	No	Left	Caudal	Left caudal lung lobectomy	
OSUK9PAPADO	Adenocarcinoma-Papillary	ND	Right	Cranial	Right cranial and caudal lung lobectomies	
CCB050354	Adenocarcinoma-Papillary	Pneumocystosis	Right	Middle	Right middle lung lobectomy; vinorelbine: 15 mg/m <sup>2</sup> , 14.4 mg intravenously	
OSUK9FAPADRe	Adenocarcinoma-Mucinous papillary	ND	Right	Cranial	Right cranial lung lobectomy	
OSU419040	Adenocarcinoma-Papillary	No	Right	Caudal and middle	Left caudal lung lobectomy (partial debulking)+ vinblastine and carboplatin	
CCB030381	Adenocarcinoma-Papillary	Anthraxosis	Right	Caudal	Right caudal lung lobectomy	
CCB060143	Adenocarcinoma-Solid	No	Right	ND	Right caudal lung lobectomy	
CCB070294	Adenocarcinoma-Papillary	No	Left	Caudal	Left caudal lung lobectomy +torceranib	
CCB050356	Adenocarcinoma	No	Left	Caudal	None	
CLAC	Adenocarcinoma	ND	ND	ND	ND	
OSU429271	Adenocarcinoma	No	Left	Cranial	Left cranial lung lobectomy	
CCB070214	Adenocarcinoma-Acinar	No	Left	Cranial	Left cranial lung lobectomy	
CCB070142	Adenocarcinoma-Acinar	Anthraxosis	Left	Cranial and Caudal	Left cranial and caudal lung lobectomies, gemcitabine, carboplatin	
CCB050081	Adenocarcinoma-Papillary	No	Left	Caudal	Left caudal lung lobectomy	
OSU431895	Adenocarcinoma-Tubulopapillary	No	Right	Caudal	Right caudal lung lobectomy	
OSUK9PADSn	Adenocarcinoma-Papillary	No	Left	Cranial	Left cranial lung lobectomy	

FIG. 8E

Patient ID	Histopathological and imaging findings			Treatment
	Histopathological diagnosis	Side lung affected	Lung lobe affected	
CCB050363	Adenocarcinoma-Papillary	Right	Caudal	Right caudal lung lobectomy
CCB020198	Adenocarcinoma-Tubulopapillary	Left	Caudal	Left caudal lung lobectomy
CCB040005	Adenocarcinoma-Papillary	Left	Caudal	Left caudal lung lobectomy
OSUK9PADSQ	Adenosquamous carcinoma	Left	Caudal	Left caudal lung lobectomy
CCB050243	Adenocarcinoma-Papillary	Left	Caudal	Left caudal lung lobectomy
OSU381645	Adenocarcinoma-Papillary	Left	Caudal	Left caudal lung lobectomy
CCB050352	Adenocarcinoma-Papillary	Right	Cranial	Right cranial lung lobectomy
OSU415281	Adenocarcinoma-Papillary	Left	Cranial	Left cranial lung lobectomy
OSU422557	Adenosquamous carcinoma	Right	ND	Right caudal lung lobectomy - euthanasia 2 days postop
BACA	Adenocarcinoma	ND	ND	ND
CCB030382	Adenocarcinoma-Papillary	Right	Caudal	Right lung lobectomy - all right lung lobes
CCB070152	Squamous cell carcinoma	Right	Caudal	Right caudal and accessory lung lobectomies
CCB050346	Adenocarcinoma-Papillary	Left	Caudal	Left caudal lung lobectomy; carboplatin at 10mg/kg
CCB020070	Adenocarcinoma-Papillary	Right	Caudal	Right caudal lung lobectomy
CCB050200	Adenocarcinoma	ND	ND	ND
CCB020203	Adenocarcinoma-Papillary	Left	Caudal	Left caudal lung lobectomy
CCB060040	Adenocarcinoma-Papillary	ND	ND	Lung lobectomy
CCB060056	Adenosquamous carcinoma	Left	Cranial	Left cranial lung lobectomy
CCB040149	Adenocarcinoma-Mucinous papillary	ND	ND	Lung lobectomy
CCB010227	Adenosquamous carcinoma	ND	ND	Navelbine and lung lobectomy
CCB070114	Adenocarcinoma-Papillary	Left	Caudal	Left caudal lung lobectomy
CCB070295	Adenocarcinoma-Mucinous papillary	Left	Caudal	Left caudal lung lobectomy
CCB060157	Adenocarcinoma-Tubulopapillary	Right	Cranial	Right cranial lung lobectomy
OSUK9PAPADSh	Adenocarcinoma-Papillary	Right	Caudal	Right caudal lung lobectomy
CCB070006	Adenocarcinoma-Papillary	Right	Caudal and accessory	Right caudal and accessory lung lobectomies
CCB070296	Adenosquamous carcinoma	Left	Caudal	Left caudal lung lobectomy
OSUK9PAPADI	Adenocarcinoma-Papillary	Right	Caudal	Right caudal lung lobectomy
OSU421486	Adenocarcinoma-Papillary	Right	Caudal	Right caudal lung lobectomy + torceranib
OSUK9PADBa	Adenocarcinoma-Papillary	Left	Caudal	Left caudal lung lobectomy
CCB020251	Adenocarcinoma-Papillary	Left	Caudal	Left caudal lung lobectomy
CCB040011	Adenosquamous carcinoma	ND	ND	Cytotoxic chemotherapy
CCB010336	Adenocarcinoma-Papillary	ND	ND	Vinorelbine
CCB050346	Adenocarcinoma-Acinar	Left	Cranial	Left cranial lung lobectomy, radiation
CCB010105	Adenosquamous carcinoma	Left	Cranial	Left lobectomy
CCB010131	Squamous cell carcinoma	Left	Cranial	Lung lobectomy
CCB010282	Adenocarcinoma-Papillary	ND	ND	Lung lobectomy
CCB010379	Adenosquamous carcinoma	Right	ND	Right middle lung lobectomy, prednisone
CCB020051	Adenocarcinoma	Left	Caudal	Left caudal lung lobectomy

FIG. 8F

Patient ID	Histopathological and imaging findings			Lung lobe affected	Treatment
	Histopathological diagnosis	Anthracois	Side lung affected		
CCB020245	Adenocarcinoma-Solid	No	Right	Caudal	Right caudal lung lobectomy
CCB020293	Adenocarcinoma-Tubulopapillary	No	Right	Caudal	Right caudal lung lobectomy
CCB040068	Adenocarcinoma-Papillary	No	Left	ND	None
CCB050181	Adenocarcinoma-Solid	Anthracois	Right	Middle	Right middle lung lobectomy
CCB050280	Adenocarcinoma-Papillary	No	Right	Caudal	Right caudal lung lobectomy
CCB050349	Adenosquamous carcinoma	No	Right	Caudal	Right caudal lung lobectomy
OSU454468	Adenocarcinoma-Tubulopapillary	No	Right	Middle	Right middle lung lobectomy + vinorelbine 8 treatments q. 2 wks
OSU452418	Adenocarcinoma-Papillary	No	Left	Caudal	Left caudal lung lobectomy
CCB070189	Adenocarcinoma-Acinar	Anthracois	Right	ND	Lung lobectomy
CCB050362	Adenocarcinoma-Papillary	Anthracois	Right	Caudal	Right caudal and accessory lung lobectomies, vinorelbine #1 15mg/m <sup>2</sup> x 2 = 14mg IV
CCB010196	Adenosquamous carcinoma	No	Right	Caudal	Vinorelbine and Right caudal lung lobectomy
CCB010139	Adenocarcinoma-Acinar	No	Right	ND	Lornustine, CCNU, iron dextran 100mg/ml, maropitant 10mg, packed red blood cells (2 units), omeprazole 20mg, famotidine 10mg/ml, amildipine 2.5mg tabs, benazepril 20mg tabs
CCB050227	Adenocarcinoma-Papillary	Anthracois	Left	Caudal	Left caudal lung lobectomy
CCB010358	Adenocarcinoma-Papillary	Anthracois	Right	Cranial	Right cranial lung lobectomy
OSULSCC1	Squamous cell carcinoma	ND	Right	Caudal	Right caudal lung lobectomy
CCB010120	Adenocarcinoma-Papillary	No	Left	Caudal dorsal	Lung lobectomy
CCB050353	Adenocarcinoma-Papillary	Anthracois	Right	Cranial	Right cranial lung lobectomy
OSUK9PAPADRI	Adenocarcinoma-Mucinous papillary	No	Right	Cranial	Right cranial lung lobectomy

\* Only tumor data  
ND= no data

FIG. 8G

Supplementary Table 2 (cont2). Extended clinical and multiplexed analysis of primary canine lung cancer cases.

Patient ID	Sample type	Genetic analysis				Immunohistochemistry		
		Exome sequencing	Amplicon sequencing (HER2-V669E)	Sanger sequencing (whole HER2) <sup>a</sup>	Droplet digital PCR <sup>b</sup> (HER2-V669E)	Plasma droplet digital PCR (ERBB2-V669E)	RNA Expression	HER2
CCB010381	Tumor/Normal	ND	Yes	ND	ND	Yes	ND	
CCB040231	Tumor/Normal	ND	Yes	ND	ND	ND	ND	
CCB050342	Tumor/Normal	ND	Yes	ND	ND	ND	ND	
OSU398622	Tumor/Normal	Yes	ND	ND	Yes	ND	ND	
CCB010109	Tumor/Normal	ND	Yes	ND	ND	Yes	ND	
OSU381939	Tumor/Normal	ND	Yes	Yes	ND	Yes	ND	
CCB030383	Tumor/Normal	ND	Yes	ND	ND	ND	ND	
CCB050097	Tumor/Normal	ND	Yes	ND	ND	ND	ND	
CCB060186	Tumor/Normal	ND	Yes	Yes	ND	ND	ND	
OSU428073	Tumor/Normal	ND	Yes	Yes	ND	Yes	ND	
CCB050345	Tumor/Normal	ND	Yes	ND	ND	ND	ND	
CCB050350	Tumor/Normal	ND	Yes	ND	ND	Yes	ND	
OSU388265	Tumor/Normal	ND	Yes	Yes	ND	Yes	Yes	
CCB040245	Tumor/Normal	ND	Yes	ND	ND	ND	ND	
CCB040385	Tumor/Normal	ND	Yes	ND	ND	Yes	ND	
OSU424354	Tumor/Normal	ND	Yes	Yes	ND	ND	Yes	
CCB010387	Tumor/Normal	Yes	Yes	ND	ND	Yes	ND	
OSU389339	Tumor/Normal	ND	Yes	Yes	ND	ND	Yes	
OSUK9PAPADO	Cell line	ND	Yes	Yes	Yes	ND	ND	
CCB050354	Tumor/Normal	Yes	Yes	ND	ND	Yes	ND	
OSUK9PAPADRe	Cell line	ND	Yes	ND	Yes	ND	ND	
OSU419040	Tumor/Normal	ND	Yes	ND	Yes	ND	Yes	
CCB030381	Tumor/Normal	ND	Yes	ND	ND	ND	ND	
CCB060143	Tumor/Normal	ND	Yes	ND	ND	ND	ND	
CCB070294	Tumor/Normal	ND	Yes	ND	Yes	ND	ND	
CCB050356	Tumor/Normal	ND	Yes	ND	ND	ND	ND	
CLAC	Cell line	ND	Yes	Yes	ND	ND	ND	
OSU428271	Tumor/Normal	ND	Yes	Yes	ND	Yes	ND	
CCB070214	Tumor/Normal	ND	Yes	ND	ND	ND	ND	
CCB070142	Tumor/Normal	ND	Yes	ND	ND	ND	ND	
CCB050081	Tumor/Normal	ND	Yes	ND	ND	ND	ND	
OSU431895	Tumor/Normal	Yes	ND	ND	ND	Yes	ND	
OSUK9PADSn	Cell line	ND	Yes	Yes	ND	ND	ND	
CCB050363	Tumor/Normal	ND	Yes	ND	Yes	ND	ND	
CCB020198	Tumor/Normal	ND	Yes	ND	ND	Yes	ND	
CCB040005	Tumor/Normal	ND	Yes	Yes	ND	ND	ND	
OSUK9PADSQ	Cell line	ND	Yes	Yes	ND	ND	ND	
CCB050243	Tumor/Normal	ND	Yes	Yes	Yes	ND	ND	

FIG. 8H

Patient ID	Sample type	Genetic analyses				Immunohistochemistry			
		Exome sequencing	Amplicon sequencing	Sanger sequencing* (HER2-V689E)	Sanger sequencing (whole HER2)*	Droplet digital PCR* (HER2-V689E)	Plasma droplet digital PCR (HERB2-V689E)	RNA Expression	HER2
OSU381846	Tumor/Normal	ND	Yes	Yes	ND	ND	ND	Yes	Yes
CCB050352	Tumor/Normal	ND	Yes	ND	ND	ND	ND	Yes	ND
OSU415281	Tumor/Normal	ND	Yes	Yes	ND	ND	ND	ND	ND
OSU422557	Tumor/Normal	ND	Yes	Yes	ND	ND	ND	Yes	ND
BACA	Cell line	ND	Yes	Yes	Yes	Yes	ND	ND	ND
CCB030382	Tumor/Normal	ND	Yes	ND	ND	ND	ND	Yes	ND
CCB070152	Tumor/Normal	ND	Yes	ND	ND	ND	ND	ND	ND
CCB050346	Tumor/Normal	ND	Yes	ND	ND	ND	ND	Yes	ND
CCB020070	Tumor/Normal	ND	Yes	Yes	ND	ND	ND	Yes	ND
CCB020203	Tumor/Normal	ND	Yes	Yes	ND	ND	Yes	Yes	ND
CCB060040	Tumor/Normal	ND	Yes	ND	ND	ND	ND	Yes	ND
CCB060066	Tumor/Normal	ND	Yes	ND	ND	ND	ND	Yes	ND
CCB040149	Tumor/Normal	ND	Yes	ND	ND	ND	ND	Yes	ND
CCB010227	Tumor/Normal	ND	Yes	Yes	ND	ND	ND	Yes	ND
CCB070114	Tumor/Normal	ND	Yes	ND	ND	ND	ND	ND	ND
CCB070286	Tumor/Normal	ND	Yes	ND	ND	Yes	ND	Yes	ND
CCB060157	Tumor/Normal	ND	Yes	ND	ND	ND	ND	ND	ND
OSUK9PAPADSh	Cell line	ND	Yes	ND	Yes	Yes	ND	ND	ND
CCB070008	Tumor/Normal	ND	Yes	Yes	ND	ND	ND	ND	ND
CCB070286	Tumor/Normal	ND	Yes	ND	ND	ND	ND	Yes	ND
OSUK9PAPADI	Cell line	ND	Yes	ND	Yes	Yes	ND	ND	ND
OSU421496	Tumor/Normal	ND	Yes	Yes	ND	ND	ND	Yes	Yes
OSUK9PADBa	Cell line	ND	Yes	ND	Yes	Yes	ND	ND	ND
CCB020251	Tumor/Normal	ND	Yes	ND	ND	Yes	ND	Yes	ND
CCB040011	Tumor/Normal	ND	Yes	ND	ND	ND	ND	Yes	ND
CCB010336	Tumor/Normal	ND	Yes	ND	ND	ND	ND	Yes	ND
CCB050348	Tumor/Normal	ND	Yes	ND	ND	ND	ND	Yes	ND
CCB010105	Tumor/Normal	ND	Yes	ND	ND	ND	ND	Yes	ND
CCB010131	Tumor/Normal	ND	Yes	ND	ND	ND	ND	Yes	ND
CCB010282	Tumor/Normal	ND	Yes	ND	ND	ND	ND	Yes	ND
CCB010379	Tumor/Normal	ND	Yes	ND	ND	ND	ND	Yes	ND
CCB020051	Tumor/Normal	ND	Yes	Yes	ND	ND	Yes	Yes	ND
CCB020245	Tumor/Normal	ND	Yes	Yes	ND	ND	Yes	Yes	ND
CCB020283	Tumor/Normal	ND	Yes	ND	ND	Yes	Yes	Yes	Yes
CCB040088	Tumor/Normal	ND	Yes	ND	ND	ND	ND	Yes	ND
CCB050181	Tumor/Normal	ND	Yes	ND	ND	ND	ND	Yes	ND
CCB050280	Tumor/Normal	ND	Yes	Yes	ND	Yes	ND	Yes	ND
CCB050349	Tumor/Normal	ND	Yes	ND	ND	ND	ND	Yes	ND
OSU454408	Tumor/Normal	ND	Yes	Yes	ND	ND	ND	ND	Yes
OSU452418	Tumor/Normal	ND	Yes	ND	ND	ND	ND	Yes	ND
CCB070189	Tumor/Normal	ND	Yes	ND	ND	ND	ND	Yes	ND

FIG. 8I

Patient ID	Sample type	Genetic analyses						Immunohistochemistry		
		Exome sequencing	Amplicon sequencing	Sanger sequencing* (HER2-V659E)	Sanger sequencing (whole HER2)*	Droplet digital PCR* (HER2-V659E)	Plasma droplet digital PCR (ERBB2-V659E)	RNA Expression	HER2	
CC8050362	Tumor/Normal	ND	Yes	Yes	ND	ND	ND	ND	Yes	ND
CC8010198	Tumor/Normal	ND	Yes	ND	ND	ND	ND	ND	ND	ND
CC8010139	Tumor/Normal	ND	Yes	ND	ND	ND	ND	ND	Yes	ND
CC8060227	Tumor/Normal	Yes	ND	ND	ND	Yes	ND	ND	ND	ND
CC8010358	Tumor/Normal	ND	Yes	ND	ND	ND	ND	ND	Yes	ND
OSULSCC1	Cell line	ND	Yes	Yes	Yes	Yes	ND	ND	ND	ND
CC8010120	Tumor/Normal	ND	Yes	Yes	ND	ND	ND	ND	Yes	ND
CC8050353	Tumor/Normal	ND	Yes	ND	ND	ND	ND	ND	ND	ND
OSUK9PAPADRI	Cell line	ND	ND	Yes	Riley	ND	ND	ND	ND	ND

\* Only tumor data  
 ND= no data

FIG. 8J

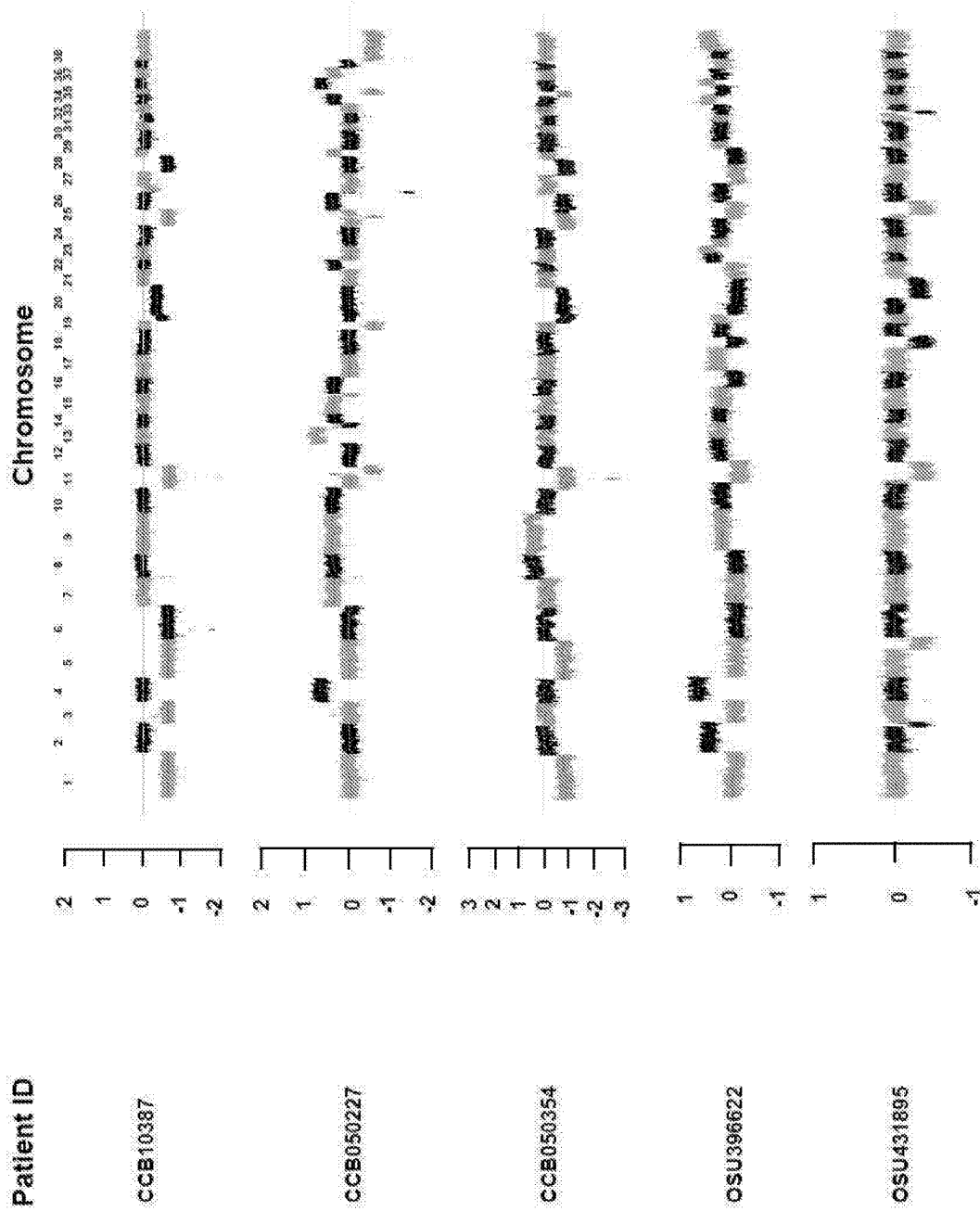


FIG. 9



Supplementary Table 4. Somatic coding SNVs identified by exome sequencing of primary canine lung cancers.

Patient ID	Gene symbol	Transcript accession	Nucleotide (genomic)	rs ID (dbSNP151)	Nucleotide (cDNA)	Amino acid (protein)	Mutation type	% mutant reads
CCB010387	ENSCAFG000000024198	ENSCAF000000048683.2	chr11:103124016A>G	.	c.547A>G	p.Asn183Asp	Missense variant	13%
CCB010387	ENSCAFG000000031824	ENSCAF000000044443.1	chr11:110344193G>A	.	c.746G>A	p.Arg249His	Missense variant	58%
CCB010387	ENSCAFG000000001785	ENSCAF00000002802.3	chr10:31022318G>A	.	c.529G>A	p.Asp177Asn	Missense variant	21%
CCB010387	KCNK12	ENSCAF000000046978.1	chr10:49871039G>T	.	c.349C>A	p.Pro117Thr	Missense variant	17%
CCB010387	KDR	ENSCAF00000003300.3	chr13:47443884G>T	.	c.3846-1G>A		Splice acceptor variant	41%
CCB010387	TMPRSS11F	ENSCAF00000004486.3	chr13:58599540G>C	.	c.128C>A	p.Thr43Asn	Missense variant	15%
CCB010387	HGF	ENSCAF00000010286.3	chr18:21342802AC>A	.	c.1618+1delG		Splice donor variant	34%
CCB010387	ENSCAFG000000024737	ENSCAF00000023283.3	chr19:51478247A>C	.	c.1055T>G	p.Leu352Arg	Missense variant	23%
CCB010387	ENSCAFG000000030414	ENSCAF000000046090.1	chr22:59203429G>A	.	c.728C>T	p.Thr243Ile	Missense variant	11%
CCB010387	ARPP21	ENSCAF00000007650.4	chr23:5811527C>A	.	c.1354+8C>A		Splice region variant	25%
CCB010387	PRKG1	ENSCAF000000044295.2	chr26:35767262C>T	.	c.812G>A	p.Arg271Gln	Missense variant	15%
CCB010387	ACTA2	ENSCAF000000024881.3	chr26:38707206G>A	.	c.289C>T	p.Arg97Cys	Missense variant	38%
CCB010387	UNC13C	ENSCAF000000025186.3	chr30:19556056A>T	.	c.607A>T	p.Met203Leu	Missense variant	37%
CCB010387	ISLR	ENSCAF000000028352.3	chr30:37326596G>A	.	c.1447G>A	p.Val483Ile	Missense variant	30%
CCB010387	HLC5	ENSCAF000000015393.3	chr31:31943202C>T	.	c.1682G>A	p.Ser661Asn	Missense variant	34%
CCB010387	ENSCAFG000000032143	ENSCAF000000046642.1	chr33:5301141T>A	.	c.794T>A	p.Val265Asp	Missense variant	40%
CCB010387	PHLDB1	ENSCAF000000019942.4	chr5:15101566G>A	.	c.3517C>T	p.Arg1173Trp	Missense variant	50%
CCB010387	IOCE	ENSCAF000000036668.3	chr6:14540101C>T	.	c.217-3C>T		Splice region variant	6%
CCB010387	ENSCAFG000000018634	ENSCAF000000026354.3	chr6:17505745C>G	.	c.583G>C	p.Asp195His	Missense variant	8%
CCB010387	USP33	ENSCAF000000032445.3	chr6:69155689G>T	.	c.1509G>T	p.Glu503Asp	Missense variant	54%
CCB010387	MIS18BP1	ENSCAF000000023361.4	chr6:22847439A>C	.	c.2037T>G	p.Cys879Trp	Missense variant	13%
CCB010387	ERBB2	ENSCAF000000025936.3	chr9:22765127A>T	.	c.1976T>A	p.Val659Glu	Missense variant	44%
CCB010387	SLC43A2	ENSCAF000000030472.2	chr9:45767181C>A	.	c.202G>T	p.Glu88*	Stop-gained variant	8%
CCB010387	ENSCAFG000000019755	ENSCAF000000031414.3	chr9:49869729T>G	.	c.374A>C	p.Tyr125Ser	Missense variant	27%
CCB010387	ACE2	ENSCAF000000019262.3	chrX:11618518G>T	.	c.1034C>A	p.Pro345His	Missense variant	28%
CCB010387	TNMD	ENSCAF000000027750.3	chrX:74474211T>C	.	c.622T>C	p.Phe208Leu	Missense variant	28%
CCB050227	SYNE1	ENSCAF00000000760.4	chr1:42441824C>G	.	c.23289G>C	p.Leu7763Phe	Missense variant	10%
CCB050227	FREM1	ENSCAF00000002397.3	chr11:35220245G>C	.	c.4600C>G	p.Leu1534Val	Missense variant	70%
CCB050227	COL14A1	ENSCAF00000001452.3	chr13:19125873G>A	.	c.2302G>A	p.Val768Met	Missense variant	37%
CCB050227	MPP8	ENSCAF00000004508.3	chr14:58182881A>C	.	c.1042A>C	p.Lys348Ser	Missense variant	48%
CCB050227	ZNF800	ENSCAF000000002714.3	chr14:8880781C>A	.	c.158-7C>A		Splice region variant	23%
CCB050227	PABPC4	ENSCAF000000004949.4	chr15:3292275C>A	.	c.407C>A	p.Ser136Tyr	Missense variant	39%
CCB050227	GIMAP8	ENSCAF00000007370.2	chr16:14757724G>C	.	c.638G>C	p.Ser213Thr	Missense variant	5%
CCB050227	C5MD1	ENSCAF000000013889.4	chr16:55503451C>A	.	c.1307G>T	p.Arg436Ile	Missense variant	42%
CCB050227	MFSDB2B	ENSCAF000000006341.3	chr17:18504848G>A	.	c.1249G>A	p.Ala417Thr	Missense variant	35%
CCB050227	PCLO	ENSCAF000000010157.3	chr18:22512128C>T	.	c.8742G>A	p.Ala3248Thr	Missense variant	38%
CCB050227	CR4P4	ENSCAF000000012973.3	chr18:40239473C>A	.	c.802G>T	p.Val268Leu	Missense variant	39%
CCB050227	SART1	ENSCAF000000020808.3	chr18:51298894G>A	.	c.1741C>T	p.Arg581Trp	Missense variant	51%
CCB050227	CAPN1	ENSCAF000000021965.3	chr18:52006009T>TA	.	c.942_943insT	p.Asn315fs	Frameshift variant	30%
CCB050227	MBS5	ENSCAF000000008917.3	chr19:50235818G>A	.	c.4331G>A	p.Ser1444Asn	Missense variant	39%
CCB050227	PTAFR	ENSCAF000000018894.3	chr2:72255041G>A	.	c.673G>A	p.Ala225Thr	Missense variant	20%

FIG. 10A

Patient ID	Gene symbol	Transcript accession	Nucleotide (genomic)	rs ID (dbSNP151)	Nucleotide (cDNA)	Amino acid (protein)	Mutation type	% mutant reads
CCB050227	EEFSEC	ENSCAF0000006626.3	chr20:2273718C>T	.	c.1073C>T	p.Ser358Phe	Missense variant	66%
CCB050227	FANCD2	ENSCAF0000008366.3	chr20:8253068C>T	.	c.3274G>A	p.Glu1092Lys	Missense variant	79%
CCB050227	ENSCAF00000005230	ENSCAF0000008452.3	chr21:22004023G>A	.	c.1532G>A	p.Arg511>Gln	Missense variant	45%
CCB050227	ORS1G2	ENSCAF00000019854.3	chr21:27360444C>T	.	c.883G>A	p.Val295Ile	Missense variant	33%
CCB050227	ENSCAF00000006321	ENSCAF00000010223.3	chr21:28981291G>T	.	c.852G>T	p.Leu284Phe	Missense variant	8%
CCB050227	MBNL2	ENSCAF00000008902.3	chr22:47695351C>A	.	c.844C>A	p.Glu282Lys	Missense variant	43%
CCB050227	FBXO25	ENSCAF00000018193.2	chr25:37451577C>T	.	c.235C>T	p.Gln79*	Stop-gained variant	69%
CCB050227	ADAMTSL3	ENSCAF00000021096.3	chr3:55577631G>A	.	c.1849G>A	p.Glu617Lys	Missense variant	33%
CCB050227	IRX4	ENSCAF00000016576.3	chr34:10928900G>C	.	c.685G>C	p.Glu229Gln	Missense variant	44%
CCB050227	CNTN2	ENSCAF00000037921.2	chr38:1585482G>A	.	c.1081G>A	p.Glu361Lys	Missense variant	41%
CCB050227	NIPBL	ENSCAF00000044310.2	chr4:71598459T>C	.	c.6682A>G	p.Ile2228Val	Missense variant	48%
CCB050227	DNAH2	ENSCAF00000026606.3	chr5:32634372C>A	.	c.2918C>A	p.Ser973Tyr	Missense variant	66%
CCB050227	MYH13	ENSCAF00000027662.3	chr5:34638774G>A	.	c.2891C>T	p.Thr964Met	Missense variant	13%
CCB050227	ZSWIM7	ENSCAF00000028717.3	chr5:396868255G>C	.	c.48G>C	p.Glu16Asp	Missense variant	74%
CCB050227	ENSCAF00000014044	ENSCAF00000022201.3	chr6:8811223G>C	.	c.7728C>G	p.Ser2576Arg	Missense variant	6%
CCB050227	MYBPH	ENSCAF00000016341.3	chr7:41892G>A	.	c.1003G>A	p.Gly335Arg	Missense variant	24%
CCB050227	NLRP3	ENSCAF00000017002.3	chr8:259283G>T	.	c.1687G>T	p.Glu563*	Stop-gained variant	30%
CCB050227	ERBB2	ENSCAF00000025936.3	chr9:22765127A>T	.	c.1976T>A	p.Val659Glu	Missense variant	54%
CCB050227	CACNA1G	ENSCAF00000027129.5	chr9:28518243G>A	.	c.3288G>A	p.Ala1090Thr	Missense variant	7%
CCB050227	ENTPD2	ENSCAF00000031028.1	chr9:46590998G>A	.	c.433G>A	p.Asp45Asn	Missense variant	26%
CCB050227	SLITRK2	ENSCAF00000030252.3	chrX:114581830T>C	.	c.781T>C	p.Val254Ala	Missense variant	38%
CCB050227	CITED1	ENSCAF00000027168.3	chrX:56327283G>T	.	c.565C>A	p.Leu189Met	Missense variant	43%
CCB050227	DIAPH2	ENSCAF00000035855.2	chrX:71042970A>C	.	c.3308A>C	p.Lys1103Thr	Missense variant	8%
CCB050354	ENSCAF00000026536	ENSCAF0000001265.3	chr1:54190681C>T	.	c.539G>A	p.Arg180His	Missense variant	22%
CCB050354	ENSCAF00000001339	ENSCAF0000002078.3	chr1:73521101C>A	.	c.684C>A	.	Splice region variant	18%
CCB050354	MICALL1	ENSCAF0000002244.4	chr10:26726936C>A	.	c.928+1G>T	.	Splice donor variant	49%
CCB050354	ENSCAF00000005307	ENSCAF00000029311.2	chr10:38390829C>A	.	c.283C>A	p.Ala88Asp	Missense variant	12%
CCB050354	ENSCAF00000001853	ENSCAF0000002921.4	chr12:11995302C>A	.	c.1825C>A	p.Pro808Thr	Missense variant	17%
CCB050354	CSMD3	ENSCAF0000001236.4	chr13:12453038C>A	.	c.8200G>T	p.Arg3087Ile	Missense variant	40%
CCB050354	WDR35	ENSCAF00000006134.4	chr17:15030766C>A	.	c.255G>T	p.Lys85Asn	Missense variant	14%
CCB050354	APOB	ENSCAF00000008266.2	chr17:15888008G>A	.	c.4987C>T	p.Arg1683Cys	Missense variant	38%
CCB050354	MAML3	ENSCAF00000005950.3	chr19:2891218T>G	.	c.108T>G	p.Phe36Leu	Missense variant	19%
CCB050354	ATP9A	ENSCAF00000018585.3	chr24:37804580A>G	.	c.2732T>C	p.Leu911Pro	Missense variant	20%
CCB050354	SLC6B1	ENSCAF00000046446.2	chr26:10679000C>G	.	c.568G>C	p.Ala190Pro	Missense variant	18%
CCB050354	LCOR	ENSCAF00000048723.1	chr28:10333164A>G	.	c.1801A>G	p.Thr601Ala	Missense variant	22%
CCB050354	POLK	ENSCAF00000014935.3	chr3:30811008C>A	.	c.1089+1G>T	.	Splice donor variant	24%
CCB050354	PDE5B	ENSCAF00000026577.3	chr3:91751745A>C	.	c.1786T>G	p.Cys598Gly	Missense variant	11%
CCB050354	ENSCAF00000024680	ENSCAF00000038074.3	chr30:31947438C>G	.	c.911C>G	p.Ser304Cys	Missense variant	19%
CCB050354	ZSCAN12	ENSCAF00000018931.3	chr35:25550627C>A	.	c.421G>T	p.Val141Phe	Missense variant	17%
CCB050354	ERBB4	ENSCAF00000022535.3	chr37:19041081C>T	.	c.3007-8G>A	.	Splice region variant	13%
CCB050354	ENSCAF00000016100	ENSCAF00000048260.1	chr4:34757218C>T	.	c.1082G>A	p.Gly361Asp	Missense variant	14%
CCB050354	CALB2	ENSCAF00000037964.2	chr5:77189552C>A	.	c.56C>A	p.Ala19Asp	Missense variant	21%
CCB050354	RNPEP	ENSCAF00000016772.3	chr7:970490A>AG	.	c.1239dupC	p.Tyr414fs	Frameshift variant	21%

FIG. 10B

Patient ID	Gene symbol	Transcript accession	Nucleotide (genomic)	rs ID (dbSNP151)	Nucleotide (cDNA)	Amino acid (protein)	Mutation type	% mutant reads
CSU030354	ERBB2	ENSCAF00000025836.3	chr9:227650771>C	.	c.2026A>G	p.Lys679Glu	Missense variant	35%
CSU030354	CALCOCCO	ENSCAF00000026722.3	chr9:250580080>T	.	c.154C>T	p.Arg52*	Stop-gained variant	23%
CSU030354	UNC45B	ENSCAF00000029046.3	chr9:381190461C>G	.	c.2653G>C	p.Val885Ileu	Missense variant	17%
CSU030354	COL5A1	ENSCAF00000031582.4	chr9:50832901G>C	.	c.4007G>C	p.Gly1336Ala	Missense variant	32%
CSU030354	CERCAM	ENSCAF00000031918.3	chr9:55110594G>A	.	c.1717C>G	p.Arg573Cys	Missense variant	19%
CSU030354	AFF2	ENSCAF00000030321.3	chrX:117131625C>T	.	c.2085C>T	p.Pro689Ser	Missense variant	23%
CSU030354	ARSH	ENSCAF00000017754.3	chrX:1579713A>G	.	c.961A>G	p.Thr321Ala	Missense variant	23%
OSU396622	GLPR1L2	ENSCAF00000048594.1	chr10:15924621G>T	.	c.109G>T	p.Gly37Tyr	Missense variant	26%
OSU396622	PNPLA1	ENSCAF00000002155.3	chr12:5417391C>T	.	c.1448C>T	p.Pro483Leu	Missense variant	17%
OSU396622	POU3F2	ENSCAF00000043152.1	chr12:57104161A>C	.	c.77A>C	p.Gln26Pro	Missense variant	8%
OSU396622	MDR1	ENSCAF0000002896.3	chr14:13711741G>T	.	c.422C>A	p.Ala141Glu	Missense variant	22%
OSU396622	TLL1	ENSCAF00000014157.3	chr15:81887057G>T	.	c.1337G>T	p.Trp448Leu	Missense variant	7%
OSU396622	CSMD2	ENSCAF00000005882.4	chr15:8006138C>T	.	c.1756+8C>T	Splice region variant	14%	
OSU396622	SGCZ	ENSCAF00000010844.3	chr18:37844479A>G	.	c.277T>C	p.Tyr93His	Missense variant	6%
OSU396622	SLC7A2	ENSCAF0000011153.3	chr16:40855325C>T	.	c.20C>T	p.Ala7Val	Missense variant	24%
OSU396622	AIM1L	ENSCAF0000019865.4	chr2:73687064G>A	.	c.3371G>A	p.Gly1124Glu	Missense variant	19%
OSU396622	MYO16	ENSCAF00000008518.3	chr22:36070777G>A	.	c.1185G>A	p.Ser395Ser	Splice region variant	21%
OSU396622	NRSN1	ENSCAF00000048012.1	chr22:57655454G>T	.	c.3277G>T	p.Val1093Leu	Missense variant	23%
OSU396622	CFLAR	ENSCAF0000019278.2	chr37:103048781G>T	.	c.1021delG	p.Asp341fs	Frameshift variant	28%
OSU396622	CFLAR	ENSCAF0000019278.2	chr37:10304880G>T	.	c.1021G>T	p.Asp341Tyr	Missense variant	29%
OSU396622	NBEAL1	ENSCAF0000020215.4	chr37:11989839C>A	.	c.4376C>A	p.Ser1459Tyr	Missense variant	30%
OSU396622	SUSD4	ENSCAF0000018868.3	chr38:23671827G>A	.	c.218G>A	p.Arg73His	Missense variant	20%
OSU396622	PER1	ENSCAF0000026905.4	chr5:32962533C>T	.	c.2082G>A	p.Glu688Lys	Missense variant	24%
OSU396622	FBLX18	ENSCAF0000025425.3	chr6:12448719G>A	.	c.1096G>A	p.Glu368Lys	Missense variant	20%
OSU396622	CACNA1E	ENSCAF0000020724.5	chr7:15200535C>T	.	c.3218C>T	p.Thr1073Met	Splice region variant	20%
OSU396622	KIF21B	ENSCAF0000017574.3	chr7:2206062G>T	.	c.1467-4G>T	Splice region variant	20%	
OSU396622	MBD1	ENSCAF00000030047.3	chr7:78603634G>C	.	c.1684G>C	p.Val562Leu	Missense variant	16%
OSU396622	KCNK10	ENSCAF0000043710.2	chr8:59487970C>T	.	c.940G>A	p.Val314Ile	Missense variant	21%
OSU396622	KIF26A	ENSCAF0000029108.4	chr8:71824126G>A	.	c.4085G>A	p.Arg1362Gln	Missense variant	27%
OSU396622	ERBB2	ENSCAF0000025936.3	chr9:22765127A>T	.	c.1976T>A	p.Val659Glu	Missense variant	20%
OSU431895	TSEN34	ENSCAF0000004233.3	chr11:103021904C>A	.	c.864G>T	p.Lys288Asn	Missense variant	34%
OSU431895	PPM1N	ENSCAF0000004536.3	chr11:10068586G>C	.	c.473G>A	p.Arg158His	Missense variant	37%
OSU431895	CLPTM1	ENSCAF0000007423.3	chr11:110493865AG>A	.	c.1140-6C>G	Splice region variant	30%	
OSU431895	CCDC97	ENSCAF0000008063.4	chr11:12653365G>T	.	c.73-6delC	Splice region variant	14%	
OSU431895	PAK4	ENSCAF0000009039.4	chr11:14014367G>A	.	c.860C>T	p.Gln238Lys	Missense variant	27%
OSU431895	ZFP82	ENSCAF00000045420.1	chr11:14014367G>A	.	c.332T>A	p.Pro287Leu	Missense variant	36%
OSU431895	URI1	ENSCAF0000012164.4	chr11:121611868G>C	.	c.28C>G	p.Leu111*	Stop-gained variant	29%
OSU431895	BCLAF1	ENSCAF0000000383.4	chr11:28873817G>C	.	c.38C>G	p.Leu10Val	Missense variant	27%
OSU431895	SERAC1	ENSCAF0000000999.3	chr11:47609753C>A	.	c.1117G>T	p.Ser13*	Stop-gained variant	5%
OSU431895	LAMA2	ENSCAF0000001697.4	chr11:67645594G>T	.	c.141G>T	p.Glu373*	Stop-gained variant	23%
OSU431895	LAMA2	ENSCAF0000001697.4	chr11:67645594G>T	.	c.141G>T	p.Arg47Ser	Missense variant	10%

FIG. 10C

Patient ID	Gene symbol	Transcript accession	Nucleotide (genomic)	rs ID (dbSNP151)	Nucleotide (cDNA)	Amino acid (protein)	Mutation type	% mutant reads
OSU431895	CD274	ENSCAF0000003346.3	chr1:93598056G>C	.	c.314G>C	p.Arg105Thr	Missense variant	24%
OSU431895	ERMP1	ENSCAF0000003361.3	chr1:93880291C>T	.	c.628G>A	p.Asp210Asn	Missense variant	30%
OSU431895	PTPRB	ENSCAF0000000719.4	chr10:12302391G>A	.	c.4715-7C>T		Splice region variant	21%
OSU431895	ZFC3H1	ENSCAF0000000726.4	chr10:13201688C>G	.	c.1061G>C	p.Arg354Thr	Missense variant	23%
OSU431895	TBC1D15	ENSCAF0000000735.3	chr10:13362797G>G	.	c.206C>G	p.Ser69Cys	Missense variant	24%
OSU431895	TTIL12	ENSCAF0000001412.3	chr10:22383957G>C	.	c.1699G>C	p.Asp567His	Missense variant	21%
OSU431895	CHADL	ENSCAF0000001705.3	chr10:23996212C>A	.	c.2195C>A	p.Ser732Tyr	Missense variant	27%
OSU431895	SEPT10	ENSCAF00000047214.1	chr10:34297349C>T	.	c.991C>T	p.Gln331*	Stop-gained variant	23%
OSU431895	SLC16A7	ENSCAF0000000487.3	chr10:3491155G>C	.	c.678G>C	p.Lys228Asn	Missense variant	22%
OSU431895	EPCAM	ENSCAF00000004180.3	chr10:49493762C>G	.	c.731C>G	p.Pro244Arg	Missense variant	21%
OSU431895	FOXN2	ENSCAF00000046196.1	chr10:50260429C>G	.	c.476C>G	p.Ser159Cys	Missense variant	13%
OSU431895	SPTBN1	ENSCAF0000004367.4	chr10:55558606C>T	.	c.6301C>T	p.Pro2101Ser	Missense variant	21%
OSU431895	TEX43	ENSCAF0000000911.2	chr11:15908369G>C	.	c.300C>C	p.Leu100Phe	Missense variant	27%
OSU431895	SPAG8	ENSCAF00000044181.2	chr11:52340730C>T	.	c.891G>A	p.Glu231Lys	Missense variant	26%
OSU431895	DDX39B	ENSCAF000000336511.2	chr12:1042622G>A	.	c.113C>T	p.Ser38Phe	Missense variant	23%
OSU431895	TAP1	ENSCAF0000003306.3	chr12:2431980C>A	.	c.89S>T	p.Arg30Met	Missense variant	28%
OSU431895	TAP1	ENSCAF0000001306.3	chr12:2431981T>A	.	c.88A>T	p.Arg30Trp	Missense variant	30%
OSU431895	COL19A1	ENSCAF0000004046.4	chr12:32509880G>C	.	c.915G>C	p.Gln305His	Missense variant	23%
OSU431895	NRM	ENSCAF0000000694.5	chr12:462875C>A	.	c.2286G>T	p.Asp766Tyr	Missense variant	13%
OSU431895	MDN1	ENSCAF00000048198.2	chr12:48983311A>G	.	c.2286C>G	p.Asp762Glu	Missense variant	10%
OSU431895	SLC45A4	ENSCAF0000001916.3	chr13:35744578G>A	.	c.61C>T	p.Val631Ile	Missense variant	31%
OSU431895	CPGF1	ENSCAF0000002514.3	chr13:37818701G>T	.	c.3484G>A	p.Asp1162Asn	Stop-gained variant	19%
OSU431895	KIT	ENSCAF00000049630.2	chr13:47179167G>C	.	c.1892T>C	p.Gln21*	Missense variant	20%
OSU431895	ZFPM2	ENSCAF0000001049.4	chr13:6435763T>A	.	c.181T>A	p.Leu643Phe	Missense variant	15%
OSU431895	FAM126A	ENSCAF0000004353.3	chr14:3665783C>T	.	c.160G>A	p.Glu54Lys	Missense variant	24%
OSU431895	GPNMB	ENSCAF0000004389.2	chr14:36933881G>A	.	c.892G>A	p.Val228Met	Missense variant	18%
OSU431895	ENSCAF0000002897	ENSCAF0000004632.3	chr14:39514372G>C	.	c.167+5G>C	Splice region variant	16%	
OSU431895	ANLN	ENSCAF00000065209.3	chr14:47818863G>T	.	c.790G>T	p.Asp264Tyr	Missense variant	24%
OSU431895	ENSCAF00000023485	ENSCAF00000036126.2	chr14:5896928G>C	.	c.518G>C	p.Arg173Thr	Missense variant	24%
OSU431895	CPA1	ENSCAF0000002313.3	chr14:6565478G>C	.	c.815C>G	p.Ser272*	Stop-gained variant	7%
OSU431895	ENSCAF00000028806	ENSCAF0000004683.1	chr15:14994033G>A	.	c.662C>T	p.Ser221Phe	Missense variant	7%
OSU431895	PIIE	ENSCAF00000046878.1	chr15:3169583C>G	.	c.174+5G>C	Splice region variant	18%	
OSU431895	MMAA	ENSCAF00000012297.2	chr15:44232714G>A	.	c.229G>C	p.Glu77Lys	Missense variant	17%
OSU431895	AGBL3	ENSCAF0000005114.3	chr16:13061855C>G	.	c.1122G>C	p.Met374Ile	Missense variant	28%
OSU431895	ENSCAF0000003149	ENSCAF0000005066.3	chr16:13821050C>T	.	c.845C>T	p.Ser282Phe	Missense variant	20%
OSU431895	WDR60	ENSCAF00000045150.2	chr16:14495233G>C	.	c.121G>C	p.Glu41Gln	Missense variant	23%
OSU431895	ENSCAF00000026458	ENSCAF0000008456.3	chr16:20823434G>C	.	c.802G>C	p.Glu276Gln	Missense variant	20%
OSU431895	LONRF1	ENSCAF00000042745.1	chr16:35373460G>A	.	c.602G>A	p.Gly201Glu	Missense variant	9%
OSU431895	ENSCAF00000068873	ENSCAF00000047804.1	chr16:36244321C>G	.	c.859G>C	p.Asp287His	Missense variant	19%
OSU431895	ENSCAF00000008367	ENSCAF0000011052.3	chr16:40524050G>C	.	c.333G>C	p.Leu111Phe	Missense variant	20%
OSU431895	APOB	ENSCAF0000003291.3	chr16:51552737G>T	.	c.1460G>T	p.Arg467Leu	Missense variant	22%
OSU431895		ENSCAF0000006266.2	chr17:15886395G>C	.	c.6600C>G	p.Ile2200Met	Missense variant	28%

FIG. 10D

Patient ID	Gene symbol	Transcript accession	Nucleotide (genomic)	rs ID (dbSNP151)	Nucleotide (cDNA)	Amino acid (protein)	Mutation type	% mutant reads
OSU431895	TSSC1	ENSCAF00000005219.3	chr17:1870470C>T		c.998-1G>A		Splice acceptor variant	20%
OSU431895	DPYSL5	ENSCAF00000007378.3	chr17:20895379C>A		c.246C>A	p.Phe82Leu	Missense variant	26%
OSU431895	PLB1	ENSCAF0000000843.3	chr17:22547880G>A		c.3822G>A	p.Glu1274Gln	Splice region variant	24%
OSU431895	C2orf71	ENSCAF00000008452.3	chr17:22907687C>G		c.2851G>C	p.Asp951His	Missense variant	19%
OSU431895	CEBPZ	ENSCAF00000009851.3	chr17:29570374C>T		c.2515G>A	p.Glu839Lys	Missense variant	23%
OSU431895	NOTCH2	ENSCAF00000018889.3	chr17:56870295C>T		c.5137G>A	p.Glu1713Lys	Missense variant	28%
OSU431895	TXNIP	ENSCAF00000018124.3	chr17:58777650G>C		c.811C>G	p.Arg271Gly	Missense variant	29%
OSU431895	ZNF567	ENSCAF00000020030.3	chr17:60356209G>C		c.2200G>C	p.Glu734Gln	Missense variant	21%
OSU431895	DTX4	ENSCAF00000012238.3	chr18:37562136G>A		c.739C>T	p.Arg247Tyr	Missense variant	32%
OSU431895	ENSCAF00000025503	ENSCAF00000039659.2	chr18:38128118G>A		c.787G>A	p.Val261Ile	Missense variant	31%
OSU431895	ENSCAF00000031163	ENSCAF00000047375.1	chr18:39799037C>T		c.361G>A	p.Asp121Asn	Missense variant	24%
OSU431895	TRPM5	ENSCAF00000016218.3	chr18:46485577C>A		c.1806G>T	p.Arg602Ser	Missense variant	32%
OSU431895	ENSCAF00000032485	ENSCAF00000046317.1	chr18:51424509C>T		c.614C>G	p.Ser205Leu	Missense variant	15%
OSU431895	AHNAK	ENSCAF00000048755.1	chr18:54101249G>T		c.2728G>T	p.Gly609Val	Missense variant	23%
OSU431895	GLI3	ENSCAF00000049220.2	chr18:8054666C>G		c.1758C>G	p.Phe586Leu	Missense variant	28%
OSU431895	KIFC3	ENSCAF00000035416.2	chr2:58730820C>T		c.2314C>G	p.Arg772Cys	Missense variant	23%
OSU431895	ABCC12	ENSCAF00000016220.4	chr2:66965092G>A		c.3800G>A	p.Arg1287His	Missense variant	24%
OSU431895	DNAJC8	ENSCAF00000018890.4	chr2:72193839T>C	rs851990132	c.27>C	p.Met1?	Start-lost variant	6%
OSU431895	EXTL1	ENSCAF00000020161.3	chr2:73934088C>A		c.1516-1G>T		Splice acceptor variant	21%
OSU431895	PGD	ENSCAF00000026597.3	chr2:85397951C>G		c.780G>C	p.Gln260His	Missense variant	6%
OSU431895	ARHGAP21	ENSCAF00000044523.2	chr2:8864689G>C		c.3373G>C	p.Asp1125His	Missense variant	7%
OSU431895	FOXP1	ENSCAF00000010476.3	chr20:21009967G>T		c.1834G>T	p.Glu612*	Stop-gained variant	22%
OSU431895	FAM3D	ENSCAF00000043106.2	chr20:32037081G>C		c.417G>C	p.Glu139Asp	Missense variant	30%
OSU431895	PODNL1	ENSCAF00000007075.3	chr20:3812849G>A		c.491G>A	p.Glu161Lys	Missense variant	31%
OSU431895	ZSWIM4	ENSCAF00000026169.4	chr20:48545684C>T		c.498-3C>T		Splice region variant	33%
OSU431895	ENSCAF00000026294.4	ENSCAF00000026294.4	chr20:48633250G>A		c.1492C>T	p.Arg498Tyr	Missense variant	28%
OSU431895	ENSCAF0000007454.4	ENSCAF0000007454.4	chr20:5587327G>A		c.2626G>A	p.Asp76Asn	Missense variant	28%
OSU431895	ENSCAF00000036630.3	ENSCAF00000036630.3	chr20:57338199G>C		c.1740C>G	p.Phe580Leu	Missense variant	4%
OSU431895	INPPL1	ENSCAF00000010146.2	chr21:25992321C>A		c.2901G>T	p.Leu967Phe	Missense variant	32%
OSU431895	TRIM34	ENSCAF00000010112.4	chr21:28842194G>C		c.1476G>C	p.Glu492Asp	Missense variant	25%
OSU431895	ENSCAF00000029611	ENSCAF00000010146.2	chr21:28714549A>C		c.883A>C	p.Thr293Pro	Missense variant	33%
OSU431895	WEE1	ENSCAF00000011683.4	chr21:32843586G>T		c.239C>T	p.Pro80Leu	Missense variant	21%
OSU431895	DNAJC13	ENSCAF00000010177.3	chr23:29437196C>A		c.1350-7C>A		Splice region variant	22%
OSU431895	C2orf194	ENSCAF00000010311.3	chr24:17958191G>C		c.706G>C	p.Glu238Gln	Missense variant	16%
OSU431895	CTSA	ENSCAF00000015596.4	chr24:33188262T>TAAGGG		+2_1311-3insA		Splice region variant	42%
OSU431895	NEFM	ENSCAF00000014336.4	chr25:32494886C>G		c.1712G>C	p.Gly571Ala	Missense variant	40%
OSU431895	CODC80	ENSCAF00000015857.3	chr26:15594632G>A		c.959G>A	p.Gly320Glu	Missense variant	6%
OSU431895	CMKLR1	ENSCAF00000018084.3	chr26:18533464C>G		c.1006C>G	p.Leu338Val	Missense variant	14%
OSU431895	SFT1	ENSCAF00000049951.2	chr26:24502091G>A		c.3778G>A	p.Glu1260Lys	Missense variant	15%
OSU431895	PCDH15	ENSCAF00000024635.3	chr26:34566685C>T		c.4160C>T	p.Pro1387Leu	Missense variant	27%
OSU431895	PPHLN1	ENSCAF00000046129.1	chr27:11571694C>G		c.241G>C	p.Asp81His	Missense variant	6%
OSU431895	MAP3K12	ENSCAF00000011109.3	chr27:1731327C>G		c.997C>G	p.Leu333Val	Missense variant	34%
OSU431895	CCDC81	ENSCAF00000017424.3	chr27:19461973C>T		c.461G>A	p.Arg154Lys	Missense variant	

FIG. 10E

Patient ID	Gene symbol	Transcript accession	Nucleotide (genomic)	rs ID (dbSNP151)	Nucleotide (cDNA)	Amino acid (protein)	Mutation type	% mutant reads
OSU431895	CASC1	ENSCAF00000018157.4	chr27:22364318G>A	.	c.838G>A	p.Glu280Lys	Missense variant	29%
OSU431895	CLEC9A	ENSCAF00000021464.2	chr27:35920820G>C	.	c.472-4C>G	.	Splice region variant	19%
OSU431895	DDX11	ENSCAF00000024894.3	chr27:42079676G>C	.	c.357G>C	p.Gln119His	Missense variant	32%
OSU431895	BGALNT3	ENSCAF00000025016.4	chr27:42598333T>TA TGG	.	729_2730msATr	p.Met910fs	Frameshift variant	23%
OSU431895	SEMA4G	ENSCAF00000015460.4	chr28:13667893G>A	.	c.819+3G>A	.	Splice region variant	29%
OSU431895	PPRC1	ENSCAF00000015971.4	chr28:14677374G>GC	.	c.2798dupC	p.Pro934fs	Frameshift variant	19%
OSU431895	CHAT	ENSCAF00000010762.4	chr28:1528603C>G	.	c.2070C>G	p.Phe690Leu	Missense variant	21%
OSU431895	PCGF6	ENSCAF00000044220.2	chr28:15733030G>A	.	c.68C>T	p.Pro230Leu	Missense variant	20%
OSU431895	ENSCAF00000006847	ENSCAF00000011021.4	chr28:1916959C>T	.	c.2984C>T	p.Ser993Phe	Missense variant	28%
OSU431895	PNLIPRP1	ENSCAF00000018834.2	chr28:27169312G>C	.	c.306G>C	p.Glu102Asp	Missense variant	7%
OSU431895	PTPRE	ENSCAF00000021005.3	chr28:36867151G>A	.	c.532G>A	p.Glu178Lys	Missense variant	42%
OSU431895	ENSCAF00000013695	ENSCAF00000021723.3	chr28:40788958G>C	.	c.676G>C	p.Ala228Pro	Missense variant	27%
OSU431895	SGK3	ENSCAF00000011773.3	chr28:46344863G>C	.	c.69G>C	p.Lys23Asn	Missense variant	17%
OSU431895	ZFX4	ENSCAF00000013195.4	chr29:2483205C>T	.	c.473C>T	p.Pro1579Ser	Missense variant	18%
OSU431895	CPNE3	ENSCAF00000014109.2	chr29:32727523C>G	.	c.1580C>G	p.Pro527Arg	Missense variant	9%
OSU431895	EDL3	ENSCAF00000013454.3	chr3:23711511A>G	.	c.952-2A>G	.	Splice acceptor variant	25%
OSU431895	POLK	ENSCAF00000014935.3	chr3:30798334G>C	.	c.1731C>G	p.Phe577Leu	Missense variant	34%
OSU431895	HOMER2	ENSCAF00000020916.3	chr3:54661523C>G	.	c.895G>C	p.Glu299Gln	Missense variant	29%
OSU431895	ARAP2	ENSCAF00000025868.3	chr3:75276709C>G	.	c.2723C>G	p.Ser908Cys	Missense variant	21%
OSU431895	PPIP5K2	ENSCAF00000012054.4	chr3:8082899C>G	.	c.17G>C	p.Arg6Thr	Missense variant	23%
OSU431895	RNF11	ENSCAF00000026314.3	chr30:24024406GAC>G	.	.2786_2787delC	p.Thr928fs	Frameshift variant	21%
OSU431895	EIF2AK4	ENSCAF00000014032.4	chr30:7189333G>C	.	c.1602G>C	p.Leu534Phe	Missense variant	33%
OSU431895	IND80	ENSCAF00000015097.3	chr30:8118915G>C	.	c.3510-6C>G	.	Splice region variant	22%
OSU431895	ENSCAF00000029964	ENSCAF00000012894.3	chr31:11856097G>A	.	c.1301C>T	p.Ser434Phe	Missense variant	22%
OSU431895	PTPN13	ENSCAF00000046703.1	chr31:37278435G>C	.	c.2336G>C	p.Arg779Thr	Missense variant	26%
OSU431895	TRMT10C	ENSCAF00000014995.3	chr32:10280336G>C	.	c.2377G>C	p.Gly793Arg	Missense variant	27%
OSU431895	IRX4	ENSCAF00000048115.1	chr33:7948899TTAGA>T	.	016_1019delGA	p.Arg339fs	Frameshift variant	22%
OSU431895	CCDC127	ENSCAF00000018576.3	chr34:10928929G>C	.	c.714G>C	p.Glu238Asp	Missense variant	24%
OSU431895	PEX5L	ENSCAF00000018246.2	chr34:13199570C>A	.	c.533C>G	p.Ser176Cys	Missense variant	17%
OSU431895	PEX5L	ENSCAF00000018246.2	chr34:13292410C>A	.	c.994G>T	p.Asp332Tyr	Missense variant	22%
OSU431895	SI	ENSCAF00000022936.3	chr34:30322770G>A	.	c.97G>T	p.Glu33*	Stop-gained variant	24%
OSU431895	DLX1	ENSCAF00000020533.3	chr36:16487786G>A	.	c.848G>A	p.Trp216*	Stop-gained variant	15%
OSU431895	HOXD10	ENSCAF00000021329.3	chr36:19926791G>C	.	c.1014G>C	p.Lys338Asn	Missense variant	23%
OSU431895	MEITL21A	ENSCAF00000042739.1	chr37:16001841G>T	.	c.103C>A	p.Gln35Lys	Missense variant	27%
OSU431895	USH2A	ENSCAF00000017072.3	chr37:11478108C>T	.	c.5017G>A	p.Glu1673Lys	Missense variant	14%
OSU431895	LRRTM3	ENSCAF00000018051.3	chr38:23718354G>T	.	c.2562C>A	p.Phe654Leu	Missense variant	18%
OSU431895	AIFM2	ENSCAF00000043912.1	chr4:18322023C>G	.	c.83C>G	p.Ser28Cys	Missense variant	15%
OSU431895	MCU	ENSCAF00000022236.3	chr4:21089398G>A	.	c.968C>T	p.Pro323Leu	Missense variant	46%
OSU431895	LRRIT1	ENSCAF00000023057.4	chr4:23498898G>A	.	c.508G>A	p.Glu170Lys	Missense variant	18%
OSU431895	SYNPO	ENSCAF00000025227.3	chr4:32476147G>A	.	c.560C>T	p.Ala187Val	Missense variant	18%
OSU431895	PPARGC1B	ENSCAF00000028746.2	chr4:56504820G>T	.	c.1297C>A	p.Leu433Met	Missense variant	21%
OSU431895		ENSCAF00000029039.4	chr4:59184211C>G	.	c.2102G>C	p.Gly707Ala	Missense variant	

FIG. 10F

Patient ID	Gene symbol	Transcript accession	Nucleotide (genomic)	rs ID (dbSNP151)	Nucleotide (cDNA)	Amino acid (protein)	Mutation type	% mutant reads
OSU431895	CDH10	ENSCAF00000030188.3	chr4:81100231G>T	.	c.1984G>T	p.Gly682Cys	Missense variant	50%
OSU431895	ACTA1	ENSCAF00000013094.3	chr4:9813995G>A	.	c.802G>A	p.Asp288Asn	Missense variant	55%
OSU431895	TP53	ENSCAF00000026465.3	chr5:32564571C>T	.	c.338G>A	p.Tyr113*	Stop-gained variant	36%
OSU431895	TEK3	ENSCAF00000028445.3	chr5:36884781G>C	.	c.884C>G	p.Ser295*	Stop-gained variant	21%
OSU431895	LRRCT5A	ENSCAF00000028810.3	chr5:39486746G>A	.	c.661G>A	p.Glu221Lys	Missense variant	28%
OSU431895	C1orf168	ENSCAF00000043811.2	chr5:52680879G>T	.	c.4G>T	p.Glu2*	Stop-gained variant	7%
OSU431895	TTC22	ENSCAF00000043914.2	chr5:54379139C>G	.	c.1226C>G	p.Thr409Arg	Missense variant	31%
OSU431895	ARHGAP32	ENSCAF00000016261.3	chr5:5656288C>G	.	c.1238C>G	p.Ser413Cys	Missense variant	32%
OSU431895	MYL6P	ENSCAF00000026205.3	chr6:17721053G>C	.	c.79C>A	p.Gln27Glu	Missense variant	28%
OSU431895	USP31	ENSCAF00000028066.3	chr6:22652611C>A	.	c.677G>A	p.Ser228Tyr	Missense variant	23%
OSU431895	USP31	ENSCAF00000028068.3	chr6:22662881C>G	.	c.1120C>G	p.Leu374Val	Missense variant	4%
OSU431895	DNASE1	ENSCAF00000030587.3	chr6:37599193C>G	.	c.111G>C	p.Lys37Asn	Missense variant	22%
OSU431895	NAAB0	ENSCAF00000030602.3	chr6:37768888C>G	.	c.64G>C	p.Asp23His	Missense variant	12%
OSU431895	CLCA4	ENSCAF00000032245.3	chr6:61563679C>G	.	c.2152G>C	p.Glu718Gln	Missense variant	32%
OSU431895	PROX1	ENSCAF00000019756.3	chr7:12043975G>C	.	c.2214G>C	p.Ter738Tyr	Stop-lost variant	15%
OSU431895	HMCN1	ENSCAF00000021686.3	chr7:19225514T>G	.	c.15040T>G	p.Tyr5014Asp	Missense variant	25%
OSU431895	ADCY10	ENSCAF00000026129.3	chr7:28268707C>G	.	c.1059C>G	p.Phe353Leu	Missense variant	25%
OSU431895	POGK	ENSCAF00000024738.3	chr7:30619392G>C	.	c.2301G>C	p.Lys767Asn	Missense variant	20%
OSU431895	ARHGEF11	ENSCAF00000026129.3	chr7:41096724G>T	.	c.1421G>A	p.Arg474His	Missense variant	27%
OSU431895	ENSCAF00000016616	ENSCAF00000026393.3	chr7:41397468C>A	.	c.981+3C>A	p.Arg1497Ile	Missense variant	14%
OSU431895	DSG3	ENSCAF00000028690.2	chr7:58064476G>C	.	c.565C>G	p.Leu189Val	Splice region variant	27%
OSU431895	OSBPL1A	ENSCAF00000023469.4	chr7:5963617A>G	rs652402061	c.289T>C	p.Cys97Arg	Missense variant	9%
OSU431895	CLUL1	ENSCAF00000022395.3	chr7:64217286G>C	.	c.2611G>C	p.Asp871His	Missense variant	38%
OSU431895	MIS16BP1	ENSCAF00000029136.4	chr7:67472732G>A	.	c.631G>A	p.Glu311Lys	Missense variant	5%
OSU431895	ZBTB1	ENSCAF00000022361.4	chr8:22653637G>A	.	c.1348C>T	p.Ser449Phe	Missense variant	23%
OSU431895	ELMSAN1	ENSCAF00000043877.1	chr8:38950419G>T	.	c.149G>T	p.Arg50Ile	Missense variant	19%
OSU431895	NRXN3	ENSCAF00000026701.4	chr8:46997477G>A	.	c.1016C>T	p.Ser339Phe	Missense variant	24%
OSU431895	SERPINA6	ENSCAF00000043139.1	chr8:51608485C>G	.	c.2084C>G	p.Phe698Leu	Missense variant	22%
OSU431895	SYNE3	ENSCAF00000027978.3	chr8:93335946C>T	.	c.76G>A	p.Asp26Asn	Missense variant	20%
OSU431895	ATP6V0A1	ENSCAF00000028095.3	chr8:64304269C>T	.	c.1278G>A	p.Met426Ile	Missense variant	4%
OSU431895	MYCBPAP	ENSCAF00000023704.4	chr9:20460130C>G	.	c.457G>C	p.Asp153His	Missense variant	20%
OSU431895	COX11	ENSCAF00000027487.2	chr9:26473031G>C	.	c.1902G>C	p.Trp634Cys	Missense variant	17%
OSU431895	MED13	ENSCAF00000028083.3	chr9:30079609C>G	.	c.225G>C	p.Glu75Asp	Missense variant	27%
OSU431895	SEPT9	ENSCAF00000008383.4	chr9:34722633C>G	.	c.3663C>G	p.Ser1288Cys	Missense variant	17%
OSU431895	HEATR6	ENSCAF00000008383.4	chr9:3504856C>G	.	c.1159G>C	p.Glu387Gln	Missense variant	21%
OSU431895	MYO1D	ENSCAF00000028841.3	chr9:37581109C>A	.	c.2851G>T	p.Glu951*	Stop-gained variant	22%
OSU431895	SMG6	ENSCAF00000029185.3	chr9:40171560T>A	.	c.74T>A	p.Phe25Tyr	Missense variant	13%
OSU431895	LRRCT26	ENSCAF00000030579.3	chr9:46402631G>C	.	c.385C>G	p.Leu129Val	Missense variant	23%
OSU431895	NPDC1	ENSCAF00000031014.3	chr9:48491434C>T	.	c.440C>T	p.Ser147Phe	Missense variant	20%
OSU431895	HMCN2	ENSCAF00000031743.4	chr9:48599176G>C	.	c.125G>C	p.Cys42Ser	Missense variant	20%
OSU431895	PBX3	ENSCAF00000032127.3	chr9:53491794G>C	.	c.14144-40C>G	Splice region variant	24%	
OSU431895		ENSCAF00000032127.3	chr9:57200010C>T	.	c.1042G>A	p.Glu348Lys	Missense variant	21%

FIG. 10G

Patient ID	Gene symbol	Transcript accession	Nucleotide (genomic)	rs ID (dbSNP151)	Nucleotide (cDNA)	Amino acid (protein)	Mutation type	% mutant reads
OSU431895	FAM120C	ENSCAF100000047380.2	chrX:45984653T>A	.	c.2524-2A>T	.	Splice acceptor variant	56%
OSU431895	GNL3L	ENSCAF100000028083.3	chrX:46294904A>G	.	c.1736A>G	p.Asn579Ser	Missense variant	51%
OSU431895	ENSCAFG00000017103	ENSCAF100000043925.2	chrX:55730703G>C	.	c.4635+1G>C	.	Splice donor variant	48%

FIG. 10H



Supplementary Table 5. Somatic copy number variants identified by exome sequencing in primary canine lung cancers.

Patent ID	Region	Mutation	type	Log <sub>2</sub> ratio	Number of		Gene symbols
					genes	genes	
CCB010387	chr6:16860700-16899200	Deletion	-1.6779	2	2	ENSCAF-G000000143121TGAX	
CCB010387	chr11:41182150-41570250	Deletion	-1.8457	5	5	ENSCAF-G00000001671CDKN2A,CDKN2B,CDKN2E,AS,DMRTA1	
CCB050227	chr11:01566850-101590100	Deletion	-1.0814	1	1	ZNF583	
CCB050227	chr11:114616500-114618000	Deletion	-1.0175	1	1	GGN	
CCB050227	chr11:15940650-115971150	Deletion	-1.1607	1	1	ZNF568	
CCB050227	chr11:262250-1351300	Deletion	-1.0325	1	1	ATP9B	
CCB050227	chr11:3853250-13868550	Deletion	-1.0799	1	1	VPS4B	
CCB050227	chr11:14587900-14652700	Deletion	-1.1356	1	1	KIAA1468	
CCB050227	chr11:24470250-24495400	Deletion	-1.052	1	1	ENSCAF-G000000000172	
CCB050227	chr11:88139500-88149900	Deletion	-1.1038	1	1	TJP2	
CCB050227	chr5:16623600-16656850	Deletion	-1.0154	1	1	SIK3	
CCB050227	chr5:50042500-50060250	Deletion	-1.1865	1	1	HOOK1	
CCB050227	chr5:80028150-80046050	Deletion	-1.1114	1	1	NFAT5	
CCB050227	chr5:80637850-80668100	Deletion	-1.1047	1	1	TANGO6	
CCB050227	chr5:82027000-82068250	Deletion	-1.0996	1	1	LPRC36	
CCB050227	chr11:13400700-13453950	Deletion	-1.1525	1	1	CSNK1G3	
CCB050227	chr11:34502800-34603350	Deletion	-1.0815	1	1	NFIB	
CCB050227	chr11:53633600-53683150	Deletion	-1.0652	1	1	ZCCHC7	
CCB050227	chr20:16807200-16813950	Deletion	-1.0215	1	1	CHL1	
CCB050227	chr20:5497850-5521750	Deletion	-1.0239	1	1	TMCC1	
CCB050227	chr20:6053750-6071150	Deletion	-1.0578	1	1	TSEN2	
CCB050227	chr25:14121350-14153400	Deletion	-1.1147	1	1	NUPL1	
CCB050227	chr25:23987000-24141250	Deletion	-1.1921	1	1	SCRG1	
CCB050227	chr25:5377350-5415550	Deletion	-1.2073	1	1	NBEA	
CCB050227	chr26:16636650-16760250	Deletion	-1.0642	1	1	SBPL3	
CCB050227	chr26:23276850-23287100	Deletion	-1.0595	1	1	HORMAD2	
CCB050227	chr28:12949400-12961950	Deletion	-1.1368	1	1	ERLIN1	
CCB050227	chr28:16317950-16344200	Deletion	-1.1552	1	1	SLK	
CCB050227	chr28:16528300-16554600	Deletion	-1.0746	1	1	WDR96	
CCB050227	chr28:25605300-25628800	Deletion	-1.0107	1	1	FAM160B1	
CCB050227	chr28:6544760-6352100	Deletion	-1.1796	1	1	TNKS2	
CCB050227	chr28:9838900-9970600	Deletion	-1.1972	1	1	TM5SF3	
CCB050227	chr11:104802900-104871300	Deletion	-1.0366	2	2	ZNF677,ENSCAF-G0000000030568	
CCB050227	chr11:15014800-115040300	Deletion	-1.0106	2	2	WDR67,ENSCAF-G000000005986	
CCB050227	chr11:17852000-117918100	Deletion	-1.0193	2	2	WTIP,UBA2	
CCB050227	chr11:18094500-118424400	Deletion	-1.0721	2	2	LSMT4A,KC,TD15	
CCB050227	chr11:57668100-57755450	Deletion	-1.243	2	2	ROSL,DCBLD1	
CCB050227	chr11:60692600-60847950	Deletion	-1.117	2	2	TBC1D32L4	
CCB050227	chr11:93409500-93472450	Deletion	-1.1313	2	2	JAK2,INSL6	
CCB050227	chr5:12768050-12681800	Deletion	-1.0626	2	2	SC5D,TEC1A	
CCB050227	chr5:13533650-13675900	Deletion	-1.0241	2	2	ARRHGFT2,TNEM1,36	
CCB050227	chr5:22311300-22332900	Deletion	-1.0314	2	2	ARRHGAP20,ENSCAF-G000000014234	

FIG. 11A

Patient ID	Region	Mutation type	Log2 ratio	Number of genes	Gene symbols
CC8050227	chr5:22572050-22826450	Deletion	-1.177	2	RDX,ENSCAFG000000030803
CC8050227	chr5:38611050-38791800	Deletion	-1.0144	2	FIGL1,NCOR1
CC8050227	chr5:75323800-75486400	Deletion	-1.0383	2	SCAR1,P97
CC8050227	chr5:76496150-76518750	Deletion	-1.0017	2	SF3B3,SNORD111
CC8050227	chr8:45222200-45245050	Amplification	0.5121	2	PAX9,SLC25A21
CC8050227	chr8:24675500-25005850	Amplification	0.667	2	ENSCAFG000000030925,ENSCAFG000000011459
CC8050227	chr8:30604100-30734800	Amplification	0.555	2	SAMD4A,GSCH1
CC8050227	chr8:43099450-43211550	Amplification	0.6235	2	GALNT16,ERH
CC8050227	chr8:50628500-50964200	Amplification	0.7957	2	ADCK1,ENSCAFG000000017256
CC8050227	chr8:59710850-59726350	Amplification	0.5668	2	SPATA7,PIPN21
CC8050227	chr9:40651600-40727850	Amplification	0.5736	2	RHBDL3,RHOT1
CC8050227	chr9:49620900-49635200	Amplification	0.8816	2	ENSCAFG000000019749,LCN9
CC8050227	chr11:37273900-3759000	Deletion	-1.0549	2	CATLN,SH3GL2
CC8050227	chr11:45666650-45998200	Deletion	-1.1213	2	C9orf72,U6
CC8050227	chr11:50641500-50681000	Deletion	-1.1092	2	UBE2R2,UBAP2
CC8050227	chr11:51683900-51838300	Deletion	-1.0625	2	FAM214B,UNC13B
CC8050227	chr11:59243050-59630000	Deletion	-1.1042	2	CYLC2,ENSCAFG000000030806
CC8050227	chr11:66259850-66355900	Deletion	-1.0879	2	DNAJ225,C9orf84
CC8050227	chr20:19122650-19193700	Deletion	-1.1216	2	PPP4R2,GXYLT2
CC8050227	chr20:8783600-9056800	Deletion	-1.0515	2	THUMPB3,SRGAP3
CC8050227	chr20:9163300-9359800	Deletion	-1.0094	2	R4D18,OXTR
CC8050227	chr25:31211750-31478850	Deletion	-1.2779	2	PPP2R2A,EBF2
CC8050227	chr25:34763150-34859650	Deletion	-1.1124	2	PPP3CC,SLC39A14
CC8050227	chr26:14609350-14716700	Deletion	-1.073	2	TAOK3,SUDS3
CC8050227	chr26:9121150-9225900	Deletion	-1.2128	2	ATXN2,BRAP
CC8050227	chr28:2385200-2443800	Deletion	-1.0395	2	ENSCAFG000000025080,ZNF22
CC8050227	chr28:29967400-30011800	Deletion	-1.125	2	C10ORF119,SEC23IP
CC8050227	chr1:100188600-100251600	Deletion	-1.0589	3	ENSCAFG000000029340,ENSCAFG00000002408,ENSCAFG000000028494
CC8050227	chr1:108762600-108875300	Deletion	-1.0459	3	ZC3H4,SAE1,U6
CC8050227	chr1:31161550-31363550	Deletion	-1.1872	3	ENSCAFG000000000279,ABRACL,HECA
CC8050227	chr8:39141750-39307050	Amplification	0.6613	3	PLEKHG3,SPTB,CHURC1
CC8050227	chr8:50039400-50117050	Amplification	0.6604	3	TMEM63C,NG2,POMT2
CC8050227	chr8:50142700-50182850	Amplification	0.5886	3	GSTZ1,TMED8,SAMD15
CC8050227	chr9:26660200-26737000	Amplification	0.625	3	ENSCAFG000000028964,WFKIKN2,TOB1
CC8050227	chr11:2677200-26905000	Deletion	-1.1166	3	MATR3,5,8S,IRNA,MLANA
CC8050227	chr11:52896650-53068800	Deletion	-1.0224	3	GNE,RNF38,MELK
CC8050227	chr20:12487050-12643600	Deletion	-1.1602	3	ARL8B,U6,BHLHE40
CC8050227	chr20:25130300-25515200	Deletion	-1.2147	3	SLC25A26,SNORA64,ENSCAFG000000030398
CC8050227	chr20:48455100-48457600	Deletion	-1.0294	3	C19orf57,PALM3,IL27RA
CC8050227	chr25:11442900-11617250	Deletion	-1.0477	3	PAN3,U2,FLJ3
CC8050227	chr25:26545700-26716350	Deletion	-1.0077	3	ENSCAFG000000009016,MTMR9,ENSCAFG000000030648
CC8050227	chr28:13609300-13667850	Deletion	-1.0149	3	FAM176A,U2,SEMA4G

FIG. 11B

Patient ID	Region	Mutation type	Log2 ratio	Number of genes	Gene symbols
CCB050227	chr28:28978900-27145400	Deletion	-1.068	3	CCDC172,SS,IRNA,PNLIP
CCB050227	chr28:8624500-8738150	Deletion	-1.1155	3	TBC1D12,HELLS,CYP2C21
CCB050227	chr11:06859600-106876300	Deletion	-1.0013	4	PRMT1,U4,BC1L2L12,IRF3
CCB050227	chr11:48948500-49011800	Deletion	-1.0667	4	SOD2,ENSCAFG00000023207,U6atac,ACAT2
CCB050227	chr5:39243200-39386800	Deletion	-1.0097	4	ENSCAFG000000031764,SS,IRNA,ZNF624,ZNF267
CCB050227	chr9:35169500-35405000	Deletion	-1.0411	4	PODN,SCP2,HES4,ZYG11A
CCB050227	chr11:68765800-68863100	Deletion	-1.1198	4	TBX4,ENSCAFG0000001742,TBX2,BCAS3
CCB050227	chr11:70052500-70308350	Deletion	-1.0307	4	PTBP3,ENSCAFG0000002333,ENSCAFG00000003019,HSD12
CCB050227	chr8:48968700-49674550	Amplification	0.7281	5	ZNF782,ZNF510,AAED1,ENSCAFG000000030594,CCDC14B
CCB050227	chr9:43672400-43745900	Amplification	0.5282	5	ESRRB,YSK,ENSCAFG00000004150,YASH1,ANGEL1
CCB050227	chr9:41103200-41486150	Amplification	0.5367	6	COPRS,U5,cfamir-385-2,cfamir-193a,RAB11FIP4,NF1
CCB050227	chr9:60948750-61040500	Amplification	0.5768	6	LHX6,MORNS,NDUFA8,TLL11,DAB2IP,GGTA1
CCB050227	chr26:6792950-7092600	Deletion	-1.0275	6	KNTCT,RSRC2,ZCCHC8,SNORA9,CLIP1,ENSCAFG00000007919
CCB050227	chr9:46063700-46384700	Amplification	0.5435	7	RTNMR1,DPH1,DPH1,cfamir-132,cfamir-212,HIC1,SMG6
CCB050227	chr11:45083850-45278650	Deletion	-1.0307	7	CAATP,PLAA,IFT4,LRRCT9,cfamir-872,U6,TEK
CCB050227	chr9:3074200-4005250	Amplification	0.565	9	ARNA16,MGA15B,MFSD11
CCB050227	chr9:54720850-54897300	Amplification	0.5341	10	CRAT,PHYHD1,LRRRC8A,CCBL1,C8orf114,ENDOG,TBC1D13,ZERT,ZDHHC12,PKN3
CCB050227	chr9:58444650-58930100	Amplification	0.5732	10	NR6A1,U5,SF1,GPR144,PSMB7,NEK6,ENSCAFG000000031433,LHX2,DEND1A,ENSCAFG00000003064
CCB050227	chr9:42827400-43374900	Amplification	0.5401	13	TLCD1,NEK8,TRAF4,FAM22B,cfamir-451,cfamir-451,cfamir-451,FOCAD,cfamir-497,U6,SNORA30,PTPLAD2,IFNB1,ENSCAFG000000023674,IFNE,cfamir-536,PTGES,PRRX2,Y,RNA,ASB8,NTMT1,ENSCAFG00000019987,IERSL,PPP2R4,C,CRAT,DOLPP1,FAM7
CCB050227	chr11:40300200-41570200	Deletion	-2.6435	14	FNBP1,U6,USP20,ENSCAFG00000019879,TORTA,ENSCAFG000000032504,TORTB,ENSCAFG00000000030
CCB050227	chr9:53936050-54686900	Amplification	0.5133	21	3B,SH3GLB2,ENSCAFG000000020013
CCB050227	chr8:70013700-71225650	Amplification	0.535	24	DYNC1H1,ENSCAFG000000031259,HSP90AA1,WDR20,MOK,ZNF839,CINP,TECPR2,ANKRD9,RPL36,R
CCB050227	chr9:51995100-5370350	Amplification	0.5779	27	2,TNFAIP2,ENSCAFG00000018194,EJF5,SNORA28,MARK3,U2,U4
CCB050227	chr9:51995100-5370350	Amplification	0.5779	27	NTNG2,MED27,SNOR263,RAPGEF1,PRRC2B,UCK1,POMT1,SNORD62,SNORD62,PPAPDC3,FAM78A,NUP214,U6AIF,ENSCAFG000000028859,LAMC3,FIBCD1,QRFP,ABL1,EXOSC2,PRDM12,FUBP3,LAM
CCB050227	chr9:25772300-26604200	Amplification	0.5339	29	TOR5,ASS1,HMCN2,NCS1,GPR107
CCB050227	chr9:40229500-4879850	Amplification	0.5243	42	SLC35B1,FAM117A,KAT7,TAC4,DLX4,DLX3,ENSCAFG000000028938,ITGA3,SAMD14,PKK2,PPP1R9B,S
CCB050227	chr9:40229500-4879850	Amplification	0.5243	42	GCA,ENSCAFG00000017016,COL1A1,snoU2,19,snoU2
CCB050227	chr9:40229500-4879850	Amplification	0.5243	42	30,TMEM82,ENSCAFG000000017025,XYL12,MRPL27,EME1,LRRRC59,ACSF2,CHAD,MYCBPAP,EPN3,CA
CCB050227	chr9:40229500-4879850	Amplification	0.5243	42	CNA1G,ABCC3,ANKRD40
CCB050227	chr9:40229500-4879850	Amplification	0.5243	42	ENSCAFG0000000095147,METTL23,INJD6,ST6GALNAC1,ST6GALNAC2,snoR36,snoR38,ENSCAFG0000
CCB050227	chr9:40229500-4879850	Amplification	0.5243	42	0030147,PRCD,CYGB,RHEDF2,AAANAT,UBE2O,SPHK1,ENSCAFG000000028615,ENSCAFG00000003156
CCB050227	chr9:40229500-4879850	Amplification	0.5243	42	6,PRPSAP1,RNaseP_nuc,ORIC2,RNF157,FOXJ1,EXOC7,ZACN,GALR2,SRP68,ENSCAFG0000000502
CCB050227	chr9:40229500-4879850	Amplification	0.5243	42	1,CDK3,TEM1,ACOX1,FBF1,MRPL38,TRIM65,TRIM47,WBP2,UNC13D,UNK,U4,H3F3B,GALK1,ENSCAF
CCB050227	chr9:40229500-4879850	Amplification	0.5243	42	G00000028346,ENSCAFG00000004805,SAP30BP

FIG. 11C

Patient ID	Region	Mutation type	Log2 ratio	Number of genes	Gene symbols
CCB050227	chr9:48635400-51859600	Amplification	0.6491	55	LCN9, GLT1D1, ENSCAF00000019754, ENSCAF00000023097, ENSCAF00000019755, LCN1, ABO, SU, RF6, MED22, ENSCAF00000017680, SNORD34, SNORD36, SNORD38, SNORD39, SURF1, SURF2, SURF4, C8orf196, RX04, ADAMT1S3, CACFD1, SLC2A6, TMEIM8C, ADAMT1S2, ENSCAF000000031627, DBH, SAR, DH, VAV2, U6, BRD3, U6, WDR5, RXRALPHA, ENSCAF00000026559, COL5A1, ENSCAF00000030630, OL, FM1, PPP1R28, ENSCAF00000032138, MRPS2, ENSCAF000000031968, ENSCAF000000019863, GBGT, 1, RALGDS, CEL, GTF3C5, GF1B, MDH2, TSC1, C9ORF9, AK3, GTF3C4, BARHL1, C9orf171, TTF1, ENSCAF000000018285, XRCC3, ZFY, YE21, PPP1R13B, U6, RD3L, TDRD9, ASPG, cfa-mir-203, cfa-mir-203, KIF26A, ENSCAF0000000303862, U1, ENSCAF00000029088, C14orf180, TMEIM179, ENSCAF00000029862, ENSCAF000000031878, INF2, ENSCAF00000028959, ADSSL1, AKT1, ZBTB42, CEP170B, PLD4, NSCAF000000030682, ENSCAF000000030862, C14orf79, CDC44, GPR132, JAG2, NUDT14, BRF1, BTBD6, PACS2, TEX22, MTA1, CRIP2, ENSCAF000000018440, ENSCAF000000031417, C14orf80, TMEIM121, ENSC, AFG000000032358, ENSCAF000000028687, IGHE, ENSCAF000000030258, RPS24, ENSCAF000000030989, 3, ENSCAF000000023484, ENSCAF000000023480, ENSCAF00000018468, ENSCAF000000031078, EN, SCAF000000028509, ENSCAF00000030284, ENSCAF000000029986, ENSCAF000000030894, ENSCA, F, G0000000030001, ENSCAF000000030900, ENSCAF000000024111, ENSCAF00000029299, ENSCAF0000018488
CCB050227	chr8:71436200-74292900	Amplification	0.6229	61	SAP30BP, RECQL5, MYO15B, LILGL2, TSEN64, ENSCAF000000030685, CASKN2, KIAA0195, GRR2, SLC25, A19, ENSCAF00000004756, MRPS7, GGA3, NUP85, SUMO2, HNI, NT5C, ARMC7, SLC16A5, ENSCAF00000004715, ENSCAF000000032582, KCTD2, ENSCAF00000004703, ICT1, CDR2L, HID1, OTOP3, USH1G, F, ADS8, FXR, GRIN2C, TMEIM104, NAT9, SLC9A3R1, RAB37, ENSCAF00000004595, CD300E, ENSCAF000000028609, ENSCAF00000024944, ENSCAF000000024942, ENSCAF000000028912, ENSCAF000000024792, CD300LB, ENSCAF000000032631, GPRC5C, GPR142, BTBD17, ENSCAF000000032340, KIF19, D, NA12, TTYH2, SDK2, CDC42EP4, C17orf80, FAM104A, CCG1, SSTR2, SLC39A1, U6, ENSCAF00000003158, 3, ENSCAF00000004401, SOX9, ENSCAF000000031779, ENSCAF00000015160, EFCAB13, GP1HA, MYL, 4, CDC27
CCB050227	chr9:4907300-9309800	Amplification	0.525	68	HOMER, PPP1R3E, BCL2L2, PABPN1, SLC22A17, EFS, IL25, CMTM5, cfa-mir-208a, MYH7, cfa-mir-208b, NGDN, ZFHX2, APIG2, THPA, DHRS2, ENSCAF00000025298, DHRS4, LRRC4, LRRC18B, CPNE6, NRL, PCK, 2, DCAF11, FITM1, PSME1, EMC9, PSME2, ENSCAF00000011993, IRF9, REC8, IPO4, ENSCAF0000000120, 71, TSSK4, NEDD8, GMPR2, TNF2, TGM1, RABGGTA, DHRS1, C14ORF21, CIDEB, LTB4R, ADCY4, RIPK3, U6, TXBP9, ENSCAF00000013905, RNaseP, nuc, U6, NOVA1, ENSCAF000000025404, CTSG, GZMB, U6, S, 18, U6, ENSCAF000000012522, ENSCAF00000012527, FOXG1, ENSCAF00000008062, ENSCAF000000029701, U6, ENSCAF000000028819, U6, PRKD1, U6, ENSCAF00000012573, G2E3
CCB050227	chr8:3546450-9927850	Amplification	0.5262	77	CSNK1D, SLC16A3, RFXNG, SNORA62, CCDC57, FASN, DUS1L, GPS1, DCXR, RAC3, LRRC45, STRA13, ASP5, CRI1, TSPAN10, NOTUM, MYADM12, PYCR1, MAFG, SIRT7, PCYT2, NPB, ANAPC11, ALYREF, ARHGDB1, P4H, B, PPP1R27, FAM195B, GCGR, ENSCAF00000005812, HGS, ARL16, CCDC137, OXLD1, PDE5G, NPLOC4, ENSCAF000000030278, C17orf70, FSCN2, ACTG1, ENSCAF000000032216, ENSCAF00000005732, SLC, 38A10, C17orf89, ENTHD2, AZI1, AATK, cfa-mir-338, BAIAP2, CHMP6, RPTOR, U6, NPTX1, RNF213, ENDOV, SLC28A11, SGSH, CARD14, EIF4A3, ENSCAF00000005596, GAA, CCDC40, TBC1D16, CBX4, CBX8, CBX2, ENPP7, Y, RNA, RBFOX3, ENGASE, C10TNF1, CANT1, LGALS3BP, ENSCAF000000030984, ENSCAF00000005532, TIMP2, USP38, CYTH1, U6, DNAH17, PGS1, SOCS3, ENSCAF00000014766, TMEIM235, BIRC5, AFMID, TK1, SYNGR2, C17orf89, TMC8, TMC6, TN, RC6C
CCB050227	chr9:96600-3044550	Amplification	0.6024	91	

FIG. 11D



Patient ID	Region	Mutation type	Log2 ratio	Number of genes	Gene symbols
CCB050354	chr17:2238650-2307200	Amplification	0.5278	1	DDC2C
CCB050354	chr23:8581930-8604600	Amplification	0.6679	1	SCN11A
CCB050354	chr23:13703900-13719600	Amplification	0.6981	1	MYH15
CCB050354	chr4:10980800-11387500	Amplification	0.866	2	BICCT1,ENSCAFG00000012382
CCB050354	chr33:31341000-31360250	Amplification	0.573	2	LRRC15,CPN2
CCB050354	chr4:59459200-59580900	Amplification	0.513	4	ENSCAFG00000018286, cfa-mir-145, cfa-mir-143, IL17B
CCB050354	chr2:1320800-1772700	Amplification	0.5012	5	FZD8,ENSCAFG00000023176,CCNY,7SK,CREM
CCB050354	chr2:55236650-55920250	Amplification	0.5192	8	MAP1B,MRPS27,PT,CD2,SS,IRNA,ZNF366,ENSCAFG00000031745,TNPO1,FCHO2
CCB050354	chr4:74862650-75922050	Amplification	0.5435	8	GOLPH3
CCB050354	chr4:71943650-74862350	Amplification	0.7323	28	GLAST,ENSCAFG00000029561,RANBP3L,ENSCAFG0000001830,SKP2,LMBRD2,ENSCAFG0000000023 144,ENSCAFG00000032039,CAPSL,IL7R,SPEF2,U6,PRU,AGXT2,DNAJC21,BRIX1,RAD1,TTCC23L,U6, RAH14,U6,ENSCAFG00000018825,AMACR,SLC45A2,PKFP3,ADAMTS12,TARS,NPR3
CCB050354	chr4:75351000-88273150	Amplification	0.7176	29	PDZD2,C5orf22,ENSCAFG00000031829,ENSCAFG00000018939,CDH6,ENSCAFG00000018956,U6,CD H9,ENSCAFG00000018960,7SK,CDH10,ENSCAFG00000017424,ENSCAFG00000019017,ENSCAFG000 00019023,CDH12,ENSCAFG000000031957,CDH16,SNORA62,U2,7SK,RNF167,BASP1,FAM134B,MYO10 ZNF622,MARCH11,FBXL7,ENSCAFG00000019108,ANKH
CCB050354	chr4:69500-4248700	Amplification	0.6936	35	IFT2,IFT3,U4,IFT1,IFT5,ZNF246,ZNF25,ENSCAFG00000028519,ENSCAFG00000029103,ENSCAFG0 000024143,U6,ZNF37A,CHRM3,ENSCAFG00000009885,ENSCAFG00000008991,ENSCAFG00000000999 98,ZP4,RYR2,7SK,ENSCAFG00000008063,SNORA25,U6,SNORA2,ENSCAFG00000010041,MTR,U6,AC TN2,HEATR1,LGALS8,EDARADD,ERO1LB,GPR137B,ENSCAFG00000030984,NID1,LYST
CCB050354	chr23:4141650-8581200	Amplification	0.5057	40	PDCD6IP,ENSCAFG00000030719,SS,IRNA,U6,ENSCAFG00000004734,U6,U4,ENSCAFG00000010012, ARPP21,cfa-mir-128
CCB050354	chr4:57768650-59458950	Amplification	0.6725	41	2,ENSCAFG000000004758,ENSCAFG00000028672,STAC,ENSCAFG00000028737,DCLK3,TRANK1,EPH 2AIP1,MLH1,LRRFIP2,ENSCAFG00000029996,GOLGA4,ITGA9,cfa-mir-26a- 1,VILL,PLCD1,DLEC1,ACAA1,MYD88,OXS1,ENSCAFG00000031028,ENSCAFG000000032364,SLC22A 13,SLC22A14,XYLB,ACVR2B,EXOC,PP2S,SCN5A,SCN10A,SCN11A
CCB050354	chr4:11446750-19604000	Amplification	0.6615	45	FAT2,SLC36A1,SLC26A2,SLC36A3,GM2A,ENSCAFG00000028627,CCDC69,U6,ANXA8,TNIP1,GPX3,EN SCAFG00000017961,ENSCAFG00000029257,ZNF390,U6,SMIM3,7SK,DC1N4,RBM22,MYO23,SYNPO,N DST1,RP514,CD74,TCOF1,LARS1,CAMK2A,SLC6A7,CDX1,PDGFRB,CSF1R,HMGXB3,ENSCAFG000000 24412,ENSCAFG00000013277,ENSCAFG00000006036,DNAJC12,ENSCAFG00000028988,HNRNPA1L2 SIRT1,ENSCAFG00000013319,HERC4,U6,SS,IRNA,MYPN,ATOH7,PBLD,HNRNPH3,RUFY2 MYH15,KIAA1524,DZIP3,7SK,TRA11,GUCA1C,MORC1,ENSCAFG00000010327,ENSCAFG0000001033 1,ENSCAFG00000010335,PVRL3,CD96,ZBED2,PLCXD2,PHLDB2,ABHD10,TAGLN3,TMPRSS7,C3orf52, GCSAM1,SLC9C1,ENSCAFG00000032420,ENSCAFG00000029117,CD200,ENSCAFG00000010477,BTL A,ENSCAFG00000010493,SLC35A5,CCDC80,ENSCAFG00000010546,ENSCAFG00000025131,GTPBP8 C3orf17,ENSCAFG00000028163,BOC,WDR52,SPICE1,SIDT1,KIAA2018,NAAS50,ATP6V1A,GRAMD1C,S NORD16,ENSCAFG0000003955,ZDHHC23,KIAA1407

FIG. 11F

Patient ID	Region	Mutation type	Log2 ratio	Number of genes	Gene symbols
CCB050354	chr4:4275550-10980450	Amplification	0.6742	66	LYST, ENSCAF00000031911, GNG4, B3GALNT2, TBCE, GGF1, ARID4B, RBM34, TOMM20, SNORA14, U6 ENSCAF00000032166, IRF2BP2, TARBP1, COA6, SLC35F3, 7SK, KCHN1, ENSCAF00000001566, PCNX LZ, NTPCR, 5S_rRNA, ENSCAF00000011616, SIPA1L2, DISC1, SNORA25, ENSCAF00000030882, EGLN 1, SNORD35, SPRTN, EXOC8, GNPAT, C1orf131, TRIM67, FAM89A, ARV1, TTC13, CAPN9, C1orf198, AGT, cfa- miR-1841, cfa-mir- 1841, U6, PCBD5, GALNT2, ENSCAF00000024420, URB2, TAF5L, ABCB10, NUP133, ACTA1, CCSAP, RAB4 A, U6, RHOU, ENSCAF00000012252, U6, 5S_rRNA, 5S_rRNA, 5S_rRNA, 5S_rRNA, BICC1, 5S_rRNA, E NSCAF00000027921, ENSCAF00000032217
CCB050354	chr4:59561200-71867800	Amplification	0.665	99	IL17B, PCYOX1L, GRPEL2, AFAP1L1, ABI, IM3, U6, SH3TC2, ADRB2, HTR4, FBXC38, SPINK9, SPINK7, GZMK, ESM1, ENSCAF00000008488, ENSCAF00000018385, ENSCAF00000031454, SNX18, HSPB3, ENSCA FG0000002726, LITAF, ARL15, FST, ENSCAF00000018410, ENSCAF00000028642, ENSCAF00000001 8414, ENSCAF00000031599, MOCS2, ITGA2, ENSCAF00000018434, ITGA1, U2, U6, ISL1, U6, U6, PARP8, U6, EMB, HCN1, U6, ENSCAF00000018512, MRPS30, FGF10, SNORA54, U6, NNT, SNORA33, PAIP1, ENSC AF00000031903, C5orf34, 5S_rRNA, C5orf28, CCL28, ENSCAF00000018572, ENSCAF00000030435, NI M1K, ZNF131, SEPP1, CCDC152, GHR, ENSCAF00000023056, FBXC4, C5orf51, LEEF1A1, OXCT1, PLCXD3, C6, MROH2B, C7, CARD6, SNORD72, PRKAA1, TTC33, PTGER4, ENSCAF0000001877, DAB2, C9, FYB, RI CTOR, OSMR, ENSCAF00000018652, LIFR, U2, EGFLAM, ENSCAF00000018671, U6, GDNF, WDR70, EN SCAF00000018679, SNORA67, SNORD22, NUP155, U6, SNORA30, 7SK, U6, C5orf42, NIPBL

FIG. 11G

Patient ID	Region	Mutation type	Log2 ratio	Number of genes	Gene symbols
CCB050354	chr4:19724800-57765800	Amplification	0.6697	336	SLC23A16, E11, U6, SS, RNA, UCAR1, U6, ST, UXT1, DD, X3, DDX21, KNA1Z179, U4, SK, G, V, PS, Z8, A, S, U, P, V, Z, L, 1, HKDC1, HK1, TACR2, TSPAN15, NEUROG3, C10orf95, COL13A1, SS, RNA, HZAFY2, AIFM2, TY, SND1, PPA1, ENSCAF00000014038, LRR020, EIF4EBP2, NODAL, PALD1, PRF1, ENSCAF00000014078, ADAMTS14, TBATA, SGP11, PCBD1, UNC5B, SLC29A3, ENSCAF00000014229, U2, C10orf105, C10orf64, PSAP, U6, C, HST3, SPOCK2, ASCC1, ANAPC16, DDI4, DNAJB12, MICU1, U6, ENSCAF00000014500, MUCJ, OIT3, PLA2, G12B, U6, ENSCAF00000014550, P4HA1, NUDT13, ECD, FAMI149B1, DNAJC9, ENSCAF00000014586, TT, C18, ANXA7, U6, MSS51, PPP3CB, USP54, MYO21, SYNPO2L, SEC24C, FUT11, CHCHD1, ZSWIM8, ENSCAF00000015059, CAMK2C, PLAU, ENSCAF00000015053, VCL, AP3M1, ADK, U6, SNORD2, stnd, U2-30, U6, KAT16B, ENSCAF000000152859, ENSCAF00000013198, SAMD8, VDAC2, COMTD1, ZNF503, C10orf11, U6, ENSCAF000000130490, KCNMA1, U6, DLG5, POLR3A, RPS24, U6, U6, ENSCAF00000013222, ZMIZ1, 1, PPIF, ZCCHC24, ANXA11, TIME254, 7SK, ENSCAF00000013232, SFTPD, ENSCAF00000015754, MAT1A, DYDC1, DYDC2, FAM213A, TSPAN14, SH2D4B, SS, RNA, DNAJB6, NRG3, ENSCAF00000015886, 7SK, GHITM, CDHRT1, LRIT2, LRIT1, ENSCAF00000015927, RGR, ENSCAF000000132581, CCSER2, U6, GRID1, ENSCAF000000131941, cfa-mir-
OSU431895	chr13:10017000-10023000	Amplification	0.5342	1	PKHD1L1
OSU431895	chr7:12365100-12371250	Amplification	0.5386	1	PTPNT4
OSU431895	chr13:58435300-58440350	Amplification	0.5417	1	IMPRSS11A
OSU431895	chr16:6344700-6351450	Amplification	0.5454	1	CLON1
OSU431895	chr34:11295750-11300350	Amplification	0.5474	1	ERT
OSU431895	chr6:27340800-27357600	Amplification	0.5493	1	IRI18
OSU431895	chr10:45370600-45374900	Amplification	0.5575	1	HAO
OSU431895	chr15:8168500-8183050	Amplification	0.5726	1	CSMD2
OSU431895	chr37:14353200-14361200	Amplification	0.5807	1	NRP2
OSU431895	chr36:10308100-10318750	Amplification	0.7701	1	SCN3A
OSU431895	chr13:37487200-37489050	Amplification	0.9482	1	PLEC
OSU431895	chr22:48571700-48587350	Amplification	0.5304	2	FARP1, STK24
OSU431895	chr16:16489650-16522550	Amplification	0.537	2	ACTR3B, U6
OSU431895	chr7:6101100-6162800	Amplification	0.548	2	FCAMR, C1orf116
OSU431895	chr10:26004900-26034450	Amplification	0.5519	2	NPTXR, DNAL4
OSU431895	chr22:60977950-60981700	Amplification	0.5581	2	TIME255B, GAS6

FIG. 11H



Patient ID	Region	Mutation type	Log2 ratio	Number of genes	Gene symbols
OSU431895	chr9:28459350-28469900	Amplification	0.5604	2	MYCBPAP, EPN3
OSU431895	chr34:18785700-18840750	Amplification	0.5732	2	ETV5, DGKG
OSU431895	chr7:43173400-43180800	Amplification	0.5938	2	SLC39A1, CRTC2
OSU431895	chr10:38061150-38082800	Amplification	0.6231	2	FHL2, C2orf49
OSU431895	chr4:62227650-62303450	Amplification	0.5052	3	ITGA2, ENSCAF00000018434, ITGA1
OSU431895	chr7:57557250-57585800	Amplification	0.5268	3	ENSCAF000000031963, U6, RNAF125
OSU431895	chr8:43338250-43458900	Amplification	0.5862	3	ENSCAF000000016579, U6, KIAA0247
OSU431895	chr8:32475550-32498600	Amplification	0.8189	3	LRIT1, ENSCAF00000015827, RGR
OSU431895	chr7:7049100-8257550	Amplification	0.5814	8	PLXNA2, ENSCAF000000026765, ENSCAF00000010678, U6, ENSCAF0000000000
OSU431895	chr36:10329750-11130100	Amplification	0.6732	8	11883, cfa-mir-205, CAMK1G
OSU431895	chr26:356689700-36917000	Deletion	-1.3683	29	SCN3A, SCN2A, U6, CSRNIP3, GALTN3, U6, TTC21B, SCNTA, DRK1, PRKGT, C, STP2, ENSCAF000000023426, ATCF, ENSCAF000000015600, U6, SCMS178K, MINIP1, PAPS2, A, TAD1, ENSCAF000000028370, ENSCAF000000031669, PTEN, RNLS, ENSCAF000000032091, LIP, LIPF, LIPK, LIPM, ANKRD22, ENSCAF000000029090, ENSCAF000000030844, STAMBPL1, ACTC, FAS, CH25H, LIPA, SCNTA, SCN8A, SCNTA, ENSCAF00000011673, XIRP2, ENSCAF00000011707, S3GAL1, STR39, CERS8, NOSTRIN, SPC25, G6PC2, ABCB1, DHR59, ENSCAF000000031746, LRP2, ENSCAF000000012276, KHL41, U6, FAS, TKD1, PPI, G, CDC173, PHOSPHO2, KHL23, ENSCAF000000029231, SSB, METTL5, UBR3, MYO3B, ENSCAF000000012501, SP, 5, ERICH2, GAD1, ENSCAF000000032252, U6, GORASP2, TLK1
OSU431895	chr36:11157950-15533500	Amplification	0.6229	37	PCAT1, U6, U6, U6, PAPPB, U6, ENHB, HCHT, U6, ENSCAF000000018512, MRPS30, FGF10, SNORA54, U6, NNT1, NOR33, PAIP1, ENSCAF000000031903, C5orf84, 5S, rRNA, C5orf28, CCL28, ENSCAF000000019572, ENSCAF000000030435, NIMTK, ZNF131, SEPP1, CCDC152, GHR, ENSCAF000000023056, FBXO4, C5orf615, EEF1A1, OXCT1, PLCXD3, C6, MROH2B, C7, CARD6, SNORD72, PRKAA1, ACP3, ENSCAF000000033638, ENSCAF000000026150, PDE11A, RSM45, U6, SNORD112, ENSCAF000000028429, O, SBPL6, DFNBS6, PRKRA, FKBP7, PLEKH43, TTN, ENSCAF000000028776, CCDC141, SESTD4, ZNF388B, CMC22, U6, U, BEZES, ITGA4, CERKL, ENSCAF000000014194, SSPA2, PPP1R1C, PDE1A, SNORD22, ENSCAF000000030266, Y, rRNA, A, DNAJC10, FRZB, NCKAP1, U6, DUSP19, ITGDI1, NUP35, STK19, ZNF804A, U6, FSIIP2, ZC3H15, ITGAV, FAM171B, ZSWI, MZ, CALCR1, TFP1, TSK, 7SK, GULP1, U6, COL3A1, COL5A2, TLK1, ENSCAF000000026775, U6, METTL8, DCAF17, CYBRD1, DYNLC12, SLC25A12, HATT, ENSCAF000000012900, M, ETAP1D, U6, DLX1, DLX2, SCARNA17, SCARNA18, ITGA6, ENSCAF000000013080, RAPGEF4, ENSCAF000000013140, ENSCAF000000013159, TSK, ISP3, OLA1, SP9, GPR155, SCRN3, U6, WIPF1, CHRNA1, CHN1, AIF2, ENSCAF000000013386, U6, ENSCAF000000013374, U1, ENSCAF000000030714, KIAA1715, ENSCAF000000013399, EVX2, HOXD12, HO, XB11, HOXD10, HOXD8, cfa-mir-10b, HOXD4, HOXD3, HOXD1, MTX2, TUG1, _1, ENSCAF000000030694, ENSCAF000000032718, HMRNP3, NFE2L2, A, GPS
OSU431895	chr36:15542950-21175300	Amplification	0.6498	55	GALTN3, HSPD1, 5S, rRNA, KCNJ3, ENSCAF000000009188, U6, ENSCAF0000000029956, NIK4A2, GPD2, ENSCAF000000009244, ENSCAF000000009250, ENSCAF000000009252, GALTN3, UGT2B31, UGT2A3, ENSCAF000000024836, ENSCAF000000002C148, 5S, rRNA, PKP4, DAPL1, TANC1, WDSUB1, ENSCAF000000009377, BAZ2B, ENSCAF000000013858, 5S, rRNA, MARCH7, CD302, ENSCAF000000023972, PLA2R1, ITGB6, RBMS1, TANK, PSMD14, 5S, rRNA, TBR1, SLC44A10, DPPA, GLP, T, PAP, IFIH1, GCA, KCNIF7, ENSCAF000000010515, ENSCAF000000010520, FIGL1, U6, SNORA25, GRB14, COBL1, 1, EN, SCAF000000031461, SLC39A11, SCN3A
OSU431895	chr36:686800-10307250	Amplification	0.6344	56	TMPRSS11A, ENSCAF000000032430, TMPRSS11F, TMPRSS11B, TMPRSS11E, U6, YTHDC1, ENSCAF000000030336, 7, ENSCAF000000002628, ENSCAF000000029376, UGT2B31, UGT2A3, ENSCAF000000024836, ENSCAF000000002857, SUL1, TEB1, ENSCAF00000002873, ENSCAF00000002875, SUL1, TE1, CSN1S1, CSN2, C4orf40, ODAM, CSN8, EN, SCAF000000028873, ENSCAF00000002890, CABSI1, ENSCAF000000029608, C, AMTN, AMBN, ENAM, IGL1, UTP3, RUFY, 3, GRSF1, SNORA62, MOB1B, DCK, ENSCAF00000002934, SLC44A, GC, NIPFFR2, ENSCAF00000002958, ENSCAF00000002959, COX18, ANKRD17, ALB, AFP, AFM, RASSF16, IL6, U6, ENSCAF000000025016, PPBP, ENSCAF000000030003, 1464, MTHFD2L, ENSCAF00000003069, EPICN, ENSCAF00000003071, EREG, ENSCAF00000003075

FIG. 111

Patient ID	Region	Mutation type	Log2 ratio	Number of genes	Gene symbols
OSU431895	chr13:92500-10016800	Amplification	0.726	76	LAP1M4, MATKZ, ENSCAF000000031952, SNORA72, C26orf47, ENSCAF000000030250, POP1, NIPAL2, ENSCAF000018581, KCNS2, STK3, U6, OSR2, VPS13B, U6, cfa-mir-599, cfa-mir-875, RGS22, ENSCAF00000000532, FBXO43, ENSCAF00000001661, SPAG1, RNF19A, 5S, rRNA, ANKRD46, SNX31, PABPC1, YWH42, Y, RNA, ZNF706, Y, RNA, GRHL2, ENSCAF000000030800, NCALD, ENSCAF000000025576, ENSCA, FG00000000598, RRM4B, UBR5, ENSCAF00000000632, ENSCAF000000030010, SNRPD2, ODF1, KLF10, AZH1, ENSCAF00000000646, ATRPV1C1, BAALC, ENSCAF00000000693, FZD6, C, THRC1, SLC25A32, DCAF13, PRMS2, ENSCA, FG00000028565, ENSCAF00000000672, DCSTAMP, DPY5, LRPI, ENSCAF000000028333, ZFPM2, OXR1, SNORA6, 2, ABRA, ENSCAF00000000963, ENSCAF00000000984, ENSCAF00000000687, ANGPT1, U6, R, SPO2, EIF3E, ENSCAF00000022583, ENSCAF00000000713, TME47A, TRHB, NUJGD1, PKHD11, TTC33, P, GER4, ENSCAF00000001977, DAB2, C9, FYB, RICTOR, OSMR, ENSCAF00000018652, LIFR, U2, EGF, LAM, ENSCAF00000018871, U6, GDNF, WDR70, ENSCAF00000018679, SNORA67, SNORD22, NUP155, U6, SNORA30, 7S, K, U6, C5orf42, NIPBL, GLAST, ENSCAF00000029561, RANBP3L, ENSCAF0000001830, SKP2, LMBRD2, ENSCAF00000023144, ENSCAF00000032039, CAPSL, IL7R, SYPEF2, U6, PRLR, AGXT2, DNA, JC21, BRX1, RAD1, TTC23L, U6, R, AH4, U6, ENSCAF00000018825, AMACR, SLC45A2, RYFP3, ADAMTS12, TARS, NPR3, 5S, rRNA, ENSCAF00000018878, ENSCAF00000018939, ZFR, ENSCAF00000027374, MTMR12, CCLPH3, PDZD2, C5orf22, ENSCAF00000031629, ENSCAF00000018939, CDH6, ENSCAF00000018956, U6, CDH8, ENSCAF00000018880, 7SK, CDH10, ENSCAF00000017424, ENSCAF00000019017, ENSCAF00000019023, CDH12, ENSCAF00000031957, CDH18, SNORA62, U2, 7SK, RNF167, BASP1, FAM134B, MYO10, ZNF622, MARCH11, FBXL7, ENSCAF00000019108, ANKH, C, OSER2, U6, GRID1, ENSCAF00000031841, cfa-mir-346, WAPAL, CPNA, LDB3, BMP1A, MMRN2, ENSCAF00000024229, SNCG, ENSCAF00000018693, ENSCAF00000018085, ENSCAF00000032460, FAM35A, SYT15, GPRIN2, NPY4R, ENSCAF00000016149, ANTXR1, ZNF488, RBP3, GDF2, GDF10, ENSCAF00000023521, DCP2, U6, MCC, FAM193B, GRK6, DDX41, DOK3, ENSCAF00000016333, DBN1, PRR7, F12, PFN3, SLC34A1, RGS14, LMAN2, MXD3, PRELID1, RAB24, NSD1, FGF4, ZNF346, ENSCAF00000016545, ENSCAF00000026478, UHMCL1, SK, U4, HK3, UNC5A, TSPAN17, EIF4E1S, SNCS, GPRIN1, CDHR2, RNF44, FAF2, C, LIT, B, NOP16, ARL10, cfa-mir-1271, U6, KIAA1191, SIMC1, SUB1, THOC3, CPLX2, HHR23, U6, 7SK, SF2X1, DRD1, MSX2, ENSCAF00000030421, C5orf4, 7, CPES4, U6, ENSCAF00000016775, BOD1, STC2, NKX2.5, ENSCAF00000016785, BNIIP1, CREBRF, ATRP, VOE1, ER, GIC1, DJSP1, NEURL1B, SH3PXD2B, U6, SNORD23, UBTD2, U6, EFCAB9, STK10, 5S, rRNA, FBXW1, SMIM23, FGF18, N, PM1, U6, TLX3, RANBP17, U6, GABRP, KCNIP1, KCNMB1, LOP2, FOXH1, DOCK2, FAM196B, SPDL1, ENSCAF00000017000, U6, SLT3, cfa-mir-218, 2, PANK3, RARS, WWC1, U6, TENM2, ENSCAF00000017171, ENSCAF00000017176, ENSCAF00000017180, SROZ5, U6, U6, MAT2B, HMMR, HMMR, NUPDC2, CCNG1, ENSCAF00000017212, 5S, rRNA, U6, GABRG2, ENSCAF00000017236, GABRA1, ENSCA, FG00000017239, GABRA6, GABRB2, ATP10B, cfa-mir-146a, ENSCAF00000017264, SLU7, C5orf54, U6, C11orf12, ENSCAF00000017274, FABP6, ENSCAF00000017689, U4, PWWP2A, TTC1, ADRA1B, ENSCAF00000029942, IL12B, UBLCP1, RNF145, EBF1, U6, CLINT1, U6, THG1L, SOX30, ADAM19, NIPAL4, CYFIP2, FNDC9, U6, ITK, FAM171B, MED7, HAVERC2, HAVCR1, TIMD4, SGGD, ENSCAF00000030235, MRPL22, ENSCAF00000017808, GEMIN5, CNOT8, FAXDC2, LARP1, ENSCAF00000029767, U6, HANDB1, SAP30L, GA, LNT10, ENSCAF00000032419, MFAP3, FAM114A2, GRIA1, NMUR2, GLRA1, G3BP1, ATOX1, ENSCAF00000030581, SPARC, FAT2, SLC39A1, SLC36A2, SLC36A3, ZNF2, ENSCAF00000026827, CCDC89, U6, ANKAG, TNIP1, GPX3, ENSCAF00000017661, ENSCAF00000023257, ZNF300, U6, SMIM3, 7SK, DCTN4, RBM22, MYO23, SYNPO, NDST1, RPS14, CD74, TCOF1, ARS1, CAMK2A, SLC6A7, GDX1, PDGFRB, CSF1R, HMGXB3, ENSCAF00000032400, TIGD8, SLC26A2, P, DEBA, PPARGC1B, cfa-mir-378, U6, ARHGGEF37, ENSCAF00000018286, cfa-mir-145, cfa-mir-143, IL17B, PCYOX1, L, GRPEL2, AFAP1L1, ABLIM3, U6, SH3TC2, ADRB2, HTR4, FBXO38, SPINK9, SPINK7, GZMK, ESM1, ENSCAF00000008488, ENSCAF00000018395, ENSCAF00000031454, SNX18, HSPB3, ENSCAF00000002728, L, ITAF, ARL15, FST, ENSCAF00000018410, ENSCAF00000026642, ENSCAF00000018414, ENSCAF000000031509, MOC52, ITGA2
OSU431895	chr4:68648500-86273150	Amplification	0.6472	90	
OSU431895	chr4:32584700-47752750	Amplification	0.6863	133	
OSU431895	chr4:47761300-62225000	Amplification	0.6827	142	

FIG. 11J



Patient ID	Region	Mutation type	Log2 ratio	Number of genes	Gene symbols
OSU431865	chr4:69700-32472150		0.6663	278	IFIT2, IFIT3, L4, IFIT1, IFIT5, ZNF248, ZNF25, ENSCAF00000028518, ENSCAF000000028103, ENSCAF000000024143, U6, ZNF37A, CHR3, ENSCAF00000008985, ENSCAF00000009691, ENSCAF00000008988, ZP4, RYR2, 7SK, ENS, CAF00000008083, SNORA25, U6, SNORA2, ENSCAF000000010041, MTR, U6, ACTN2, HEATR1, LGAL, S8, EDARADD, ERO1L, GPR137B, ENSCAF000000030894, MID1, LYST, ENSCAF000000031911, GNG4, IBSGALNT2, TBCE, GGFST1, A, RID4B, RBM34, TOMM20, SNORA14, U6, ENSCAF000000032166, IRF2BP2, TARBP1, COA6, SLC35F3, 7SK, KCKNK1, EN, SCAF000000011588, PCNXL2, NTPCR, S5, rRNA, ENSCAF00000011615, SIPA1L2, DISC1, SNORA25, ENSCAF000000030982, EGLN1, SNORD35, SPRTN, EXOC8, GNPAT, C10orf131, TRIM67, FAM89A, ARV1, TTC13, CAPN8, C10orf198, AG, T, c6a, rbc-1841, c6a, mlk-1841, U6, PGBD5, GALNT2, ENSCAF00000024420, URB2, TAF8L, ABCB10, NUP133, ACTA1, CCSAP, RAB4A, U6, RHO, U, ENSCAF000000012252, U6, S5, rRNA, S5, rRNA, S5, rRNA, UBCE2D1, TFAM, BIC1, S5, rRNA, ENSCAF00000002782, 1, ENSCAF000000032217, ENSCAF00000002392, PHYHIP, FAM13C, SLC16A8, CDC6, U6, ENSCAF00000001245, &ANK3, U6, CDK1, RHOB, T1, U2, GAPDH, ENSCAF000000012971, TMEM236, S5, rRNA, C10orf07, ARID5B, RTKN2, ZN, F365, ADO, EGR2, NRBF2, MJJD1C, ENSCAF000000028634, 7SK, REEP3, CTNNA3, ENSCAF000000013264, LRR, TM3, ENSCAF000000024412, ENSCAF000000013277, ENSCAF00000008036, DNALC12, ENSCAF000000028986, HNRN, PA1L2, SIRT1, ENSCAF000000013319, HERC4, U6, S5, rRNA, MYPN, LTOH7, PBLD, HNRNPH3, RUFY2, DNA2, SLC25A, 16, SCARNA18, SCARNA17, TET1, U6, S5, rRNA, C, CCAR1, U6, S, STOX1, LDX50, DD, X21, KIAA1278, U4, SRGN, VPS26A, SU, PV3L1, HKDC1, HK1, TACR2, TSPAN1, 5, NEUROG3, C10orf35, COL13A1, S5, rRNA, HZAFY2, AIFM2, TY, SND1, PPA1, ENS, CAF000000014038, LRR, C20, EIF4EBP2, NODAL, PALD1, PRF1, ENSCAF000000014078, ADAMTS4, TBATA, SGPL1, P, CBD1, JUNC5B, SLC28A3, ENSCAF000000014229, U2, C10orf05, C10orf54, PSAP, U6, CHST3, SPOCK2, ASCC1, ANAP, C16, DDT4, DNABP12, MICU1, U6, ENSCAF000000014500, MCU, OIT3, PLA2G12B, U6, ENSCAF000000014550, P4HA1, NUDT13, ECD, FAM149B1, DNAB, ENSCAF00000001286, TTC18, ANKX7, U6, MISS1, PPP3CB, LUSP54, MYOZ1, SYN, POZL, SEC24C, FUT11, CHCHD1, ZSWIM8, ENSCAF000000015050, CAMK2G, PLAUG, ENSCAF000000031053, VCL, AP, 3M1, ADK, U6, SNORD2, snuU2, 30, U6, KA768, ENSCAF000000022869, ENSCAF000000031398, SAMD8, VDAC2, CCMTD1, ZNF503, C10orf11, U6, ENS, CAF000000030490, KCNMA1, U6, DLG5, POLR3A, RPS24, U6, U6, ENSCAF000000030222, ZMIZ1, PPIF, ZCCHC24, ANX, A11, TMEM254, 7SK, ENSCAF00000003232, SFTPD, ENSCAF000000015754, MAT1A, DYDC1, DYDC2, FAM213A, TSP, AN14, SH2D4B, S5, rRNA, DNAB, NR53, ENSCAF000000015896, 7SK, GHITM, CDHR1, LRIT2

FIG. 11L

Supplementary Table 6. Somatic coding structural variants identified by exome sequencing of primary canine lung cancers.

Patient ID	Genomic coordinates		Rearrangement type	Gene(s) affected
	region 1	region 2		
CCB010387	chr23:44360546	chr17:63950184	Translocation	WWTR1-ATP5F1
CCB050354	chrX:103308454	chr15:59537883	Translocation	MBNL3-
OSU431895	chr9:12124378	chr9:12531743	Inversion	TEX2-PECAM1

FIG. 12

Supplementary Table 7. Canine genomic regions covered by custom amplicon panel.

Gene symbol	Chromosomal region
ABL1	chr9:53132787-53132980
ABL1	chr9:53131795-53131993
ABL1	chr9:53131719-53131931
ABL1	chr9:53129710-53129941
ABL1	chr9:53141626-53141773
ABL1	chr9:53141666-53141807
AKT1	chr8:72322531-72322699
AKT1	chr8:72326350-72326560
ALK	chr17:23025511-23025720
ALK	chr17:23035562-23035750
APC	chr3:258857-259033
APC	chr3:258218-258432
APC	chr3:257603-257802
APC	chr3:257493-257662
APC	chr3:257377-257575
APC	chr3:257323-257484
APC	chr3:257192-257389
APC	chr3:257095-257294
APC	chr3:257006-257177
APC	chr3:256898-257090
APC	chr3:256847-257042
ATM	chr5:24271300-24271494
ATM	chr5:24267485-24267645
ATM	chr5:24227983-24228182
ATM	chr5:24226702-24226901
ATM	chr5:24225744-24225929
ATM	chr5:24219490-24219708
ATM	chr5:24272535-24272754
ATM	chr5:24205249-24205465
ATM	chr5:24205240-24205437
ATM	chr5:24201430-24201627
ATM	chr5:24199499-24199678
ATM	chr5:24198654-24198849
ATM	chr5:24191423-24191602
ATM	chr5:24187574-24187742
ATM	chr5:24182536-24182771
ATM	chr5:24182478-24182675
ATM	chr5:24262108-24262315
ATM	chr5:24248285-24248459
BRAF	chr16:8296161-8296342

FIG. 13A

Gene symbol	Chromosomal region
BRAF	chr16:8274236-8274435
BCL2	chr1:13734560-13734773
BCL6	chr34:20115524-20115716
PTPRJ	chr18:41635247-41635349
PTPRJ	chr18:41610376-41610575
PTPRJ	chr18:41608739-41608930
PTPRJ	chr18:41608842-41609026
PTPRJ	chr18:41608498-41608684
PTPRJ	chr18:41607194-41607362
PTPRJ	chr18:41605254-41605452
PTPRJ	chr18:41604588-41604785
PTPRJ	chr18:41602799-41602982
PTPRJ	chr18:41599896-41600094
PTPRJ	chr18:41599639-41599857
PTPRJ	chr18:41596160-41596359
PTPRJ	chr18:41592490-41592700
PTPRJ	chr18:41591115-41591314
PTPRJ	chr18:41587706-41587924
PTPRJ	chr18:41632742-41632920
PTPRJ	chr18:41632835-41633029
PTPRJ	chr18:41629887-41630079
PTPRJ	chr18:41630032-41630209
PTPRJ	chr18:41628351-41628541
PTPRJ	chr18:41628459-41628646
PTPRJ	chr18:41624925-41625123
PTPRJ	chr18:41625081-41625280
PTPRJ	chr18:41622247-41622435
PTPRJ	chr18:41622397-41622596
PTPRJ	chr18:41617533-41617716
PTPRJ	chr18:41617662-41617861
PTPRJ	chr18:41616514-41616733
PTPRJ	chr18:41616636-41616885
PTPRJ	chr18:41614210-41614408
PTPRJ	chr18:41614356-41614555
CDH1	chr5:80784506-80784734
CDH1	chr5:80776432-80776601
CDH1	chr5:80774217-80774415
CDKN2A	chr11:41225734-41225940
CDKN2A	chr11:41225847-41226091
CDKN2A	chr11:41225923-41226135
CSF1R	chr4:59009763-59009961

FIG. 13B

Gene symbol	Chromosomal region
CSF1R	chr4:58991781-58991961
CTNNB1	chr23:10560210-10560409
DDR2	chr38:20031670-20031800
DDR2	chr38:20018886-20019053
DDR2	chr38:20011852-20012021
DDR2	chr38:20015205-20015318
DDR2	chr38:20037000-20037174
EGFR	chr18:5984689-5984867
EGFR	chr18:6009937-6010119
EGFR	chr18:6015506-6015703
EGFR	chr18:6016237-6016419
EGFR	chr18:6022048-6022235
EGFR	chr18:6022102-6022321
EGFR	chr18:6031188-6031372
EGFR	chr18:6015468-6015615
EGFR	chr18:6032170-6032301
EGFR	chr18:6036127-6036259
ERBB2	chr9:22764275-22764455
ERBB2	chr9:22763963-22764154
ERBB2	chr9:22763598-22763819
ERBB2	chr9:22773787-22773946
ERBB2	chr9:22763320-22763513
ERBB2	chr9:22765031-22765155
ERBB4	chr37:19076188-19076407
ERBB4	chr37:19283169-19283364
ERBB4	chr37:19323504-19323674
ERBB4	chr37:19325350-19325532
ERBB4	chr37:19329168-19329367
ERBB4	chr37:19332359-19332524
ERBB4	chr37:19397751-19397948
ERBB4	chr37:19542733-19542967
ERBB4	chr37:19313045-19313157
ERBB4	chr37:19289223-19289313
ERBB4	chr37:19289294-19289464
EZH2	chr16:1987314-1987557
FBXW7	chr15:50190724-50190883
FBXW7	chr15:50192437-50192618
FBXW7	chr15:50194544-50194703
FBXW7	chr15:50194506-50194656
FBXW7	chr15:50195961-50196180
FBXW7	chr15:50204776-50204983

FIG. 13C



Gene symbol	Chromosomal region
FGFR1	chr16:27068305-27068524
FGFR1	chr16:27064078-27064262
FGFR2	chr28:31322761-31322958
FGFR2	chr28:31338175-31338374
FGFR2	chr28:31342907-31343177
FGFR2	chr28:31343056-31343224
FGFR2	chr28:31313535-31313691
FGFR2	chr28:31341774-31341866
FGFR3	chr3:62316073-62316318
FGFR3	chr3:62313411-62313598
FGFR3	chr3:62311495-62311744
FGFR3	chr3:62311181-62311389
FGFR3	chr3:62310633-62310841
FLT3	chr25:11658010-11658206
FLT3	chr25:11650244-11650417
FLT3	chr25:11645983-11646179
FLT3	chr25:11644347-11644540
FLT3	chr25:11651048-11651257
FLT3	chr25:11650091-11650285
FRK	chr12:71663010-71663169
GNAQ	chr1:80927708-80927894
GNAQ	chr1:80927595-80927788
GNAQ	chr1:80914802-80914992
GNAQ	chr1:80914684-80914869
GNAQ	chr1:80853899-80854117
GNAQ	chr1:80853784-80853992
GNAQ	chr1:80851113-80851319
GNAQ	chr1:80851055-80851212
GNAS	chr24:43656666-43656897
GNAS	chr24:43656737-43656956
HNF1A	chr26:16818019-16818204
HNF1A	chr26:16818585-16818780
HRAS	chr18:25644183-25644366
HRAS	chr18:25644512-25644711
IDH1	chr37:16524257-16524455
IDH2	chr3:53075018-53075197
ITK	chr4:52913310-52913489
JAK2	chr1:93416438-93416687
JAK3	chr20:45061934-45062125
JAK4	chr20:45060022-45060184
JAK5	chr20:45054387-45054604

FIG. 13D

Gene symbol	Chromosomal region
KDR	chr13:47442807-47443005
KDR	chr13:47442922-47443121
KDR	chr13:47450231-47450424
KDR	chr13:47451501-47451693
KDR	chr13:47456971-47457187
KDR	chr13:47458307-47458469
KDR	chr13:47468134-47468322
KDR	chr13:47472965-47473163
KDR	chr13:47473656-47473869
KIT	chr13:47144443-47144632
KIT	chr13:47178311-47178450
KIT	chr13:47178426-47178639
KIT	chr13:47178530-47178716
KIT	chr13:47176964-47177163
KIT	chr13:47179068-47179254
KIT	chr13:47180332-47180521
KIT	chr13:47182346-47182529
KIT	chr13:47184222-47184406
KIT	chr13:47187866-47188075
KIT	chr13:47187759-47187888
KRAS	chr27:22279727-22279909
KRAS	chr27:22277814-22278013
KRAS	chr27:22261748-22261919
MET	chr14:55626818-55627017
MET	chr14:55627435-55627650
MET	chr14:55677379-55677569
MET	chr14:55685409-55685605
MET	chr14:55691158-55691383
MET	chr14:55699134-55699333
MLH1	chr23:6914204-6914398
MTOR	chr2:84924877-84924999
MTOR	chr2:84932668-84932872
MTOR	chr2:84927931-84928072
MTOR	chr2:84935761-84935930
MTOR	chr2:84927484-84927631
NOTCH1	chr9:49016900-49017088
NOTCH1	chr9:49010843-49011051
NOTCH1	chr9:49010128-49010283
NPM1	chr4:40756680-40756873
NRAS	chr17:52413400-52413574
NRAS	chr17:52415785-52415961

FIG. 13E

Gene symbol	Chromosomal region
NRAS	chr17:52418025-52418207
PDGFRA	chr13:46755130-46755319
PDGFRA	chr13:46758112-46758261
PDGFRA	chr13:46758431-46758605
PDGFRA	chr13:46762522-46762720
PIK3CA	chr34:12647939-12648113
PIK3CA	chr34:12648039-12648254
PIK3CA	chr34:12651012-12651167
PIK3CA	chr34:12659946-12660166
PIK3CA	chr34:12660627-12660824
PIK3CA	chr34:12660735-12660974
PIK3CA	chr34:12662924-12663096
PIK3CA	chr34:12666251-12666443
PIK3CA	chr34:12674167-12674366
PIK3CA	chr34:12675544-12675768
PIK3CA	chr34:12675591-12675825
PTEN	chr26:37878229-37878397
PTEN	chr26:37885976-37886175
PTEN	chr26:37900453-37900622
PTEN	chr26:37906248-37906447
PTEN	chr26:37906397-37906589
PTEN	chr26:37906499-37906671
PTEN	chr26:37909934-37910153
PTEN	chr26:37909981-37910174
PTEN	chr26:37910002-37910174
PTPN11	chr26:10014538-10014695
PTPN11	chr26:10052693-10052873
RB1	chr22:3173653-3173838
RB1	chr22:3163154-3163332
RB1	chr22:3150317-3150489
RB1	chr22:3139920-3140083
RB1	chr22:3086935-3087134
RB1	chr22:3074403-3074621
RB1	chr22:3073714-3073938
RB1	chr22:3151283-3151502
RB1	chr22:3141437-3141649
RB1	chr22:3080014-3080184
RET	chr28:3963179-3963336
RET	chr28:3962219-3962405
RET	chr28:3957290-3957458
RET	chr28:3955803-3956014

FIG. 13F

Gene symbol	Chromosomal region
RET	chr28:3953762-3953961
SMAD4	chr1:23912698-23912906
SMAD4	chr1:23912117-23912330
SMAD4	chr1:23907338-23907536
SMAD4	chr1:23903927-23904114
SMAD4	chr1:23902156-23902353
SMAD4	chr1:23894364-23894550
SMAD4	chr1:23893105-23893301
SMAD4	chr1:23884149-23884355
SMAD4	chr1:23882497-23882684
SMARCB1	chr26:28724265-28724461
SMARCB1	chr26:28718341-28718526
SMARCB1	chr26:28716112-28716322
SMARCB1	chr26:28692815-28693023
SMO	chr14:7525791-7525990
SMO	chr14:7524837-7525024
SMO	chr14:7524444-7524653
SMO	chr14:7521708-7521886
SMO	chr14:7520567-7520757
SRC	chr24:26017664-26017849
STK11	chr20:57578759-57578958
STK11	chr20:57566739-57566975
STK11	chr20:57566801-57567028
STK11	chr20:57565779-57565960
STK11	chr20:57563316-57563508
TP53	chr5:32562056-32562255
TP53	chr5:32562928-32563119
TP53	chr5:32563278-32563472
TP53	chr5:32563619-32563858
TP53	chr5:32563769-32563968
TP53	chr5:32563888-32564137
TP53	chr5:32564559-32564757
TP53	chr5:32565057-32565252
VHL	chr20:8210831-8211067
VHL	chr20:8209613-8209812
VHL	chr20:8206929-8207144

FIG. 13G

Supplementary Table 9. Somatic coding SNVs identified by panel sequencing of primary canine lung cancers.

Patient ID	Tumor Type	Gene symbol	Transcript accession	Nucleotide (genomic)	rs ID (dbSNP151)	Nucleotide (cDNA)	Amino acid (protein)	Mutation type	% mutant reads
BACA									
CCB010120	CPAC	CDKN2A	ENSCAF10000002623.3	chr11:41225906C>T		c.148G>A	p.Gly50Arg	Missense variant	92.5%
CCB010387	CPAC	ERBB2	ENSCAF10000025936.3	chr9:22765127A>T		c.1976T>A	p.Val659Glu	Missense variant	33.8%
CCB010387	CPAC	ERBB2	ENSCAF10000025936.3	chr9:22765127A>T		c.1976T>A	p.Val659Glu	Missense variant	46.7%
CCB020051	CPAC	KDR	ENSCAF1000003003.3	chr13:47443084C>T		c.3846-1G>A		Splice acceptor variant	43.2%
CCB020051	CPAC	ATM	ENSCAF10000023032.4	chr5:24205342T>C		c.714A>G	p.Lys2472Glu	Missense variant	34.1%
CCB020051	CPAC	ERBB2	ENSCAF10000025936.3	chr9:22765127A>T		c.1976T>A	p.Val659Glu	Missense variant	44.0%
CCB020198	CPAC	ERBB2	ENSCAF10000025936.3	chr9:22765127A>T		c.1976T>A	p.Val659Glu	Missense variant	34.1%
CCB020245	CPAC	PTEN	ENSCAF10000024821.3	chr26:37906437G>T		c.688G>T	p.Asp230Tyr	Missense variant	27.9%
CCB020251	CPAC	HNF1A	ENSCAF1000018677.2	chr26:16818740C>T		c.614C>T	p.Arg272Cys	Missense variant	22.4%
CCB020251	CPAC	PTEN	ENSCAF10000024821.3	chr26:37906437T>C		c.682T>C	p.Cys228Arg	Missense variant	21.2%
CCB040005	CPAC	SMAD4	ENSCAF100000286.3	chr11:23984419T>C		c.1052A>G	p.Asp351Gly	Missense variant	12.5%
CCB040005	CPAC	AKT1	ENSCAF10000029177.3	chr8:72328373T>C		c.157A>G	p.Asp53Asp	Missense variant	24.6%
CCB040005	CPAC	ERBB2	ENSCAF10000025936.3	chr9:22765127A>T		c.1976T>A	p.Val659Glu	Missense variant	34.8%
CCB040068	CPAC	ERBB2	ENSCAF10000025936.3	chr9:22765127A>T		c.1976T>A	p.Val659Glu	Missense variant	34.0%
CCB040149	CPAC	ERBB2	ENSCAF10000025936.3	chr9:22765127A>T		c.1976T>A	p.Val659Glu	Missense variant	22.3%
CCB040149	CPAC	TP53	ENSCAF10000028465.3	chr5:32564629C>T		c.260G>A	p.Gly94Ser	Missense variant	39.6%
CCB040231	CPAC	ERBB2	ENSCAF10000025936.3	chr9:22765127A>T		c.1976T>A	p.Val659Glu	Missense variant	20.3%
CCB050243	CPAC	ERBB2	ENSCAF10000025936.3	chr9:22765127A>T		c.1976T>A	p.Val659Glu	Missense variant	11.3%
CCB050262	CPAC	ERBB2	ENSCAF10000025936.3	chr9:22765127A>T		c.1976T>A	p.Val659Glu	Missense variant	10.0%
CCB050344	CPAC	TP53	ENSCAF10000028485.3	chr5:32564027G>A		c.380C>T	p.Ala127Val	Missense variant	12.3%
CCB050344	CPAC	ERBB2	ENSCAF10000025936.3	chr9:22765127A>T		c.1976T>A	p.Val659Glu	Missense variant	30.5%
CCB050350	CPAC	KRAS	ENSCAF10000010525.3	chr27:222261798G>T		c.35G>T	p.Gly12Val	Missense variant	28.8%
CCB050354	CPAC	ERBB2	ENSCAF10000025936.3	chr9:22765077T>C		c.2026A>G	p.Lys76Glu	Missense variant	36.9%
CCB050356	CPAC	TP53	ENSCAF10000028465.3	chr5:32563074G>A		c.768C>T	p.Arg257Cys	Missense variant	48.8%
CCB050362	CPAC	ERBB2	ENSCAF10000025936.3	chr9:22765127A>T		c.1976T>A	p.Val659Glu	Missense variant	10.6%
CCB050363	CPAC	APC	ENSCAF10000011749.3	chr3:256868T>A		c.2915A>T	p.Glu972Val	Missense variant	33.4%
CCB050363	CPAC	FGFR1	ENSCAF10000009709.3	chr16:27068444G>A		c.749G>A	p.Arg250Gln	Missense variant	24.7%
CCB050363	CPAC	FGFR1	ENSCAF10000009748.4	chr28:31343109T>C		c.862A>G	p.Thr288Ala	Missense variant	25.6%
CCB060040	CPAC	PIK3CA	ENSCAF10000017863.3	chr34:12875674A>T	rs651387419	c.3140A>T	p.His1047Leu	Missense variant	20.5%
CCB060143	CPAC	TP53	ENSCAF10000028485.3	chr5:32563918C>T		c.491G>A	p.Arg184His	Missense variant	55.4%
CCB060156	CPAC	ERBB2	ENSCAF10000025936.3	chr9:22765127A>T		c.1976T>A	p.Val659Glu	Missense variant	15.6%
CCB060156	CPAC	TP53	ENSCAF10000028465.3	chr5:32563971C>A		c.438G>T	p.Val146Phe	Missense variant	34.4%
CCB070114	CPAC	ERBB2	ENSCAF10000025936.3	chr9:22765127A>T		c.1976T>A	p.Val659Glu	Missense variant	18.5%
CCB070142	CPAC	VHL	ENSCAF10000046552.2	chr20:8210849A>G		c.334T>C	p.Tyr112His	Missense variant	26.5%
CCB070294	CPAC	ERBB2	ENSCAF10000025936.3	chr9:22765127A>T		c.1976T>A	p.Val659Glu	Missense variant	9.42%
CCB070294	CPAC	SMAD4	ENSCAF100000286.3	chr11:23984419T>C		c.1572G>T	p.Trp524Cys	Missense variant	19.3%
CCB070295	CPAC	ERBB2	ENSCAF10000025936.3	chr9:22765127A>T		c.1976T>A	p.Val659Glu	Missense variant	40.8%
CCB070295	CPAC	TP53	ENSCAF10000028465.3	chr5:32563388C>T	rs651620436	c.716G>A	p.Arg239Gln	Missense variant	57.6%
CLAC		TP53	ENSCAF10000028465.3	chr5:32563028C>T	rs852440243	c.815G>A	p.Arg272His	Missense variant	96.5%
OSU361939	CPAC	ERBB2	ENSCAF10000025936.3	chr9:22765127A>T		c.1976T>A	p.Val659Glu	Missense variant	38.8%
OSU381645	CPAC	KRAS	ENSCAF10000010525.3	chr27:222261798G>T		c.35G>T	p.Gly12Val	Missense variant	56.8%
OSU388285	CPAC	ERBB2	ENSCAF10000025936.3	chr9:22765127A>T		c.1976T>A	p.Val659Glu	Missense variant	17.0%
OSU389339	CPAC	PTEN	ENSCAF10000024821.3	chr26:37906437C>T		c.574C>T	p.Gln192*	Stop-gained variant	23.2%
OSU416281	CPAC	HRAS	ENSCAF10000046281.1	chr18:25644252A>G		c.233T>C	p.Phe78Ser	Missense variant	20.9%
OSU419040	CPAC	CSF1R	ENSCAF10000028942.3	chr4:56991931A>G		c.953A>G	p.Lys318Arg	Missense variant	24.6%
OSU419040	CPAC	ERBB2	ENSCAF10000025936.3	chr9:22765113C>T		c.1990G>A	p.Ala654Thr	Missense variant	17.9%

FIG. 14A

Patient ID	Tumor Type	Gene symbol	Transcript accession	Nucleotide (genomic)	rs ID (dbSNP151)	Nucleotide (cDNA)	Amino acid (protein)	Mutation type	% mutant reads
OSU419040	cPAC	ERBB2	ENSCAF10000025936.3	chr9:22765127A>T	.	c.1976T>A	p.Val659Glu	Missense variant	8.39%
OSU419040	cPAC	VHL	ENSCAF10000046552.2	chr20:8210966C>T	.	c.317G>A	p.Gly106Asp	Missense variant	28.6%
OSU424354	cPAC	ERBB2	ENSCAF10000025936.3	chr9:22765127A>T	.	c.1976T>A	p.Val659Glu	Missense variant	6.52%
OSU426073	cPAC	ERBB2	ENSCAF10000025936.3	chr9:22765127A>T	.	c.1976T>A	p.Val659Glu	Missense variant	17.6%
OSU429271	cPAC	TP53	ENSCAF10000026465.3	chr5:32563389G>C	rs852661628	c.715C>G	p.Arg23Gly	Missense variant	63.4%
OSUK9PADSmicke	cPAC	KRAS	ENSCAF10000010525.3	chr27:22261798G>A	.	c.35G>A	p.Gly12Asp	Missense variant	73.4%
OSUK9PADSmicke	cPAC	SMARCB1	ENSCAF10000022399.3	chr26:28716263C>T	.	c.628G>A	p.Glu210Lys	Missense variant	30.5%
OSUK9PADSmicke	cPAC	TP53	ENSCAF10000026465.3	chr5:325633077C>A	.	c.766G>T	p.Gly256*	Stop-gained variant	98.4%
SUK9PAPADOSC	cPAC	ERBB2	ENSCAF10000025936.3	chr9:22765127A>T	.	c.1976T>A	p.Val659Glu	Missense variant	15.0%
SUK9PAPADOSC	cPAC	SMAD4	ENSCAF1000000266.3	chr11:23894420C>A	.	c.1051G>T	p.Asp351Tyr	Missense variant	28.7%
OSUK9PAPADRe	cPAC	ERBB2	ENSCAF10000025936.3	chr9:22765127A>T	.	c.1976T>A	p.Val659Glu	Missense variant	51.9%
OSUK9PAPADRe	cPAC	SMAD4	ENSCAF1000000266.3	chr11:23894420C>A	.	c.1051G>T	p.Asp351Tyr	Missense variant	99.3%
CCB010105	cPASC	KRAS	ENSCAF10000010525.3	chr27:22277968C>A	.	c.181C>A	p.Gln61Lys	Missense variant	29.4%
CCB010105	cPASC	TP53	ENSCAF10000026465.3	chr5:325633988G>A	.	c.439C>T	p.Arg147Cys	Missense variant	22.0%
CCB040011	cPASC	EGFR	ENSCAF1000005575.3	chr18:60163655G>A	.	c.2176G>A	p.Ala726Thr	Missense variant	23.4%
CCB040011	cPASC	MET	ENSCAF10000049462.2	chr14:55699187A>G	.	c.3605A>G	p.Met1269Val	Missense variant	34.5%
CCB040011	cPASC	PTPRJ	ENSCAF10000013154.3	chr18:41608559T>C	.	c.2527A>G	p.Ser643Gly	Missense variant	26.9%
CCB040385	cPASC	PTEN	ENSCAF10000024821.3	chr26:37910052T>G	.	c.893T>G	p.Leu298*	Stop-gained variant	59.5%
OSU422557	cPASC	HRAS	ENSCAF10000046281.1	chr16:25844303T>A	.	c.182A>T	p.Gln61Leu	Missense variant	11.3%
OSU422557	cPASC	KIT	ENSCAF10000049830.2	chr13:47187859A>G	.	c.2482-4A>G	.	Splice region variant	23.3%
OSUK9PADSQ	cPASC	PTEN	ENSCAF10000024821.3	chr26:37886124C>T	.	c.322C>T	p.Arg108*	Stop-gained variant	100.0%
OSUK9PADSQ	cPASC	VHL	ENSCAF10000046552.2	chr20:82109933G>A	.	c.290C>T	p.Pro91Leu	Missense variant	24.9%
CCB010131	cPSCC	PTPN11	ENSCAF10000014133.3	chr26:10052797G>T	.	c.1508G>T	p.Gly503Val	Missense variant	50.8%
OSUJSCC1	cPSCC	BRAF	ENSCAF1000006305.4	chr16:8296284T>A	.	c.1763T>A	p.Val588Glu	Missense variant	50.5%

FIG. 14B

Supplementary Table 10. Germline SNPs in COSMIC Tier 1 cancer genes identified by exome and panel sequencing in primary canine lung cancers.

Patient ID	Gene symbol	Transcript accession	Nucleotide (genomic)	dbSNP151	rsID	DogSD AF	Nucleotide (cDNA)	Amino acid (protein)	Variant type	Variant	
										germline zygosity	Variant tumor zygosity
CCB010387	CHRNA3	ENSCAF00000002688	chr13:38333887G>GC	.	.	.	c.1237dupC	p.Arg413is	Frameshift variant	Heterozygous	Heterozygous
CCB010387	CHRNA3	ENSCAF00000002688	chr13:38339420C>A	.	.	4%	c.1268C>A	p.Ala423Glu	Missense variant	Heterozygous	Heterozygous
CCB50354	CHRNA3	ENSCAF00000002689	chr13:38339420C>A	.	.	4%	c.1268C>A	p.Ala423Glu	Missense variant	Heterozygous	Heterozygous
CCB050354	CYP1B1	ENSCAF000000009970	chr17:30277509C>G	.	.	3%	c.278G>C	p.Arg93Pro	Missense variant	Homozygous	Homozygous
OSU431895	DNAH11	ENSCAF00000004311	chr14:35518785G>A	.	.	8%	c.2851G>A	p.Val851Ile	Missense variant	Heterozygous	Heterozygous
OSU431895	DNAH11	ENSCAF00000004311	chr14:35533763C>T	.	.	.	c.4378C>T	p.Arg1460Trp	Missense variant	Heterozygous	Heterozygous
OSU398622	HER2	ENSCAF00000025936	chr9:22761249C>T	.	.	4%	c.3565G>A	p.Val1189Ile	Missense variant	Heterozygous	Heterozygous
OSU431895	HER2	ENSCAF00000025936	chr9:22761249C>T	.	.	4%	c.3565G>A	p.Val1189Ile	Missense variant	Heterozygous	Heterozygous

FIG. 15

Supplementary Table 11. Multi-platform validation of HER2 mutations.

Patient ID	Tumor or Cell Line	Gene symbol	Transcript accession	Mutation (genomic nucleotide)	Nucleotide (cDNA)	Amino acid (protein)	Mutation type	Exome
BACA	Cell Line	HER2	ENSCAF00000025936.3	WT	n/a	n/a	WT	.
CLAC	Cell Line	HER2	ENSCAF00000025936.3	WT	n/a	n/a	WT	.
OSUK9PADBa	Cell Line	HER2	ENSCAF00000025936.3	WT	n/a	n/a	WT	.
OSUK9PADI	Cell Line	HER2	ENSCAF00000025936.3	WT	n/a	n/a	WT	.
OSUK9PADSh	Cell Line	HER2	ENSCAF00000025936.3	WT	n/a	n/a	WT	.
OSUK9PADSQ	Cell Line	HER2	ENSCAF00000025936.3	WT	n/a	n/a	WT	.
OSUK9PAPADO Passage 15	Cell Line	HER2	ENSCAF00000025936.3	WT	n/a	n/a	WT	.
OSUK9PAPADO Passage 4	Cell Line	HER2	ENSCAF00000025936.3	chr9:22765127A>T	c.1976T>A	p.Val659Glu	Missense variant	.
OSUK9PAPADRE	Cell Line	HER2	ENSCAF00000025936.3	chr9:22765127A>T	c.1976T>A	p.Val659Glu	Missense variant	.
OSUK9PAPADRI	Cell Line	HER2	ENSCAF00000025936.3	chr9:22765127A>T	c.1976T>A	p.Val659Glu	Missense variant	.
OSULSCC1	Cell Line	HER2	ENSCAF00000025936.3	WT	n/a	n/a	WT	.
OSUPaPADSh	Cell Line	HER2	ENSCAF00000025936.3	WT	n/a	n/a	WT	.
CCB010120	Tumor	HER2	ENSCAF00000025936.3	chr9:22765127A>T	c.1976T>A	p.Val659Glu	Missense variant	.
CCB010387	Tumor	HER2	ENSCAF00000025936.3	chr9:22765127A>T	c.1976T>A	p.Val659Glu	Missense variant	44%
CCB020051	Tumor	HER2	ENSCAF00000025936.3	chr9:22765127A>T	c.1976T>A	p.Val659Glu	Missense variant	.
CCB020198	Tumor	HER2	ENSCAF00000025936.3	chr9:22765127A>T	c.1976T>A	p.Val659Glu	Missense variant	.
CCB040005	Tumor	HER2	ENSCAF00000025936.3	chr9:22765127A>T	c.1976T>A	p.Val659Glu	Missense variant	.
CCB040068	Tumor	HER2	ENSCAF00000025936.3	chr9:22765127A>T	c.1976T>A	p.Val659Glu	Missense variant	.
CCB040149	Tumor	HER2	ENSCAF00000025936.3	chr9:22765127A>T	c.1976T>A	p.Val659Glu	Missense variant	.
CCB040231	Tumor	HER2	ENSCAF00000025936.3	chr9:22765127A>T	c.1976T>A	p.Val659Glu	Missense variant	.
CCB050227	Tumor	HER2	ENSCAF00000025936.3	chr9:22765127A>T	c.1976T>A	p.Val659Glu	Missense variant	54%
CCB050243	Tumor	HER2	ENSCAF00000025936.3	chr9:22765127A>T	c.1976T>A	p.Val659Glu	Missense variant	.
CCB050260	Tumor	HER2	ENSCAF00000025936.3	chr9:22765127A>T	c.1976T>A	p.Val659Glu	Missense variant	.
CCB050345	Tumor	HER2	ENSCAF00000025936.3	chr9:22765127A>T	c.1976T>A	p.Val659Glu	Missense variant	.
CCB050354	Tumor	HER2	ENSCAF00000025936.3	chr9:22765127A>T	c.2026A>G	p.Lys676Glu	Missense variant	35%
CCB050362	Tumor	HER2	ENSCAF00000025936.3	chr9:22765127A>T	c.1976T>A	p.Val659Glu	Missense variant	.
CCB060156	Tumor	HER2	ENSCAF00000025936.3	chr9:22765127A>T	c.1976T>A	p.Val659Glu	Missense variant	.
CCB070114	Tumor	HER2	ENSCAF00000025936.3	chr9:22765127A>T	c.1976T>A	p.Val659Glu	Missense variant	.
CCB070294	Tumor	HER2	ENSCAF00000025936.3	chr9:22765127A>T	c.1976T>A	p.Val659Glu	Missense variant	.
CCB070295	Tumor	HER2	ENSCAF00000025936.3	chr9:22765127A>T	c.1976T>A	p.Val659Glu	Missense variant	.
OSU361939	Tumor	HER2	ENSCAF00000025936.3	chr9:22765127A>T	c.1976T>A	p.Val659Glu	Missense variant	.
OSU388285	Tumor	HER2	ENSCAF00000025936.3	chr9:22765127A>T	c.1976T>A	p.Val659Glu	Missense variant	.
OSU389339	Tumor	HER2	ENSCAF00000025936.3	chr9:22765127A>T	c.1976T>A	p.Val659Glu	Missense variant	.
OSU396622	Tumor	HER2	ENSCAF00000025936.3	chr9:22765127A>T	c.1976T>A	p.Val659Glu	Missense variant	20%
OSU419040	Tumor	HER2	ENSCAF00000025936.3	chr9:22765127A>T	c.1976T>A	p.Val659Glu	Missense variant	.
OSU419040	Tumor	HER2	ENSCAF00000025936.3	chr9:22765113C>T	c.1990G>A	p.Ala684Thr	Missense variant	.
OSU424354	Tumor	HER2	ENSCAF00000025936.3	chr9:22765127A>T	c.1976T>A	p.Val659Glu	Missense variant	.
OSU428073	Tumor	HER2	ENSCAF00000025936.3	chr9:22765127A>T	c.1976T>A	p.Val659Glu	Missense variant	.

FIG. 16A



Patient ID	HER2 Mutant reads (%) or Profiling Result					
	Targeted panel	HER2 659 locus		HER2 all coding regions		Digital droplet PCR
		Sanger sequencing	WT	Sanger sequencing	WT	
BACA	0.0%	WT	WT	WT	0.0%	No HER2 Amp
CLAC	0.0%	WT	WT	WT	0.0%	No HER2 Amp
OSUK9PADBa	0.0%	.	WT	WT	0.0%	.
OSUK9PADI	0.0%	.	WT	WT	0.0%	.
OSUK9PADSn	0.0%	WT	WT	WT	0.0%	.
OSUK9PADSQ	0.0%	WT	WT	WT	0.0%	.
OSUK9PAPADO Passage 15	15.0%	.	.	.	16.0%	.
OSUK9PAPADO Passage 4	51.9%	.	.	.	50.5%	.
OSUK9PAPADRe	.	Mut	.	.	.	.
OSUK9PAPADRI	.	WT	WT	WT	0.0%	.
OSULSCC1	0.0%	WT	WT	WT	.	.
OSUPaPADSh	0.0%	Mut	.	.	.	.
CCB010120	33.8%	.	.	.	.	.
CCB010387	46.7%	.	.	.	39.0%	.
CCB020051	44.0%	Mut	.	.	.	.
CCB020198	34.1%	Mut	.	.	.	.
CCB040005	34.8%	Mut	.	.	.	.
CCB040068	34.0%	.	.	.	.	.
CCB040149	22.3%	.	.	.	.	.
CCB040231	20.3%	.	.	.	.	.
CCB050227	.	.	.	.	59.2%	.
CCB050243	11.3%	WT	WT	WT	33.0%	.
CCB050260	10.0%	WT	WT	WT	10.5%	.
CCB050345	30.5%	.	.	.	.	.
CCB050354	36.9%	.	.	.	.	.
CCB050362	10.6%	Mut	Mut	Mut	.	.
CCB060156	15.6%	Mut	Mut	Mut	.	.
CCB070114	18.5%	Mut	Mut	Mut	.	.

FIG. 16B

Patient ID	Targeted panel	HER2 659 locus Sanger sequencing	HER2 all coding regions Sanger sequencing	Digital droplet PCR	aCGH from Clemente-Vicario et al. <sup>21</sup>
CCB070294	9.42%	.	.	10.4%	.
CCB070295	40.8%	.	.	36.5%	.
OSU361939	38.8%	Mut	.	.	.
OSU388285	17.0%	Mut	.	.	.
OSU389339	47.7%	Mut	.	.	.
OSU396622	.	.	.	27.0%	.
OSU419040	17.9%	.	.	11.6%	.
OSU419040	8.39%	.	.	11.6%	.
OSU424354	8.52%	Mut	.	.	.
OSU428073	17.8%	Mut	.	.	.

FIG. 16C

Supplementary Table 12. Non-invasive detection of HER2 V659E in the plasma of primary canine lung cancer patients.

Sample ID	Sample type	HER2 <sup>V659E</sup> allele frequency in tumor	Total droplets assayed	Poisson corrected mutant droplet count (HER2 <sup>V659E</sup> )	Poisson corrected wild type droplet count (HER2 <sup>V659E</sup> )	HER2 <sup>V659E</sup> allele frequency by ddPCR
Bioreclamation IVT	Canine plasma (negative control)	na	10000000	0	207	0.0%
Bioreclamation IVT	Canine plasma (negative control)	na	10000000	0	313	0.0%
Bioreclamation IVT	Canine plasma (negative control)	na	10000000	0	237	0.0%
Bioreclamation IVT	Canine plasma (negative control)	na	10000000	0	202	0.0%
Bioreclamation IVT	Canine plasma (negative control)	na	10000000	1	241	0.5%
Bioreclamation IVT	Canine plasma (negative control)	na	10000000	0	186	0.0%
CCB020245	Canine plasma	0.0%	10000000	0	97	0.0%
OSU3889339	Canine plasma	47.7%	10000000	1	232	0.6%
CCB020203	Canine plasma	0.0%	10000000	0	510	0.0%
OSU429271	Canine plasma	0.0%	10000000	0	221	0.0%
CCB020051	Canine plasma	44%	10000000	11	493	2.3%
OSU361939	Canine plasma	36.8%	10000000	0	517	0.0%
OSU428073	Canine plasma	17.8%	10000000	58	3022	1.9%
CCB020293	Canine plasma	0.0%	10000000	0	1936	0.0%
OSU431895	Canine plasma	0.0%	10000000	0	846	0.0%
CCB020198	Canine plasma	34.1%	10000000	0	420	0.0%
OSU388285	Canine plasma	17.0%	10000000	0	454	0.0%
NTC	Water (negative control)	na	10000000	0	0	0.00%
NTC	Water (negative control)	na	10000000	0	0	0.00%
NTC	Water (negative control)	na	10000000	0	0	0.00%
NTC	Water (negative control)	na	10000000	0	0	0.00%
NTC	Water (negative control)	na	10000000	0	0	0.00%
NTC	Water (negative control)	na	10000000	0	1	0.00%
NTC	Water (negative control)	na	10000000	0	0	0.00%
CCB030383	Tumor (negative control)	0.0%	10000000	0	14584	0.0%
OSU415281	Tumor (negative control)	0.0%	10000000	1	16164	0.0%
OSU396622	Tumor (positive control)	19.5%	10000000	2696	7254	27.1%
CCB050227	Tumor (positive control)	54.16%	10000000	14889	10248	59.2%
CCB010387	Tumor (positive control)	43.9%	10000000	6486	10122	39.1%
CCB050260	Tumor (positive control)	10.0%	10000000	1970	17222	10.3%
CCB050260	Tumor (positive control)	10.0%	10000000	1963	17194	10.2%
CCB050260	Tumor (positive control)	10.0%	10000000	2123	18109	10.5%

NTC = Non-template control  
na = not applicable

FIG. 17

Supplementary Table 13. HER2 protein expression and quantification by immunohistochemistry.

Patient ID	HER2 Mutation Status	Slide ID	HER2 Connectivity	Her2 Score	Specimen Total Area (um <sup>2</sup> )	Tumor Area (um <sup>2</sup> )	Tumor Area Ratio	Tumor Area %	HER2	
									Normal Lung Area (um <sup>2</sup> )	Normal Lung %
OSU381645	WT	31 07-2904-1 HER2 Cell Sig #4290 RA W	0.514878988	2	272740982	166064000	0.608894028	60.88939996	13714500	0.050283998
OSU421496	WT	31 12-369-7 HER2 Cell Sig #4290 RA W	0.256812906	1	443500000	363710016	0.819741004	88.97409821	45009500	0.101715997
CCB020293	WT	31 12-524-2 HER2 Cell Sig #4290 RA W	0.366387983	1	385816000	364611008	0.945527971	94.55280304	0	0
OSU454408	WT	31 16-447-1 HER2 Cell Sig #4290 RA W	0.209876003	1	202884000	185584992	0.915636003	91.56359963	13918100	0.066868798
OSU424354	V659E	31 12-1293-3 HER2 Cell Sig #4290 RA W	0.127762005	1	463207008	396947008	0.856953979	85.69539643	7454920	0.0163942
OSU388285	V659E	31 07-2241-3 HER2 Cell Sig #4290 RA W	0.161900987	1	269351008	253427008	0.940877974	94.08779907	13320800	0.049454998
OSU389339	V659E	7-2765-3 HER2 Cell Sig #4290 RA W (2)	0.239398003	1	358744992	344496992	0.960285008	96.02850342	10340400	0.0288238
OSU419040	A664T	31 11-2041-3 HER2 Cell Sig #4290 RA W	0.184890002	1	247571008	233272992	0.942003012	94.20030212	2537650	0.0102502

Patient ID	Normal Lung Area (um <sup>2</sup> )	Normal Lung Ratio	Normal Lung %	Necrosis Area (um <sup>2</sup> )	Necrosis Ratio	Necrosis %	Tumor Positive Stain Area (um <sup>2</sup> )	Tumor Positive Stain Ratio	Tumor Positive Stain %
OSU421496	2932200	0.00662645	0.662644982	45009500	0.101715997	10.17160034	121066000	0.307500432	30.7500432
C-CB020293	20504800	0.053174101	5.317409892	0	0	0	147372992	0.404192382	40.41923825
OSU454408	3081890	0.0152054	1.520539999	13918100	0.066868798	6.68687994	107836000	0.521059917	58.10599187
OSU424354	58112200	0.125456005	12.54559994	7454920	0.0163942	1.609419942	189723008	0.475436278	47.54362779
OSU388285	2603700	0.00966656	0.966656029	13320800	0.049454998	4.945499897	109380000	0.431603665	43.16036645
OSU389339	3907720	0.0106913	1.069130044	10340400	0.0288238	2.882380009	123256000	0.357794126	35.77941255
OSU419040	11500900	0.0464551	4.645510197	2537650	0.0102502	1.025020003	59016800	0.25303393	25.30339395

FIG. 18A

Patient ID	Tumor Negative		Tumor		Tumor Mean Stain		Tumor Mean Stain		Tumor Mean	
	Stain Area (µm <sup>2</sup> )	Negative Stain Ratio	Stain Ratio	Tumor Negative Stain %	Intensity [Optical Density (OD)]	Intensity Ratio	Intensity Ratio	Stain Intensity %	Stain Intensity %	Stain Intensity %
OSU381645	66323772	0.399410866	39.94108663	188.3329826	0.739560021	0.739560021	73.85600281			
OSU421496	269952000	0.685662008	68.56620076	207.6439972	0.814291	0.814291	81.42910004			
CCB020293	212390000	0.582511212	58.25112115	199.7879944	0.783483982	0.783483982	78.3483983			
OSU454408	80216896	0.432238055	43.22380551	183.6880035	0.720346987	0.720346987	72.03469849			
OSU424354	210760992	0.530954983	53.09549833	203.7700043	0.799097002	0.799097002	79.90969849			
OSU388285	146023008	0.576193552	57.61935523	200.0599976	0.784546971	0.784546971	78.45469666			
OSU389339	224224000	0.650873608	65.08736076	203.2279968	0.796971977	0.796971977	79.69719696			
OSU419040	174642000	0.748851934	74.88519336	205.3119965	0.805144012	0.805144012	80.51439667			

Patient ID	Tumor Maximum		Tumor Minimum		Tumor Maximum		Tumor Minimum	
	Maximum Stain Intensity (OD)	Stain Intensity Ratio	Maximum Stain Intensity Ratio	Minimum Stain Intensity (OD)	Minimum Stain Intensity Ratio	Minimum Stain Intensity Ratio	Minimum Stain Intensity %	
OSU381645	247.3170013	0.969869018	96.98690033	129.5850067	0.508177996	0.508177996	50.81779861	
OSU421496	248.1320038	0.973065972	97.30660248	120.7210007	0.473417014	0.473417014	47.34170151	
CCB020293	248.4869995	0.974458992	97.44589996	150.6159973	0.590651989	0.590651989	59.06520081	
OSU454408	245.0140076	0.96083802	96.08380127	118.0469971	0.46292901	0.46292901	46.29290009	
OSU424354	245.8159943	0.963982999	96.39830017	161.6629944	0.633973002	0.633973002	63.39730072	
OSU388285	246.3119965	0.965930998	96.5931015	148.2330017	0.581306994	0.581306994	58.13069916	
OSU389339	246.3410034	0.966041982	96.60420227	149.1239929	0.584798992	0.584798992	58.47990036	
OSU419040	241.3739929	0.946564019	94.65640259	102.4860001	0.401905	0.401905	40.19049835	

FIG. 18B

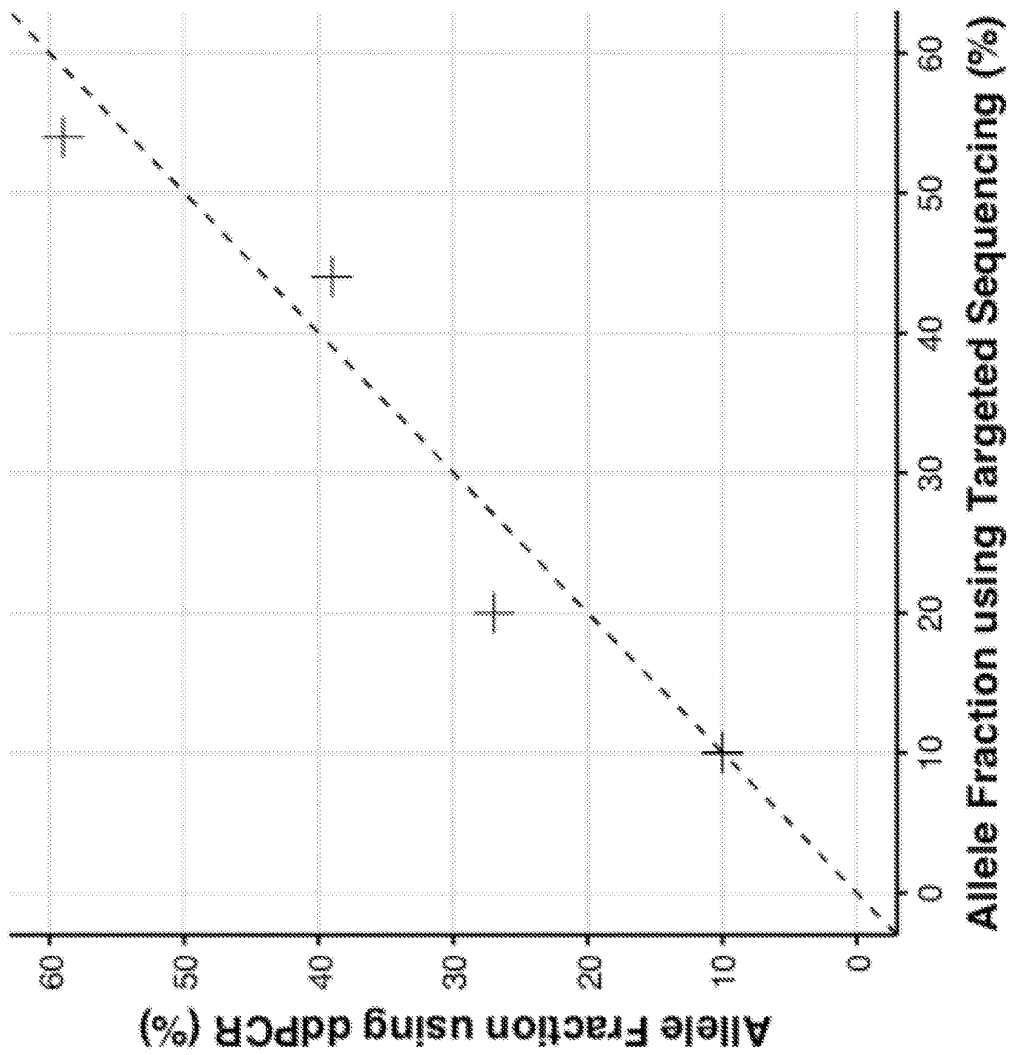


FIG. 19

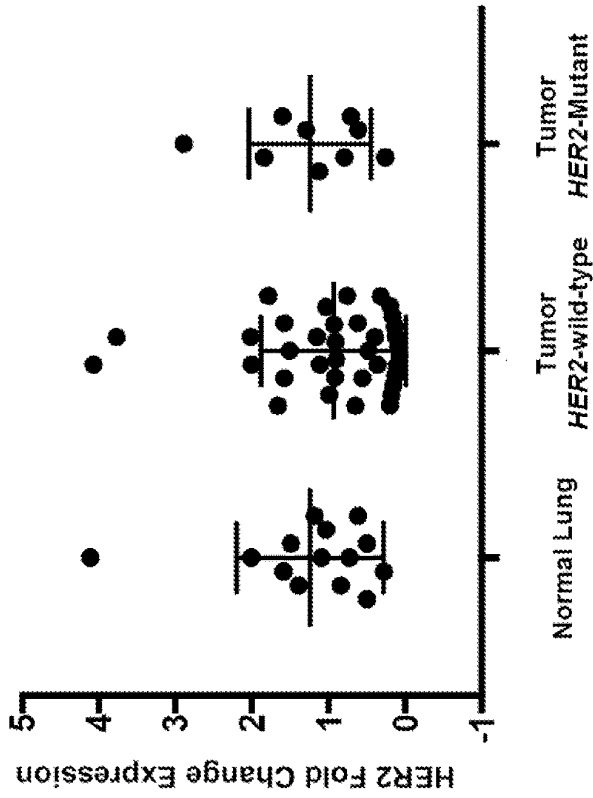


FIG. 20B

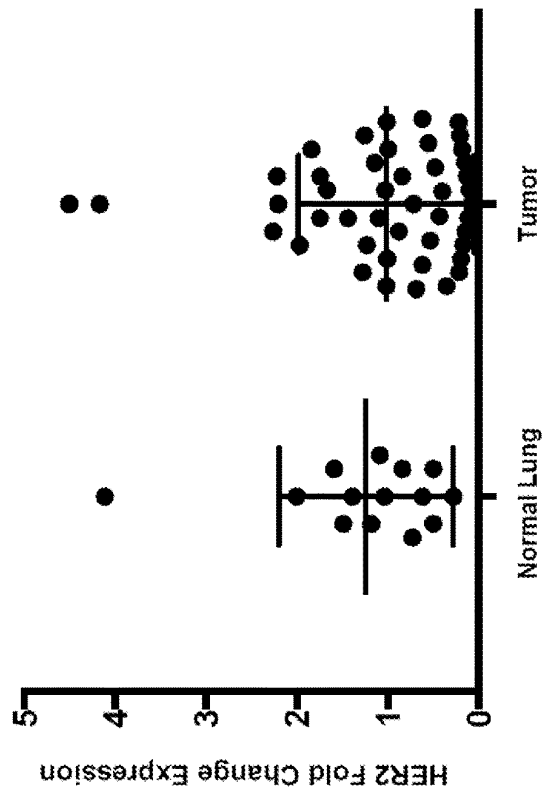
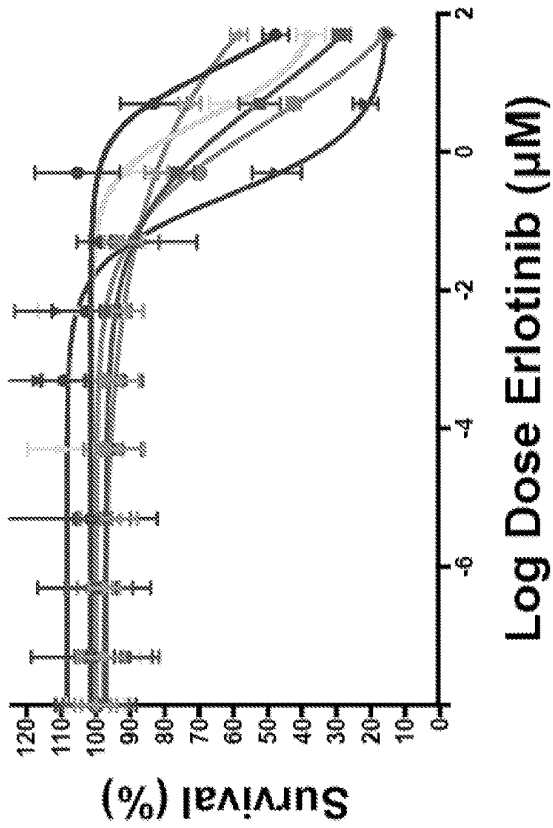


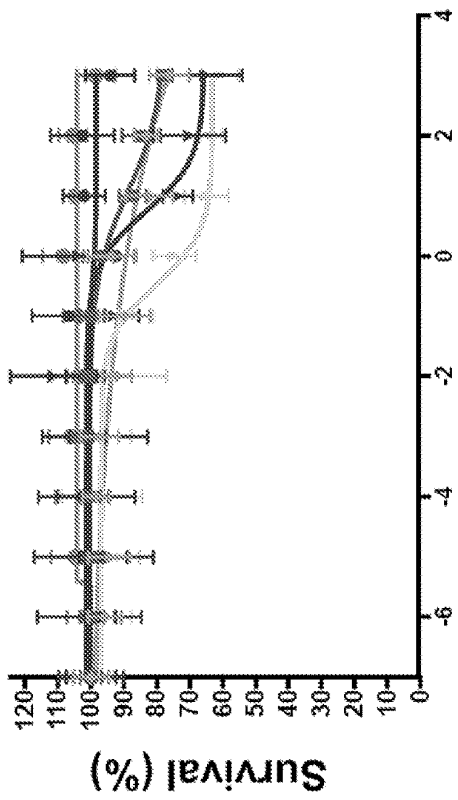
FIG. 20A



	Sample	IC50 (nM)
●	BACA (HER2 <sup>WT</sup> )	15380
■	OSUK9PADSn (HER2 <sup>WT</sup> )	1920
▲	OSUK9PAPADO (HER2 <sup>WT</sup> )	1100
◆	OSUK9PAPADRe (HER2 <sup>V659E</sup> )	220
▼	OSUK9PAPADRI (HER2 <sup>V659E</sup> )	1170
◻	BT474 (HER2 <sup>amp</sup> )	3130

FIG. 21





Log Dose Trastuzumab (µg/ml)







	Sample	Growth Inhibition Relative to BT474
	BACA (HER2 <sup>WT</sup> )	-0.05
	OSUK9PADSn (HER2 <sup>WT</sup> )	0.37
	OSUK9PAPADO (HER2 <sup>WT</sup> )	0.51
	OSUK9PAPADRe (HER2 <sup>V659E</sup> )	0.75
	OSUK9PAPADri (HER2 <sup>V659E</sup> )	-0.14
	BT474 (HER2 <sup>amp</sup> )	1

FIG. 22

## IDENTIFICATION OF HER2 MUTATIONS IN LUNG CANCER AND METHODS OF TREATMENT

### CROSS-REFERENCE TO RELATED APPLICATIONS

**[0001]** This application claims the benefit of U.S. Provisional Patent Application No. 62/778,282, filed on Dec. 11, 2018, the contents of which are incorporated herein by reference in its entirety.

### REFERENCE TO SEQUENCE LISTING SUBMITTED ELECTRONICALLY

**[0002]** The official copy of the sequence listing is submitted electronically via EFS-Web as an ASCII-formatted sequence listing with a file named "279PCT\_Sequence\_Listing\_ST25" created on Dec. 11, 2019, and having a size of 1.51 kilobytes, and is filed concurrently with the specification. The sequence listing contained in this ASCII-formatted document is part of the specification and is herein incorporated by reference in its entirety.

### FIELD

**[0003]** The present invention relates to methods for assessing and treating cancer, and in particular, canine lung cancers, and most particularly, canine pulmonary adenocarcinomas, adenosquamous and squamous cell carcinomas.

### BACKGROUND

**[0004]** Naturally occurring primary canine lung cancer is clinically challenging (1), with a disease course and underlying biology that resemble human lung cancer in never-smokers. Human never-smoker lung cancer accounts for 10% to 25% of lung cancers, causes approximately 26,000 deaths annually, and has a high incidence of erb-B family gene mutations such as those affecting epidermal growth factor receptor (EGFR). Although the incidence of smoking-related lung cancer is decreasing, lung cancer incidence in never-smokers is increasing (2). Never-smoker lung cancer is primarily non-small cell lung cancer (NSCLC), arising from lung tissue, as opposed to small cell lung cancer arising in bronchi of smokers. NSCLC histologies include adenocarcinoma (AC) and squamous cell carcinoma (SCC). The etiology of never-smoker lung cancer is also distinct from that of smokers. It is associated with factors including environmental exposures (secondhand smoke, radon, asbestos, arsenic, silica, and pollution) as well as age, sex, family history, and genetic loci (3). Unique genomic characteristics of human never-smoker lung cancer include low somatic mutation burden, enrichment for C:G>T:A transitions, and somatic activating point mutations or fusions affecting EGFR (45%), ALK (5%-11%), ROS (1.5%-6%), HER2 (3%-5%), and RET (2%) (4). The five-year overall survival is estimated at 23%, but outcomes are dependent on molecular subtype and treatment regimen. For example, EGFR inhibitors can improve outcomes in EGFR-mutant lung cancers; however, 85% of never-smoker lung AC and SCC cases are EGFR wild-type (WT) in the United States. Clinical trials of immune-checkpoint inhibitors have recently shown improved outcomes for human lung cancers, but analysis of large phase II immunotherapy trials suggests that benefits are limited in low-mutation-burden (<10 mutations/Mb) cases such as those found in never-smokers (5).

**[0005]** Lung cancer in pet dogs has limited standard of care beyond surgery, and little is known of canine lung cancer molecular underpinnings (1). Primary lung tumors typically arise in older dogs (>11 years) and resemble human NSCLC histotypes including canine pulmonary adenocarcinoma (cPAC), canine adenosquamous carcinoma (cPASC), and canine pulmonary squamous cell carcinoma (cPSCC). These subtypes collectively represent 13% to 15% of primary lung tumors (6,7). Patients are often diagnosed late with lesions incidentally discovered during routine geriatric evaluation or due to nonspecific symptoms including dyspnea (6% to 24%) and cough (52% to 93%) that do not manifest until the tumor is more than 3 centimeters (cm). The detection of canine lung cancers has significantly increased over the past 20 years not only because of improved animal healthcare and diagnostics, but also possibly due to increased companion animal exposures to pollutants. These tumors can be diagnostically challenging. Rates at which ultrasound or CT-guided fine-needle aspirates of the pulmonary mass provide cytologic diagnosis range from 38% to 90% of cases, varying broadly based on tumor accessibility and aspirate quality. At diagnosis, 71% of malignant canine lung tumors show signs of invasion and 23% show distant metastasis. Partial or complete lung lobectomy is standard of care, dependent on the extent of disease spread. Median survival is 345 days for localized disease without nodal involvement where surgical remission can be achieved, but only 60 days when nodes are involved. Responses to cytotoxic chemotherapy (cisplatin, vindesine, doxorubicin, and mitoxantrone) in the setting of disseminated disease are limited.

**[0006]** Targeted small molecules and immune-checkpoint inhibitors have not been extensively studied in part because the molecular underpinnings of canine lung cancer remain largely unknown. In naturally occurring canine NSCLC, although comprehensive genomic profiling has been limited, KRAS hotspot mutation prevalence estimates from targeted studies have varied from 0% to 25% (7-9). We have previously shown that EGFR mutation, overexpression, or phosphorylation is rare in cPAC compared with matched nonaffected chemotherapy-naïve lung tissue whereas significant overexpression and/or phosphorylation of PDGFR $\alpha$ , ALK, and HER2 are present (10).

### SUMMARY

**[0007]** A need exists for improved biological understanding and development of new models to fuel translational research in never-smoker lung cancer. Further, a need exists for methods determining a sensitivity of a subject to a HER2 inhibitor and identification of one or more markers that indicate sensitivity of the subject to the HER2 inhibitor. Methods are provided herein for assessing, characterizing, diagnosing and treating lung cancer and for comparative oncology techniques.

**[0008]** In some embodiments, methods for treating lung cancer in a subject are disclosed. A biological sample from the subject is analyzed for a mutation in HER2. If a HER2 V659E mutation is present, the patient is treated with an inhibitor of HER2. The HER2 inhibitor may be selected from the group comprising trastuzumab, neratinib, lapatinib, erlotinib, and pertuzumab. In various embodiments, the subject is canine, and the lung cancer is pulmonary adenocarcinoma. The biological sample may be a tumor sample or

a plasma sample. The step of analyzing the biological sample may comprise subjecting the sample to amplification and exome sequencing.

**[0009]** In various embodiments, the methods include receiving a biological sample from the subject, adding to a mixture comprising the sample a first primer consisting of SEQ ID NO: 1 and a second primer consisting of SEQ ID NO: 2, subjecting the mixture to conditions that allow nucleic acid amplification, detecting the presence of one or more markers selected from the group consisting of HER2 V659E, HER2 A664T, and HER2 K676E by detecting the nucleic acid amplification, and treating the subject with an inhibitor of HER2 if one or more of the markers is present. The detecting step may comprise sequencing a product of the nucleic acid amplification. The HER2 inhibitor may be selected from the group comprising trastuzumab, neratinib, lapatinib, erlotinib, and pertuzumab. The method may further include adding to the mixture a probe consisting of SEQ ID NO: 3, for example, prior to detecting the nucleic acid amplification.

**[0010]** In various embodiments, the methods of treating lung cancer in a subject include receiving a biological sample from the subject, analyzing the biological sample for one or more mutations selected from the group consisting of HER2 V659E, HER2 A664T, HER2 K676E, KRAS G12DN, SMAD4 D351Y/G, and TP53 R239Q/G, and administering, if one or more of the mutations is present, a therapeutically effective amount of a pharmaceutical composition selected from the group consisting of trastuzumab, neratinib, lapatinib, erlotinib, and pertuzumab. The step of analyzing the biological sample may comprise subjecting the biological sample to amplification and exome sequencing. In various embodiments, the subject is canine, and the lung cancer is pulmonary adenocarcinoma. The biological sample may be a tumor sample or a plasma sample.

**[0011]** Methods of characterizing lung cancer in a canine subject are disclosed. The methods may include the steps of receiving a biological sample from the subject, adding to a mixture comprising the biological sample a first primer consisting of SEQ ID NO: 1 and a second primer consisting of SEQ ID NO: 2, subjecting the mixture to conditions that allow nucleic acid amplification, detecting the presence of one or more markers selected from the group consisting of HER2 V659E, HER2 A664T, and HER2 K676E by detecting the nucleic acid amplification, and determining a sensitivity of the canine subject to a HER2 inhibitor if the one or more of the markers is present.

**[0012]** The foregoing features and elements may be combined in various combinations without exclusivity, unless expressly indicated otherwise. These features and elements as well as the operation thereof will become more apparent in light of the following description. It should be understood, however, the following description is intended to be exemplary in nature and non-limiting.

#### BRIEF DESCRIPTION OF THE DRAWINGS

**[0013]** The subject matter of the present disclosure is particularly pointed out and distinctly claimed in the concluding portion of the specification. A more complete understanding of the present disclosure, however, may best be obtained by referring to the detailed description and claims when considered in connection with the figures, wherein like numerals may denote like elements.

**[0014]** FIGS. 1A-1E illustrate the genomic landscape of primary canine lung cancer; FIG. 1A illustrates recurrent likely pathogenic somatic mutations in cancer genes identified in primary canine lung cancers through multi-platform sequencing; single nucleotide variants (SNVs) were determined from combined tumor/normal exome and/or amplicon sequencing across 88 total tumors and cell lines; FIG. 1B illustrates copy number variations (CVs) determined from tumor/normal exome data in five cPAC cases; FIG. 1C illustrates Somatic mutation burden (SNVs, CNVs, and SVs) identified by exome sequencing of five tumor/normal cPAC cases; FIG. 1D illustrates a distribution of somatic HER2 mutations within the HER2 protein identified in primary canine lung cancers; the length of the lollipops is proportional to the number of mutations found; FIG. 1E illustrates the detection of HER2 hotspot mutations in plasma from 11 canine primary lung cancer cases;

**[0015]** FIGS. 2A-2C illustrate results showing canine lung cancer HER2 mutant HER2 V659E constitutively activates downstream HER2 signaling and is associated with response to HER2 inhibitors in primary canine pulmonary adenocarcinoma (cPAC) cell lines; FIG. 2A illustrates downstream HER2 signaling in canine lung cancer cell lines; levels of phospho-Akt and Akt were assessed by Western blot under serum starvation in the presence and absence of EGFR activation by hNRG in HER2 V659E and HER2 WT cPAC cell lines; FIG. 2B illustrates canine lung cancer cell line sensitivity to neratinib; neratinib drug-dose-response studies in primary lung cancer cell lines; five canine cell lines (three HER2 WT and two HER2 V659E) and two human lung cancer positive controls with known HER2 activating mutations (BT474-HER2-amplified, and H1781-HER2 G776V) and HER2 inhibitor responses were treated with 14 neratinib doses ranging from 100  $\mu$ M to  $5.5 \times 10^{-2}$  nM for 72 hours with CellTiterGlo viability endpoints; survival is shown relative to DMSO vehicle control; FIG. 2C illustrates dose effect of the HER2 inhibitor neratinib on downstream AKT activation; phospho-AKT and AKT levels were assessed in two canine lung cancer cell lines—OSUK9PAPADO (HER2 WT) and OSUK9PAPADRI (HER2 V659E)—and compared to a well-characterized human lung cancer cell line (BT474, HER2-amplified) by Western blot under serum starvation in the presence of 5 doses (20-2000 nmol/L) of neratinib;

**[0016]** FIGS. 3A-3F illustrate extended clinical annotation of primary canine lung cancer patients; FIG. 3A shows affected breeds distribution; FIG. 3B shows age at diagnosis (Yr=years); FIG. 3C shows primary tumor location distribution; FIG. 3D shows sex distribution; FIG. 3E shows adenocarcinoma subtype distribution; FIG. 3F shows treatment of the canine lung cancer patients;

**[0017]** FIGS. 4A and 4B illustrate mutation signatures identified by exome sequencing in primary canine lung cancers; FIG. 4A illustrates the distribution of somatic single nucleotide mutation types in their trinucleotide context from tumor/normal exome sequencing of five cPAC cases; FIG. 4B illustrates the most common mutation signatures based on trinucleotide context and frequency of somatic single nucleotide mutations from tumor/normal exome sequencing of the five cPAC cases;

**[0018]** FIGS. 5A-5D illustrate the characterization of HER2 cellular location and function in primary canine lung cancer; FIG. 5A illustrates canine papillary adenocarcinoma with intense, complete, circumferential membrane (white arrow) and lateral cytoplasmic membrane (black arrow)

anti-HER2 antibody positive staining (brown) in a patient with wild-type HER2; FIG. 5B illustrates canine papillary adenocarcinoma with moderate cytoplasmic (black arrow) anti-HER2 antibody positive staining (light brown) in a patient with wild-type HER2,  $\times 40$ ; bar 50  $\mu\text{m}$ ; FIG. 5C illustrates anti-HER2 immunohistochemistry of a Grade 1 canine papillary adenocarcinoma wild type for HER2,  $\times 20$ ; FIG. 5D illustrates segmentation mark-up of the tumor from adjacent normal lung; tumor is identified by green, whereas red is area inside of tumor that contains no tissue, yellow represents areas of non-tumor such as necrosis or tumor stroma,  $\times 20$ ;

[0019] FIG. 6 illustrates canine lung cancer cell line sensitivity to lapatinib and shows four canine cell lines (three HER2 WT and one HER2 V659E) were treated with 14 lapatinib doses ranging from 100  $\mu\text{M}$  to  $5.5 \times 10^{-2}$  nM for 72 hours; survival rates were assessed by luminescence using Synergy Mx (Biotek plate reader) and expressed as the percentage of survival compared to DMSO vehicle control;

[0020] FIGS. 7A-7C illustrate a table of informatic tools utilized in primary canine lung cancer genomic analyses;

[0021] FIGS. 8A-8J illustrate a table of extended clinical and multiplatform annotation of primary canine lung cancer patients;

[0022] FIG. 9 illustrates somatic copy number plots derived from exome sequencing of five primary canine pulmonary adenocarcinomas (cPAC) and matched constitutional DNA; tumor copy number states determined by tCoNut analysis of tumors and matched constitutional DNA from five cPAC cases is shown with each canine chromosome plotted on the x-axis (shown in alternating green and black) and  $\log_2$  fold change shown on the y-axis;

[0023] FIGS. 10A-10H illustrate a table of somatic coding single nucleotide variants (SNVs) identified by exome sequencing of primary canine lung cancers;

[0024] FIGS. 11A-11L illustrate a table of somatic coding copy number variations (CNVs) identified by exome sequencing of primary canine lung cancers;

[0025] FIG. 12 illustrates a table of somatic coding structural variants (SVs) identified by exome sequencing of primary canine lung cancers;

[0026] FIGS. 13A-13G illustrates a table of canine genomic regions covered by custom amplicon panel;

[0027] FIGS. 14A-14B illustrate a table of somatic coding SNVs identified by panel sequencing of primary canine lung cancers;

[0028] FIG. 15 illustrates a table of germline SNPs in COSMIC Tier 1 cancer genes identified by exome and panel sequencing in primary canine lung cancers;

[0029] FIGS. 16A-16C illustrate a table of results of multi-platform validation of HER2 mutations;

[0030] FIG. 17 illustrates a table of non-invasive detection of HER2 V659E mutations in the plasma of primary canine lung cancer patients;

[0031] FIGS. 18A-18B illustrate a set of tables showing HER2 protein expression and quantification by immunohistochemistry;

[0032] FIG. 19 illustrates a comparison of HER2 mutant allele fractions measured using droplet digital PCR and targeted sequencing in tumor tissue; HER2 V659E was evaluated by ddPCR in tumor DNA samples in which these mutations were also detected using amplicon sequencing; a high correlation was observed between allele fractions measured using both techniques (Pearson's  $r$  0.976,  $p=0.0008$ );

[0033] FIGS. 20A-20B illustrate HER2 expression in primary canine lung cancer based on quantitative real-time PCR analyses; box plots are shown for HER2  $2^{(-\Delta\Delta\text{Ct})}$  expression fold-change relative to the housekeeping gene HPRT (x-axis) in 49 tumors and 14 matched normal lung tissues comparing; FIG. 20A illustrates normal lung tissue versus tumor tissue;

[0034] FIG. 20B illustrates normal lung tissue versus HER2-wild-type tumor tissue versus HER2-mutant tumor tissue;

[0035] FIG. 21 illustrates canine primary lung cancer cell line sensitivity to erlotinib; five canine cell lines (three HER2 WT and two HER2 V659E) and one human cell line BT474 (HER2 amp) were treated with 10 erlotinib doses ranging from  $5 \times 10^{-8}$  to 50  $\mu\text{M}$  for 72 hours with CellTiterGlo viability endpoints measured and shown as percent growth inhibition relative to DMSO vehicle control; and

[0036] FIG. 22 illustrates canine primary lung cancer cell line sensitivity to trastuzumab; five canine cell lines (three HER2 WT and two HER2V 659E) and one human cell line BT474 (HER2 amp) were treated with 10 trastuzumab doses ranging from  $1 \times 10^{-6}$   $\mu\text{g/ml}$  to 1000  $\mu\text{g/ml}$  for 72 hours with CellTiterGlo viability endpoints measured and shown as percent growth inhibition relative to PBS vehicle control. Relative survival was measured with respect of the sensitive cell line BT474.

#### DETAILED DESCRIPTION

[0037] It is to be understood that unless specifically stated otherwise, references to "a," "an," and/or "the" may include one or more than one and that reference to an item in the singular may also include the item in the plural. Reference to an element by the indefinite article "a," "an" and/or "the" does not exclude the possibility that more than one of the elements are present, unless the context clearly requires that there is one and only one of the elements. As used herein, the term "comprise," and conjugations or any other variation thereof, are used in its non-limiting sense to mean that items following the word are included, but items not specifically mentioned are not excluded.

[0038] The present disclosure characterizes the genetic underpinnings of naturally occurring canine lung cancers and identified novel recurring mutations including HER2 V659E mutations occurring in 37% of canine pulmonary adenocarcinomas. The present disclosure further includes a digital PCR assay for detection of these recurrent hotspot mutations, including HER2 mutations.

[0039] The sample in the disclosed method is preferably a biological sample from a subject. The term "sample" or "biological sample" is used in its broadest sense. Depending upon the embodiment of the invention, for example, a sample may comprise a bodily fluid including whole blood, serum, plasma, urine, saliva, cerebral spinal fluid, semen, vaginal fluid, pulmonary fluid, tears, perspiration, mucus and the like; an extract from a cell, chromosome, organelle, or membrane isolated from a cell; a cell; genomic DNA, RNA, or cDNA, in solution or bound to a substrate; a tissue; a tissue print, or any other material isolated in whole or in part from a living subject or organism. Biological samples may also include sections of tissues such as biopsy and autopsy samples, and frozen sections taken for histologic purposes such as blood, plasma, serum, sputum, stool, tears, mucus, hair, skin, and the like. Biological samples also include explants and primary and/or transformed cell cul-

tures derived from patient tissues. In some embodiments, sample or biological sample may include a bodily tissue, fluid, or any other specimen that may be obtained from a living organism that may comprise additional living organisms. The subject may be any organism subject or susceptible to lung cancer including mammals, further including canines or humans.

**[0040]** As used herein, the term “subject” or “patient” is used in its broadest sense and may refer to any vertebrate including, without limitation, humans and other primates (e.g., chimpanzees and other apes and monkey species), domestic mammals (e.g., dogs and cats), laboratory animals (e.g., rodents such as mice, rats, and guinea pigs), farm animals (e.g., cattle, sheep, pigs, goats and horses), and birds (e.g., domestic, wild and game birds such as chickens, turkeys and other gallinaceous birds, ducks, geese, and the like). In some implementations, the subject may be a mammal, preferably a canine or a human.

**[0041]** The term “extraction” as used herein refers to any method for separating or isolating the nucleic acids from a sample, more particularly from a biological sample, such as blood or plasma. Nucleic acids such as RNA or DNA may be released, for example, by cell lysis. Moreover, in some aspects, extraction may also encompass the separation or isolation of extracellular RNAs (e.g., extracellular miRNAs) from one or more extracellular structures, such as exosomes. Some embodiments of the invention include the extraction of one or more forms of nucleic acids from one or more samples. In some aspects, the extraction of the nucleic acids can be provided using one or more techniques known in the art. In other embodiments, methodologies of the invention can use any other conventional methodology and/or product intended for the isolation of intracellular and/or extracellular nucleic acids (e.g., DNA or RNA).

**[0042]** The term “nucleic acid” as referred to herein comprises all forms of RNA (mRNA, miRNA, rRNA, tRNA, piRNA, ncRNA), DNA (genomic DNA, mtDNA, cfDNA, ctDNA, cDNA), as well as recombinant RNA and DNA molecules or analogs of DNA or RNA generated using nucleotide analogues. The nucleic acids may be single-stranded or double-stranded. The nucleic acids may include the coding or non-coding strands. The term also comprises fragments of nucleic acids, such as naturally occurring RNA or DNA which may be recovered using one or more extraction methods disclosed herein. “Fragment” as referred to herein comprises a portion of nucleic acid (e.g., RNA or DNA).

**[0043]** An “allele” includes any form of a particular nucleic acid that may be recognized as a form of the particular nucleic acid on account of its location, sequence, or any other characteristic that may identify it as being a form of the particular gene. Alleles include but need not be limited to forms of a gene that include point mutations, silent mutations, deletions, frame shift mutations, single nucleotide polymorphisms (SNPs), inversions, translocations, heterochromatic insertions, and differentially methylated sequences relative to a reference gene, whether alone or in combination. An allele of a gene may or may not produce a functional protein; may produce a protein with altered function, localization, stability, dimerization, or protein-protein interaction; may have overexpression, under-expression or no expression; may have altered temporal or spatial expression specificity; or may have altered copy number (e.g., greater or less numbers of copies of the allele). An

allele may also be called a mutation or a mutant. An allele may be compared to another allele that may be termed a wild type form of an allele. In some cases, the wild type allele is more common than the mutant.

**[0044]** The term “housekeeping genes” as used herein is meant to refer to genes that encode protein products that are not connected to, involved in or required for processes specific to a disease state (e.g., cancer) in cells, and thus, exhibit a fixed expression level in diseased and healthy cells.

**[0045]** Generally, some embodiments of the invention may include assessing, determining, quantifying, or altering the expression of one or more markers. Expression may be assessed by any number of methods used to detect material derived from a nucleic acid template used currently in the art and yet to be developed. Examples of such methods include any nucleic acid detection method including the following nonlimiting examples, microarray analysis, RNA in situ hybridization, RNase protection assay, Northern blot, reverse transcriptase PCR, quantitative PCR, quantitative reverse transcriptase PCR, quantitative real-time reverse transcriptase PCR, droplet digital PCR, amplicon sequencing, reverse transcriptase treatment followed by direct sequencing, or any other method of detecting a specific nucleic acid now known or yet to be disclosed.

**[0046]** Some embodiments of the present invention can be used to identify, quantify, detect, assess, isolate, and/or augment expression levels of one or more markers. A marker may be any molecular structure produced by a cell, expressed inside the cell, accessible on the cell surface, or secreted by the cell. Some embodiments of the invention may include a method of comparing a marker in a sample relative to one or more control samples. A control may be any sample with a previously determined level of expression. A control may comprise material within the sample or material from sources other than the sample. Alternatively, the expression of a marker in a sample may be compared to a control that has a level of expression predetermined to signal or not signal a cellular or physiological characteristic. This level of expression may be derived from a single source of material including the sample itself or from a set of sources.

**[0047]** As used herein, “primer/probe set” refers to a grouping of a pair of oligonucleotide primers and an oligonucleotide probe that hybridize to a specific nucleotide sequence. Said oligonucleotide set consists of: (a) a forward discriminatory primer that hybridizes to a first location of a nucleic acid sequence; (b) a reverse discriminatory primer that hybridizes to a second location of the nucleic acid sequence downstream of the first location and (c) a fluorescent probe labeled with a fluorophore and a quencher, which hybridizes to a location of the nucleic acid sequence between the primers. In other words, a primer/probe set consists of a set of specific PCR primers capable of initiating synthesis of an amplicon specific to a nucleic acid sequence, and a fluorescent probe which hybridizes to the amplicon.

**[0048]** An “amplicon” refers to a nucleic acid fragment formed as a product of natural or artificial amplification events or techniques. For example, an amplicon can be produced by PCR, ligase chain reaction, or gene duplication.

**[0049]** The various and non-limiting embodiments of the PCR-based method detecting marker expression level as described herein may comprise one or more probes and/or primers. Generally, the probe or primer contains a sequence complementary to a sequence specific to a region of the

nucleic acid of the marker gene. A sequence having less than 60% 70%, 80%, 90%, 95%, 99% or 100% identity to the identified gene sequence may also be used for probe or primer design if it is capable of binding to its complementary sequence of the desired target sequence in marker nucleic acid.

**[0050]** An oligonucleotide may be any polynucleotide of at least 2 nucleotides. Oligonucleotides may be less than 10, 15, 20, 30, 40, 50, 75, 100, 200, or 500 nucleotides in length. While oligonucleotides are often linear, they may assume a circular or other two dimensional structure. Oligonucleotides may be chemically synthesized by any of a number of methods including sequential synthesis, solid phase synthesis, or any other synthesis method now known or yet to be disclosed. Alternatively, oligonucleotides may be produced by recombinant DNA based methods. In some aspects of the invention, an oligonucleotide may be 2 to 1000 bases in length. In other aspects, it may be 5 to 500 bases in length, 5 to 100 bases in length, 5 to 50 bases in length, or 10 to 30 bases in length. One skilled in the art would understand the length of oligonucleotide necessary to perform a particular task. Oligonucleotides may be directly labeled, used as primers in PCR or sequencing reactions, or bound directly to a solid substrate as in oligonucleotide arrays. For example, as described in greater detail herein, in some aspects of the invention, a first reagent and a second reagent can be used to detect HER2 mutations, such as HER2 V659. In some embodiments, the first and/or the second reagents may comprise one or more oligonucleotides (e.g., primers) that can specifically bind to DNA, RNA, and/or cDNA to detect the presence and/or expression of nucleic acids that correspond to HER2 V659 (SEQ ID NOS: 1 and 2).

**[0051]** As used herein, “digital PCR” refers to an assay that provides an end-point measurement that provides the ability to quantify nucleic acids without the use of standard curves, as is used in real-time PCR. In a typical digital PCR experiment, the sample is randomly distributed into discrete partitions, such that some contain no nucleic acid template and others contain one or more template copies. The partitions are amplified to the terminal plateau phase of PCR (or end-point) and then read to determine the fraction of positive partitions. If the partitions are of uniform volume, the number of target DNA molecules present may be calculated from the fraction of positive end-point reactions using Poisson statistics, according to the following equation (1):

$$\lambda = -\ln(1-p) \quad (1)$$

wherein  $\lambda$  is the average number of target DNA molecules per replicate reaction and  $p$  is the fraction of positive end-point reactions. From  $\lambda$ , together with the volume of each replicate PCR and the total number of replicates analyzed, an estimate of the absolute target DNA concentration is calculated. Digital PCR includes a variety of formats, including droplet digital PCR, BEAMing (beads, emulsion, amplification, and magnetic), and microfluidic chips.

**[0052]** “Droplet digital PCR” (ddPCR) refers to a digital PCR assay that measures absolute quantities by counting nucleic acid molecules encapsulated in discrete, volumetrically defined, water-in-oil droplet partitions that support PCR amplification (Hinson et al., 2011, Anal. Chem. 83:8604-8610; Pinheiro et al., 2012, Anal. Chem. 84:1003-1011). A single ddPCR reaction may be comprised of at least 20,000 partitioned droplets per well.

**[0053]** A “droplet” or “water-in-oil droplet” refers to an individual partition of the droplet digital PCR assay. A droplet supports PCR amplification of template molecule(s) using homogenous assay chemistries and workflows similar to those widely used for real-time PCR applications (Hinson et al., 2011, Anal. Chem. 83:8604-8610; Pinheiro et al., 2012, Anal. Chem. 84:1003-1011).

**[0054]** Droplet digital PCR may be performed using any platform that performs a digital PCR assay that measures absolute quantities by counting nucleic acid molecules encapsulated in discrete, volumetrically defined, water-in-oil droplet partitions that support PCR amplification. The strategy for droplet digital PCR may be summarized as follows: a sample is diluted and partitioned into thousands to millions of separate reaction chambers (water-in-oil droplets) so that each contains one or no copies of the nucleic acid molecule of interest. The number of “positive” droplets detected, which contain the target amplicon (i.e., nucleic acid molecule of interest), versus the number of “negative” droplets, which do not contain the target amplicon (i.e., nucleic acid molecule of interest), may be used to determine the number of copies of the nucleic acid molecule of interest that were in the original sample. Examples of droplet digital PCR systems include the QX100™ Droplet Digital PCR System by Bio-Rad, which partitions samples containing nucleic acid template into 20,000 nanoliter-sized droplets; and the RainDrop™ digital PCR system by RainDance, which partitions samples containing nucleic acid template into 1,000,000 to 10,000,000 picoliter-sized droplets.

**[0055]** The term “template” refers to nucleic acid originating from a sample that is analyzed for the presence of a marker of interest. In contrast, “background template” or “control” is used in reference to nucleic acid other than sample template that may or may not be present in a sample. Background template is most often inadvertent. It may be the result of carryover, or it may be due to the presence of nucleic acid contaminants sought to be purified out of the sample. For example, nucleic acids from organisms other than those to be detected may be present as background in a test sample.

**[0056]** “Amplification” includes a special case of nucleic acid replication involving template specificity. Amplification may be a template-specific replication or a non-template-specific replication (i.e., replication may be specific template-dependent or not). Template specificity is here distinguished from fidelity of replication (synthesis of the proper polynucleotide sequence) and nucleotide (ribo- or deoxyribo-) specificity. Template specificity is frequently described in terms of “target” specificity. Target sequences are “targets” in the sense that they are sought to be sorted out from other nucleic acid. Amplification techniques have been designed primarily for this sorting out.

**[0057]** The present invention further provides kits to be used in assessing the expression of a marker in a subject to assess the risk of developing disease, diagnosing the subject as having a stage of the disease, or determining to which stage the disease has progressed. Kits include any combination of components that facilitates the performance of an assay. A kit that facilitates assessing the expression of the markers may include suitable nucleic acid-based and immunological reagents as well as suitable buffers, control reagents, and printed protocols.

**[0058]** Overall, some embodiments of the invention include systems and methods for the diagnosis of a condi-

tion, assessing the prognosis of the condition, and treating the condition. The one or more markers can be used to diagnose and/or assess the likely sensitivity of the cancer to a particular therapy or pharmaceutical composition. For example, the method of treatment may comprise determining an expression of a marker, such as a HER mutation, for example HER2 V659, to determine sensitivity of the cancer to an anti-HER agent, and subsequently administering to the patient the anti-HER agent, such as a tyrosine kinase inhibitor, for example neratinib, lapatinib, and erlotinib or a HER2 recombinant monoclonal antibody, for example trastuzumab.

**[0059]** Moreover, some embodiments of the invention may further provide treating a cancer, such as non-small cell lung cancer. Some embodiments of the invention may include the administration of one or more pharmaceutical compositions to a subject that has been diagnosed with cancer. Such pharmaceutical compositions may take any physical form necessary depending on a number of factors including the desired method of administration and the physicochemical and stereochemical form taken by the compound or pharmaceutically acceptable salts of the compound. Such physical forms include a solid, liquid, gas, sol, gel, aerosol, or any other physical form now known or yet to be disclosed.

**[0060]** The following examples are given for purely illustrative and non-limiting purposes of the present invention.

#### EXAMPLES

**[0061]** We have discovered recurrent somatic HER2 (ERRB2) point mutations in 38% of canine pulmonary adenocarcinomas (cPAC) which confer both constitutive activation of proliferative signaling and also sensitivity to the HER2 inhibitors lapatinib and neratinib.

**[0062]** Through multi-platform sequencing of 90 primary canine lung tumors or cell lines, we discovered somatic, coding HER2 (ERRB2) point mutations in 38% of canine pulmonary adenocarcinomas (cPAC, 28 of 74), but none in adenocarcinomas (cPASC, 0 of 11) or squamous cell carcinomas (cPSCC, 0 of 3). In cPAC, recurrent somatic mutation of TP53, SMAD4, PTEN, and VHL were also identified. cPACs assessed by exome sequencing displayed a low mutation burden (median 64 SNVs, 19 CNVs and 1 SV). The majority (93%) of HER2 mutations are hotspot V659E transmembrane domain (TMD) mutations comparable to activating mutations at this same site in human cancer. Other HER2 mutations identified in this study were located in the extracellular and TMD. The HER2 V659E mutation was detected in the plasma of 33% (2 of 6) of dogs with localized tumors bearing this mutation. HER2 V659E correlated with constitutive phosphorylation of Akt in cPAC cell lines and HER2 V659E-mutant lines displayed hypersensitivity to the HER2 inhibitors lapatinib and neratinib relative to HER2 wild-type cell lines. These findings have immediate translational and comparative relevance for lung cancer and mutant HER2 inhibition.

#### Methods

**[0063]** Sample Collection: Tumors and cell lines from 89 dogs from the Canine Comparative Oncology and Genomics Consortium (CCOGC) (11) and The Ohio State University (OSU) College of Veterinary Medicine Biospecimen Repository were included. Board-certified veterinary

pathologists confirmed tumor diagnosis based on histopathology. Tumor and normal tissue samples were flash frozen in liquid nitrogen or formalin-fixed and paraffin-embedded (FFPE). Cell lines were maintained in RPMI 1640 with GlutaMAX™ (Gibco™, Thermo Fisher Scientific, #61870036) supplemented with 10% heat-inactivated fetal bovine serum at 37° C. and 5% CO<sub>2</sub> and passaged at 90% confluence. Cell lines with known passage data (except BACA) were sequenced within the first eight passages of derivation and subsequently expanded for phenotypic studies, and were authenticated by IDEXX BioResearch (Columbia, Mo.) using the Cell Check Canine STR Profile and Interspecies Contamination Test or by Nkx2 (or TTF-1) RT-PCR. Human cell lines included BT474 (ATCC #HTB20, HER2 focal amplification) and H1781 (ATCC #CRL-5894, HER2 G776V). Blood for cell-free DNA (cfDNA) and germline DNA extraction was collected in 10 ml K<sub>2</sub> EDTA Blood tubes (Thermo Fisher Scientific #22-253-145). Plasma separation was performed at room temperature within 1 hour (2× serial centrifugation at 2000 rpm×15 minutes). Plasma aliquots were stored frozen at -80° C. DNA extraction from plasma, white blood cells and tissue was performed with MagMAX Cell-Free DNA Isolation Kit (Thermo Fisher Scientific #A29319), DNeasy Blood and Tissue Kit (QIAGEN #69504) and Qiagen All-Prep DNA/RNA Mini Kit (QIAGEN #80204), respectively.

**[0064]** Exome Sequencing and Analysis: Informatic tools, versions, and flags are shown in FIGS. 7A-7C. We utilized a custom Agilent SureSelect canine exome capture kit with 982,789 probes covering 19,459 genes. Exome libraries were sequenced on the Illumina HiSeq2000 producing paired end reads of 85 bp. FASTQ files were aligned to the canine genome (CanFam3.1) using BWA v0.7.8. Aligned BAM files were realigned and recalibrated using GATK v3.3.0 and duplicate pairs were marked with Picard v1.128. Somatic copy number variants (CNVs), and structural variants (SVs) were called with tCoNUT and DELLY v0.76. Somatic single nucleotide variants (SNV) were identified from two or more of the following callers: Seurat v2.6, Strelka v1.0.13 and MuTect v1.1.4. Germline SNVs were called using Haplotype Caller (GATK v3.3.0) and Freebayes. Variant annotation was performed with SnpEff v3.5. The SomaticSignatures R package was used to identify mutation signatures.

**[0065]** Targeted Amplicon Sequencing and Analysis: The present disclosure, and method used herein, includes a custom-developed canine cancer amplicon sequencing panel consisting of 281 amplicons targeting exons and hotspot regions in 57 genes. Using this panel, the amplification was performed independently in each drop and resulted in amplicon sizes ranging from 91 to 271 base pair (bp) (FIGS. 13A-13G). Primers were pooled in two multiplexed pools to separate adjacent amplicons and any amplicons that showed cross-amplification using in silico PCR. Sequencing libraries were prepared using digital PCR amplification following the manufacturer's protocols for the ThunderBolts Cancer Panel (RainDance Technologies) with modifications (52). Sequencing of the amplicons was performed on the Illumina MiSeq generating paired-end 275 bp reads. Sequencing reads were demultiplexed and extracted using Picardtools. Sequencing adapters were trimmed using ea-utils and fastq files were assessed for quality using FASTQC. Sequencing reads were aligned to CanFam3.1 using BWA-mem and converted to BAM using Samtools (53). Scripts were devel-

oped based on Samtools and were used to create pileups for every sample with attached amplicon IDs. The pileups were analyzed in R to call SNVs and indels (insertions/deletions). For each potential non-reference allele at each targeted locus in a sample, we evaluated the distribution of background noise across all other sequenced samples. Variants were filtered based on stringent cutoffs to enable calling high-confidence somatic variants. To call a variant, we required the observed non-reference allele is an outlier from the background distribution with a Z-score >5. The variant filters included tumor depth ( $\geq 100\times$ ), allele frequency ( $\geq 10\%$ ), number of reads supporting the variation ( $\geq 10$ ), and germline background ( $< 0.01$ ) or allele fraction in the germline sample ( $< 1\%$ ). Variants were manually curated by visualization in IGV v2.3.71.

**[0066]** Sanger Sequencing: Twenty-three primer pairs covering all exons of HER2 were designed using Primer 3 including a universal M13 tag. Amplicons were Sanger sequenced at the DNASU sequencing facility at Arizona State University on an ABI 3730XL (Applied Biosystems, Foster City, Calif.) and analyzed with Mutation Surveyor DNA Variant Analysis Software (SoftGenetics, State College, Pa.).

**[0067]** HER2 Inhibitor Drug Dose-response Studies: HER2 inhibitors lapatinib (Selleckchem, #S2111), neratinib (Puma Biotechnology, Los Angeles, Calif.), and trastuzumab (Selleckchem, #A2007), as well as the EGFR inhibitor erlotinib (Selleckchem, #S1023) were assessed in 10-16 point 72 hour drug-dose response screens (from  $2\times 10^{-7}$  nM to 100  $\mu$ M) with CellTiter-Glo<sup>®</sup> luminescent cell viability assay (Promega, #G7570) endpoints. Cells were cultured in RPMI supplemented with 10% FBS and 1% Penicillin/Streptomycin. Luminescence was read using Synergy Mx (Biotek) plate reader. Six replicates were performed for each dose. Curve-fitting and  $IC_{50}$  calculations were performed using GraphPad Prism v7.00 (GraphPad Software).

**[0068]** Droplet Digital PCR: HER2 V659E genotyping was performed on tumor samples and plasma cell-free DNA with droplet digital PCR (ddPCR). 50 microliter (up reactions contained 2xKAPA PROBE FAST Master Mix (Kapa Biosystems, #KK4701), 200  $\mu$ M dNTP Mix (New England BioLabs Inc, #N04775), 1x Droplet Stabilizer (RainDance Technologies, #30-00826), 1  $\mu$ M pooled primer mix (IDT), 1  $\mu$ M mutant (FAM labeled) or wild type (TET labeled) HER2 V659E probe (IDT), and 21.75  $\mu$ L of template DNA. Each reaction was partitioned into 10,000,000 droplets using the RainDrop Digital PCR Source (RainDance). PCR amplification was performed as follows: 1 cycle 3 min at 95° C., 50 cycles 15 sec at 95° C. and 1 min at 60° C. with a 0.5° C./sec ramping from 95° C. to 60° C., 1 cycle 98° C. for 10 min and hold at 4° C. Droplet fluorescence was measured using RainDrop Digital PCR Sense and analyzed using accompanying RainDrop Analyst II Software v.1.0 (RainDance).

**[0069]** The primer and probe sequences used for HER2 V659 detection in ctDNA were forward primer: 5'-CC-CACGACCACAGCCA-3' (SEQ ID NO: 1), reverse primer: 5'-CCCTGTGACATCCATCATTGC-3' (SEQ ID NO: 2) and probe: 5'-CAGAATGCCC(T/A)CCACAGC-3'(SEQ ID NO: 3).

**[0070]** TABLE 1 shows an assay for the detection of HER2 V659, including primer and probe sequences.

TABLE 1

	Seq Type	Sequence	SEQ ID NO
HER2 V659 detection in ctDNA	Forward Primer	CCCACGACCACAGCCA	1
HER2 V659 detection in ctDNA	Reverse Primer	CCCTGTGACATCCATCATTGC	2
HER2 V659 detection in ctDNA	Probe	CAGAATGCCC (W) CCACAGC W = A/T Alternatively written as: CAGAATGCCC (T/A) CCACAGC	3

**[0071]** qRT-PCR: cDNA was obtained by reverse transcription with iScript (Biorad, #1708891) and samples were subjected to HER2 (target) and HPRT1 (reference) amplification in a QuantStudio™ 6 Flex Real-Time PCR System under standard conditions with Syber Green technology (KapaBiosystems, #KK4602).

**[0072]** Primer sequences were: HER2-Forward: 5'-CATCTGCACCATTGATGTCTA-3' (SEQ ID NO: 4), HER2-Reverse: 5'-GGCCCAAGTCTTTCATTCTGA-3' (SEQ ID NO: 5), HPRT1-Forward: 5'-GCAGCCCCAGCGTCGTGATT-3' (SEQ ID NO: 6), HPRT1-Reverse: 5'-CATCTCGAGCAAGCCGCTCAGT-3' (SEQ ID NO: 7).

**[0073]** Data was analyzed with Quantstudio Real Time PCR software v1.1. Values for  $\Delta C_t$ ,  $\Delta\Delta C_t$ , and fold changes were calculated as follows:  $\Delta C_t = C_t \text{ HER2} - C_t \text{ HPRT1}$ ;  $\Delta\Delta C_t = \Delta C_t \text{ tumor sample} - \Delta C_t \text{ average of normal samples}$ ; and fold change =  $2^{(-\Delta\Delta C_t)}$ .

**[0074]** TABLE 2 shows an assay for amplification of the HER2 target, including the primer sequences used for qRT-PCR.

TABLE 2

	Seq Type	Sequence	SEQ ID NO
HER2-Forward	Forward Primer	CATCTGCACCATTGATGTCTA	4
HER2-Reverse	Reverse Primer	GGCCCAAGTCTTTCATTCTGA	5
HPRT1-Forward	Forward Primer	GCAGCCCCAGCGTCGTGATT	6
HPRT1-Reverse	Reverse Primer	CATCTCGAGCAAGCCGCTCAGT	7

**[0075]** Immunohistochemistry: HER2 protein expression was evaluated on FFPE sections (4  $\mu$ m) of normal lung and tumor mounted on SuperFrost™ Plus glass slides (Fisher Scientific #12-550-15). Slides were deparaffinized in xylene and rehydrated in an ethanol gradient. Antigen retrieval was performed with 1 mM EDTA adjusted to pH 9.0. An autostainer (Dako, model 53400) was used to carry out immunostaining. A HER2 rabbit monoclonal antibody (Cell Signaling Technology, #4290) was used at 1:400 dilution followed by secondary biotinylated rabbit anti-goat IgG (Vector Laboratories, BA-1000) diluted 1:200. Detection was performed with VECTASTAIN® Elite® ABC System



(#PK-6100). IHC positive controls for HER2 tyrosine kinase receptor expression were single tissue samples of two canine complex mammary carcinomas (54). Negative controls were performed on all tissues using a universal rabbit negative isotype control not directed against any known antigen (Dako, #IR600).

**[0076]** Quantitative Image Analysis: Immunostained and control 1x3-inch microscope slides were scanned at 40x on a high-resolution Scanscope XT (Leica Biosystems). For quantification of immunoreactivity, images were imported into Visiopharm Image Analysis software (Visiopharm, Horsholm, Denmark version 2017.27.0.3313), segmented into areas of tumor, necrosis, and normal lung tissue using color labels for each tissue type. HER2 connectivity was scored using the modified 10007-HER2, Breast Cancer APP (Visiopharm). Thresholds were adjusted to match specimen HER2 stain intensities for accurate scoring. Area ( $\mu\text{m}^2$ ) was quantified for each tissue type and percentages derived from specimen total tissue area. Tumor areas were further segmented into staining and non-staining categories and their percentages were calculated based on total tumor area in  $\mu\text{m}^2$ . Maximum, mean, and minimum intensities were also quantified using a built-in software calculation. Staining is expressed as percentage of stain present with 100% equal to black (maximum dark brown) and 0% equal to white (no stain present). Initial thresholds and tissue types were established and mark-ups reviewed in consultation with a pathologist board-certified by the ACVP to ensure accurate measurements and to differentiate between tissue types.

**[0077]** Immunoblot Analyses: Subconfluent cells were serum starved overnight, then treated with 20 nM neuregulin for 15 min prior to harvest. Cells were lysed in RIPA buffer with cOmplete™ Mini Protease Inhibitor (Roche, #11836153001) and PhosSTOP™ (Roche, #4906845001) and loaded in Laemmli buffer at 1  $\mu\text{g}/\mu\text{l}$ . Samples were separated on 4-15% SDS-PAGE Criterion Gels (BioRad, #5671085) and transferred to Immobilon-FL PVDF membrane (MilliporeSigma, #IEVH7850). Membranes were blocked for 1 hour in LiCor blocking buffer and incubated with primary antibody at 4° C., overnight, followed by fluorescence-conjugated secondary antibodies. Membranes were scanned using the LiCor Odyssey CLx instrument. Primary antibodies were AKT (CST #4691S, 1:1000), phospho-AKT (CST #4060P, 1:1000), and  $\beta$ -actin (CST #4970S, 1:1000).

## Results and Discussion

**[0078]** The results herein describe the genomic landscape of naturally occurring primary canine lung cancer. In order to map the genomic landscape of canine lung cancer, we undertook multi-platform next-generation sequencing of 88 NSCLC cases including 77 tumor/normal matched pairs and 11 cell lines (TABLE 3). The cohort included 74 cPAC (Canine Pulmonary Adenocarcinoma) samples, 11 cPASC (Canine Pulmonary Adenocarcinoma) samples, and 3 cSCC (Canine Squamous Cell Carcinoma) samples. Labrador Retrievers represented the most commonly affected pure breed dog (21%) with mixed breeds (25%) and multiple other single pure breeds. The predominant cPAC subtype was papillary adenocarcinoma (62%). The cohort was gender-balanced (52% females) and primarily neutered/spayed (92%) with a median age at diagnosis of 11 years.

Smoking status in the pet's household was not available. Extended clinical annotation is shown in FIGS. 3A-3F and FIGS. 8A-8I.

TABLE 3

Genomic analyses performed in primary canine lung cancer		
Analysis	Samples analyzed*	Type of alteration
Platform Exome	5 cPAC and matching normal	Germline and somatic SNVs, CNVs, and SVs in coding regions
Amplicon	61 cPAC and matching normal**, 8 cell lines	Germline and somatic SNVs in 53 cancer genes
Amplicon	10 cPASC and matching normal, 1 cell line	Germline and somatic SNVs in 53 cancer genes
Amplicon	2 cSCC and matching normal, 1 cell line	Germline and somatic SNVs in 53 cancer genes

\*an additional cell line (OSUK9PADRi) was analyzed by Sanger sequencing  
 \*\*all matching normal samples were available except one (CCB30381).

**[0079]** In order to identify somatic point mutations, copy number changes, and translocations we first sequenced the coding genomic regions of five cPAC tumors and matching normal samples using a custom Agilent SureSelect canine exome capture kit comprising 982,789 probes covering 19,459 genes. Tumors were exome sequenced with a mean target coverage of 298x, and matching normal samples were exome sequenced with a mean target coverage of 263x, each with 99% of target bases covered  $\geq 40\times$  (TABLE 4). TABLE 4 shows a table of sequencing metrics for primary canine lung cancer exome analysis, where the metrics were obtained using picardtools.

TABLE 4

Sequencing metrics for primary canine lung cancer exome analysis.		
Metrics	Normal	Tumor
Total number of reads	1,074,194,664	1,185,003,340
Average number of reads (range)	214,838,933 (162,303,724-255,845,742)	237,000,668 (217,580,754-245,842,622)
% of passing filter (PF) reads	100%	100%
Mean % of PF reads aligned (range)	99.79% (99.78-99.80%)	99.18% (96.68-99.815)
Mean target coverage (range)	263.5 (204.11-313.46)	298.79 (274.02-311.19)
% of bases at 40X	98.54 (97.92-98.97%)	98.66% (98.23-98.84%)

**[0080]** A total of 648 high confidence somatic SNVs (median 64, range 37-406), 165 focal copy number variants (CNVs) (median 19, range 0-116), and 3 structural variants (SVs) (median 1, range 0-1) were identified (FIGS. 1A-1C, 10A-10H, 11A-11L, and 12). The average tumor mutation burden (TMB) for somatic point mutations per haploid callable megabase (Mb) in these cases was 2.04 mutations/Mb (range 0.58-6.38). Among these somatic variants, we identified mutations in genes whose human orthologs have been implicated in human cancer according to COSMIC (11) Tiers 1 and 2 including somatic SNVs (FIGS. 10A-10H), focal CNVs (FIG. 1B and FIGS. 11A-11L), SVs and numerical chromosomal changes (whole chromosome or arm-level

gains/losses) (FIG. 9). The sole gene bearing recurrent nonsynonymous SNVs was HER2 (80%) with the missense mutation V659E occurring in three cases and the missense mutation K676E in a fourth case (FIG. 1D). No HER2 amplifications were detected in these five tumors.

**[0081]** FIGS. 4A and 4B show the assessed somatic point mutation signatures according to their trinucleotide context (12, 13). The most common signature in these five cases was the age-associated COSMIC Signature 1A in 4 of 5 cases (80%). FIG. 4B shows COSMIC Signature 1A (C>T substitutions at NpCpG trinucleotides that are associated with age) was present in four cases. COSMIC Signature 2, C>T and C>G substitutions at TpCpN, associated with APOBEC cytidine deaminase activity was present in two cases, CCB050227 and OSU431895.

**[0082]** To identify somatic point mutations across a broader cohort of canine lung cancers, we used a custom canine cancer amplicon-based next generation sequencing panel (FIGS. 13A-13G) in 73 additional lung tumors (61 cPAC, 10 cPASC, 2 cPSCC), two previously exome-sequenced tumors with matched normal tissue, and 10 cell lines (8 cPAC, 1 cPASC, and 1 cPSCC). These cases were sequenced to an average depth of 3,383× (TABLE 5).

TABLE 5

Sequencing metrics for primary canine lung cancer amplicon analysis	
Metrics	
Number of amplicons	281
Number of genes	53
Number of amplicons passing threshold	264
Median sample depth (range)	158 (64-19640)
Median amplicon depth (range)	1989 (1-9466)

**[0083]** A median of 1 somatic coding point mutation (range 0-3) within sequenced panel regions was identified across all cases. Likely pathogenic recurrent point mutations included HER2 V659E (29.8%), KRAS G12DN (3.4%), SMAD4 D351Y/G (3.4%) and TP53 R239Q/G (2.2%) (FIGS. 14A and 14B). Two additional somatic missense mutations in HER2 were identified in single cases, including A664T and K676E (FIG. 1D). Overall, recurrently mutated genes containing somatic potentially pathogenic SNVs included TP53 (12.5%), PTEN (5.7%), SMAD4 (4.5%), KRAS (4.5%), VHL (3.4%) and HRAS (2.3%).

**[0084]** Based on both exome and amplicon sequencing, we evaluated germline SNPs to identify putatively pathogenic rare variants (i.e. those not previously identified in dogs based on review of presence in dbSNP 151 (14) and/or >10% frequency in DogSD (15) in 81 genes potentially associated with susceptibility to human lung cancer (16). We identified nine rare putatively pathogenic SNPs in five dogs in the genes CHRNA3, CYP1B1, DNAH11 and HER2 (FIG. 15). Of these SNPs, the only variant with an equivalent in its human orthologous gene was DNAH11 R1460W corresponding to human DNAH11 R1444W (rs1035326227, MAF<0.01%). The human SNP has not been associated with disease. HER2 V1189I variants occurred in two cases without somatic HER2 tumor mutations. The human orthologous position, V1184, has not shown human variation. The canine variant has been identified in 4% of cases in DogSD and

based on functional effect prediction (FATHMM), it is likely neutral. None of the genes bearing rare SNPs showed second hits in tumor tissue.

**[0085]** We additionally performed matched tumor/normal amplicon sequencing to evaluate the genomic landscapes of 11 cPASC and 3 cPSCCs, subtypes which are under-studied entities in dogs and humans, especially in never-smokers (FIG. 1A and FIGS. 14A-14B). In contrast with cPAC, no HER2 mutations were identified in these tumors. In cPASC, HRAS Q61L and KRAS Q61K each occurred in one case. Thus 18% of cases bore RAS hotspot mutations. PTEN stop gains additionally occurred in 2 of 11 (18%) cases at high tumor allele frequencies and were exclusive with RAS mutations. Additional likely pathogenic somatic mutations also occurred in a single cancer gene in a single tumor each including EGFR A726T, MET M1269V, TP53 R147C, and VHL P97L. Finally, while no recurrent mutations were identified in the three cPSCCs, we identified one case with a somatic BRAF V588E and another bearing PTPN11 G503V.

**[0086]** The results herein describe that HER2 is frequently mutated in canine pulmonary adenocarcinoma (cPAC).

**[0087]** HER2 was the most frequently mutated gene in our multi-platform next generation sequencing cohort, with missense mutations occurring exclusively in cPACs (27/74, 36.5%, two mutations occurring in a single patient) (FIG. 1A). No HER2 insertions were identified. We additionally identified a HER2 mutation in the cell line OSUK9PAPADr solely by Sanger sequencing of the codon 659 locus. We thus identified 29 total HER2 mutations overall (FIG. 1D). In 24 cases, the HER2 variants were evaluated on at least two platforms including exome sequencing, amplicon sequencing, Sanger sequencing, and/or droplet digital PCR (ddPCR) (FIGS. 16A-16C). The HER2 variant tumor allele fraction (AF) median by amplicon sequencing was 21.3% (range 8.4-51.9%). All low allele fraction (<20%) cases identified by amplicon sequencing were also validated by Sanger and/or ddPCR. Notably, one cell line, OSUK9PAPADO, contained a low AF HER2 V659E variant (AFs of 15% by amplicon and 16% by ddPCR) during early short-term culture (passage 4) that was no longer detectable by Sanger sequencing or ddPCR in later passages (passage 15). Importantly, passage 15 was utilized for all functional studies described below and it was thus considered HER2 WT in this setting. Overall, V659E missense mutations located in the HER2 TMD occurred in 93.3% of HER2-mutant cases. Additional HER2 mutations included A664T (OSU419040) and K676E (CCB050354), which have not been previously described in orthologous human HER2 regions. In some cases, HER2 mutations co-occurred with mutations in TP53, SMAD4, PTEN, VHL, AKT1 or KDR.

**[0088]** The results herein describe that HER2 mutations are detectable in canine plasma.

**[0089]** Cell-free tumor DNA (ctDNA) in plasma has been increasingly used for noninvasive genotyping in human cancer patients (17). To develop a canine blood test that could rapidly identify dogs with HER2-mutant lung cancer, we investigated whether cPAC HER2 hotspot mutations are detectable in ctDNA. We evaluated plasma from 11 dogs, 5 with HER2-wild-type tumors and 6 with HER2 V659E tumors using droplet digital PCR (ddPCR) (FIG. 17). In order to evaluate assay performance (specificity), we first analyzed wild-type tumor samples, plasma DNA from unre-

lated commercially available canine plasma samples and template-free controls to establish assay specificity (Bioreclamation/VT #BGLPLEDTA-100-P-m). Using uniform gating for all experiments, we found 1 of 7 template-free samples showed 1 wild-type droplet and no samples showed any evidence of mutant DNA amplification. In wild-type tumor and plasma DNA samples, 2 of 8 samples showed 1 mutant droplet each. Based on these results, we required at least 3 mutant droplets to confidently detect HER2 V659E. To confirm mutation detection and quantitative performance, we analyzed and detected HER2 V659E in 6 of 6 positive control tumor DNA samples where we had previously identified V659E mutations using amplicon sequencing. In these samples, we observed a high correlation between allele fractions measured using amplicon sequencing and ddPCR (Pearson's  $r = 0.976$ ,  $p = 0.0008$ ) (FIG. 19). In 11 plasma samples from dogs with cPAC tested using ddPCR, median total cell-free DNA concentration was 3.7 ng/mL plasma (range 0.7-23.0) (FIG. 17). Requiring at least three mutant droplets to support mutation detection and testing cfDNA equivalent to 435  $\mu$ L plasma, the median limit of detection (LoD) for mutation allele fraction was calculated at 0.61% (range 0.10%-3.11%). HER2 V659E mutations were detected in 2 of 6 plasma samples from dogs with HER2 V659E-positive tumors at 1.9% and 2.3% allele fractions. HER2 V659E was not detected in any plasma samples from dogs with HER2 WT tumors, confirming assay specificity (FIG. 1E). Sensitivity for mutation detection in this cohort may be limited due to low total cfDNA concentration and amounts analyzed.

**[0090]** The results herein describe HER2 expression in cPAC.

**[0091]** In human cancers, HER2 bears activating point mutations, copy number gains/amplifications, and RNA and protein overexpression. Amplification and overexpression are typically mutually exclusive with point mutations. HER2 copy number was first determined in the five exome-sequenced cases (FIG. 9 and FIGS. 11A-11L). No numerical CFA9 gains or focal HER2 amplifications were detected. However, these cases predominantly bore somatic putatively activating point mutations and might not be expected to contain concomitant gains. Therefore, we evaluated HER2 RNA and protein expression by qRT-PCR and IHC. RNA samples from 49 lung tumors (nine HER2-mutant) were evaluated alongside 14 normal lung tissue samples distal to tumor areas but from the same lung lobe. Median HER2 expression fold-change relative to expression of the housekeeping gene HPRT in normal lung samples was 1.06 (range 0.28-4.11) and in tumors was 0.85 (range 0.07-4.50) (FIGS. 20A-20B). No significant difference in relative HER2 expression was observed between tumor and normal or HER2-mutant and HER2 WT groups.

**[0092]** Additionally, in order to quantify HER2 protein expression in cPAC, digital image analysis was performed on eight tumors from FFPE. Three of the samples bore the HER2 V659E hotspot mutations, one bore HER2 A664T, and four were HER2 WT. All cases were positive for HER2 staining with homogeneous and diffuse staining of tumor cell cytoplasm and cell membrane, but no staining in adjacent stroma or vasculature (FIG. 6). Positive staining was observed in bronchial epithelium of the adjacent non-affected lung in all cases. Consistent with absence of observed HER2 amplifications, no significant differences (mean $\pm$ SEM) were detected in the tumor positivity percent-

age for HER2 ( $47\pm 5.4$  and  $35\pm 5.1$ ) between the WT and HER2-mutant groups, respectively. No significant differences in HER2 staining were present for percent minimum ( $51\pm 2.9$  WT vs.  $55\pm 5.1$ , HER2 mutations) or percent maximum ( $97\pm 0.31$  WT vs.  $96\pm 0.47$  HER2 mutations) stain intensity (FIGS. 18A-18B). Overall, most tumors showed moderate expression of HER2 based on qRT-PCR and IHC with some variability, but levels were typically consistent with those seen in normal tissue and did not vary based on HER2 mutation status.

**[0093]** The results herein describe that HER2 is constitutively active in HER2-V659E-mutant cPAC cell lines.

**[0094]** HER2 is a transmembrane receptor tyrosine kinase typically activated by homo- or hetero-dimerization with other HER family receptors. HER2 mutations or overexpression drive constitutive downstream signaling. In human cancers, HER2 V659E mutations stabilize dimers to increase HER2 autophosphorylation, EGFR phosphorylation, activation of phosphatidylinositol-3-kinase (PI3K), and activation of mitogen-activated-protein-kinase (MAPK) pro-survival signaling pathway members (e.g. AKT and ERK) relative to wild-type HER2 (18,19). To determine whether HER2 V659E constitutively activates downstream signaling in cPAC, we first validated HER2 genotype in seven canine lung cancer cell lines through amplicon sequencing, ddPCR or Sanger sequencing of the V659 locus, Sanger sequencing of all HER2 coding regions, and/or aCGH to determine HER2 copy number status as previously published (FIG. 15) (20). One cell line, OSUK9PAPADO, bore a low allele frequency HER2 V659E mutation when sequenced by amplicon panel at low passage (passage 4) as a primary culture, but had lost this allele in later established passages (passage 15) characterized by Sanger sequencing and ddPCR. The latter passage were utilized for functional studies. We thus evaluated HER2 activation in one HER2 V659E cPAC cell line, OSUK9PAPADRe, and three HER2 WT cell lines (two cPAC-CLAC and OSUK9PAPAPADO and one cPASC-OSUK9PADSQ) by Western blotting for total and phospho-AKT in the presence and absence of the ErbB ligand, neuregulin (hNRG) post-serum starvation. Only the HER2 V659E line, OSUK9PAPADRe, showed constitutively high AKT phosphorylation post-starvation even in the absence of hNRG stimulation (FIG. 2A).

**[0095]** The results herein describe that HER2-V659E-mutant cPAC cell lines are hypersensitive to HER2 inhibitors.

**[0096]** To determine the potential efficacy of anti-HER2 agents for treatment of HER2 V659E cPAC, we performed dose-response studies of selected tyrosine kinase inhibitors (TKIs: neratinib, lapatinib, and erlotinib) and a humanized HER2 recombinant monoclonal antibody (mAb), trastuzumab, which binds the extracellular juxtamembrane domain IV of HER2. We first assessed differential sensitivity of HER2 V659E and HER2 WT canine lung cancer cell lines to lapatinib (HER2 and EGFR inhibitor) and neratinib (HER2, HER4, and EGFR inhibitor). Five cPAC cell lines (two HER2 V659E and three HER2 WT) were treated with neratinib and four (one HER2 V659E and three HER2 WT) with lapatinib for 72 hours. Two HER2-mutant human cancer cell lines—BT474 (HER2 AMP) and H1781 (kinase domain HER2 G776ins)—were treated as positive drug controls (18, 21) (FIGS. 2B and 6). Significant differences in viability were observed between HER2 V659E and HER2 WT cPAC cell lines for both TKIs (IC50s < 200 nM in HER2

V659E versus IC50s>2500 nM in HER2 WT). All HER2-mutant cell lines were sensitive to neratinib with IC50s<50 nM (FIG. 2B), significantly lower than those observed for HER2WT cells (IC50s>2.7  $\mu$ M, p=0.0079). We additionally observed a neratinib dose-dependent decrease in p-AKT in the HER2-mutant cell lines OSUK9PAPADRe (HER2 V659E) and BT474 (HER2amp) whereas p-AKT levels in OSUK9PAPADO (HER2 WT) were low at all treatment levels (FIG. 2C). Given that HER2 receptors dimerize with EGFR, we then evaluated differential sensitivity of the five canine cell lines and the human BT474 control line to the EGFR inhibitor, erlotinib. HER2 V659E IC50s were greater than those of neratinib at 220 nM and 1.17  $\mu$ M. HER2 WT IC50s ranged from 1.10-15.38  $\mu$ M (FIG. 21). Finally, we evaluated the HER2-mutation-dependent effects of trastuzumab in the five cPAC cell lines described above (two HER2 V659E and three HER2 WT) and the positive control cell line, BT474, at doses ranging from 1 $\times$ 10  $\mu$ g/ml to 1 mg/ml for 72 hours. While trastuzumab did not decrease viability below 50% for any of the cell lines at 72 hours, the greatest dose-dependent responses were observed in the BT474 control line (65% viability at 10  $\mu$ g/ml, consistent with prior publications) and in the HER2 V659E line OSUK9PAPADRe (74% viability at 10  $\mu$ g/ml). More limited responses were observed in OSUK9PAPADO (HER2 V659E) and OSUK9PADSn (HER2 WT) and no responses at any dose in OSUK9PAPDRi (HER2 V659E) and BACA (HER2 WT) (FIG. 22). Overall, these studies support that HER2 V659E in cPAC is an activating event that stabilizes HER2 homo- and hetero-dimers, confers dependency on downstream signaling, and confers sensitivity to targeted HER2 tyrosine kinase inhibition.

#### DISCUSSION AND CONCLUSION

**[0097]** Through multi-platform next-generation sequencing of 88 naturally occurring primary canine NSCLC cases (77 tumors and 11 cell lines), we describe for the first time the detailed genomic underpinnings of this cancer. The cohort included major NSCLC subtypes occurring in dogs and humans: cPAC (n=74, cPASC (n=11), and cPSCC (n=3) (FIGS. 7A-7D, FIGS. 3A-3F). Although lung cancer may be over-represented in Doberman pinschers, Australian shepherds, Irish setters, and Bernese mountain dogs (7), Labrador retrievers comprised the largest pure breed in this cohort (21%) followed by mixed breeds (25%). The cohort was gender-balanced (52% females), primarily neutered/spayed (92%), and bore a median age at diagnosis of 11 years. Given that dogs are companion and service animals that typically share the same environment with humans, they may have a role to play as sentinels for human lung cancer environmental risk factors. Some data suggests that environmental risks are shared across species. For example, an increased risk of developing cPAC (OR:2.4, CI 95%:0.7-7.8; p=not given) trends towards association with having a smoker in the home in dogs with short (brachycephalic) or medium length (mesocephalic) noses, such as Labrador retrievers (22).

**[0098]** Although second-hand smoke exposure in the dogs in our cohort is possible given that exposure was not recorded, genomic landscapes of human lung cancers in never-smokers have not been shown to differ based on exposure to second-hand smoke (23). Exposure to other environmental carcinogens such as air pollutants may also play a role in development of lung cancers. For example,

increased lung cancer risk may be present in dogs with higher amounts of carbon deposits known as anthracosis (OR:2.1, CI95%: 1.20-3.70; p<0.01) (24), although in humans anthracosis has been commonly observed in normal lungs as well as tumors and lymph nodes. In this cohort, anthracosis was recorded in 15 cases and pneumoconiosis (lung disease associated with pollutant exposure) in one case. However, no associations between anthracosis annotation and genetic features of these cases were observed. Overall, our studies included broad representation of lung cancer across histologic subtypes, breeds, ages, and pollutant exposures reflective of primary canine lung cancer diversity seen in the clinical setting in the United States. Overall, support exists for shared etiologies between canine and human never-smoker lung cancer including secondhand smoke, organic dusts, and outdoor and indoor air pollution, suggesting that study of canine lung cancer can be informative for understanding human lung cancer risks and etiologies. Genomic characterization of canine lung cancers is a first major step towards understanding variables influencing lung cancer development in pet dogs.

**[0099]** Unique genomic characteristics of human never-smoker lung cancer include low somatic mutation burden, C:G>T:A enrichment, and activating mutations or fusions impacting EGFR (45%), ALK (5-11%), ROS (1.5-6%), HER2 (3-5%), and RET (2%) (4,25). Here, we also observed a low somatic burden of SNVs, CNVs, and SVs through exome sequencing in five matched tumor/normal cPAC pairs. We additionally observed that the most common mutation signature in these five cases was the age-associated COSMIC Signature 1A in 4 of 5 (80%) similar to the enrichment seen in human NSCLC (FIGS. 4A and 4B). This signature is associated with age in many human cancers, putatively the result of spontaneous deamination of 5-methyl-cytosine. COSMIC Signature 2, associated with APOBEC cytidine deaminase activity, was also present in two cases. This signature, is most prominently associated with cervical and bladder cancers, but is also commonly found in lung adenocarcinoma and squamous cell carcinoma. While these signatures are sometimes associated with APOBEC gene variants in human cancers (26), no putatively pathogenic germline or somatic APOBEC mutations were observed. Based on our studies, primary canine lung cancers bear a low mutation burden (TMB mean of 2.04 mutations/Mb) and mutation signatures reflective of those seen in human never-smoker lung cancers.

**[0100]** The most common recurrently mutated genes containing somatic potentially pathogenic SNVs in the full cohort included HER2 (31.5%), TP53 (12.5%), PTEN (5.7%), SMAD4 (4.5%), KRAS (4.5%), VHL (3.4%) and HRAS (2.3%). Recurrent CDKN2A/B focal deletions were also observed in 2 of 5 (40%) cases (FIGS. 1A and 1B) along with a homozygous missense mutation, G50R, equivalent to human codon G101 mutations. CDKN2A deletions were the most common alteration by frequency, occurring at rates comparable to those in human NSCLC. Two focal deletions were observed out of five exome-sequenced cases with signs of larger-scale CFA11 losses in remaining cases (FIG. 9). CDKN2A is mutated in approximately 30% of all human NSCLC, primarily via homozygous deletion, and this number is reduced to around 25% in never-smokers. The next most common alterations after CDKN2A and HER2 were TP53 missense and truncating mutations comparable to DNA binding domain mutations in human TP53. Similar to

human NSCLC, we observed a reduced burden of TP53 mutations (12.4%, two stop gains and nine likely pathogenic missense mutations) relative to human smoker NSCLC in which more than half of tumors are mutated. PTEN mutations were the next most common at 5.6%. PTEN is mutated in ~9% of human NSCLC, but only ~2% of never-smoker NSCLC.

**[0101]** We additionally identified four somatic mutations in the tumor suppressor SMAD4, mutated in ~5% of human NSCLC at comparable rates in smoker and never-smoker cancer. KRAS mutations are the most common oncogenic mutations in human smoker NSCLC (~30-40% of cases), but occur at reduced frequencies in never-smoker lung cancer (0-7%). KRAS mutations in our cohort were rare (2 G12V, 1 G12D, and 1 Q61K), but comparable to human hotspots. Canine HRAS missense mutations were also located in human-equivalent hotspots (Q61L, F78S). Additional likely pathogenic somatic mutations included individual cases of AKT1 amplification, KIT/KDR amplification, EGFR A726T (human A755), MET M1269V (human M1268), and VHL P97L (human P97). WWTR1, the only COSMIC gene bearing a somatic translocation in exome-sequenced cases, has been shown to undergo translocation with CAMTA1 in human epithelioid hemangioendothelioma (27). We identified a WWTR1 translocation of unknown consequence with ATP5F1. Although we identified translocations occurring in coding regions in five exome-sequenced tumors, it remains possible that, as in human never-smoker lung cancer, EML4-ALK fusions, ROS1 fusions, RET fusions, and other fusions may also be present in canine lung cancer.

**[0102]** In addition to charting the landscape of cPAC, we have found recurrent KRAS and TP53 mutations in cPASC and provide a view of possible drivers in cPASC. In cPASC, HRAS Q61L and KRAS Q61K each occurred in one case. Finally, while no recurrent mutations were identified in the three cPSCCs, we identified one case with somatic BRAF V588E (equivalent to the human V600E hotspot) and another bearing PTPN11 G503V (equivalent to the human G503V hotspot).

**[0103]** HER2 contained the most somatic mutations with hotspot mutations occurring solely in cPAC (37.8%). HER2 is a well-characterized human oncogene and drug target mutated in ~6% of all cancers based on cBioPortal query of 10,967 cases in the TCGA pan-cancer atlas (28,29). Most alterations are focal amplifications, but activating point mutations and insertions are also common. In human NSCLC, HER2 mutations are oncogenic drivers in ~1-4% of cases with mutations and insertions mostly in exon 20 at codon 776 resulting in constitutive HER2 kinase domain activation and downstream signaling through PI3K and MAPK pathways (25, 30, 31). HER2 may also be more commonly mutated in human never-smoker lung cancer, with point mutations at frequencies reported at 3-5% (32), predominately in female never-smokers who carry a median OS of ~2 years (31). HER2 TMD polar mutations (HER2 V659E/D, HER2 G660D) are present in 0.18% of human lung adenocarcinomas and are exclusive with HER2 kinase domain mutations (33). Amplicon analysis capable of identification of point mutations and small insertions or deletions covered canine HER2 exons 8 and 17-22 including transmembrane and kinase domains. Additionally, Sanger sequencing of all exons in five canine cell lines with wild-type HER2 based on amplicon sequencing

(OSUK9PAD, BACA, CLAC, K9PADSQ and OSULSCC1) found no somatic HER2 mutations in other sites (FIG. 15). It is nonetheless possible that somatic mutations occurring in other regions of HER2 were not identified in amplicon-sequenced samples even though data facilitating functional interpretation of these variants would be limited.

**[0104]** In addition to point mutations, HER2 amplification has also been identified in ~1% of human NSCLC (25), with enrichment in EGFR-inhibitor-resistant tumors (34). Protein overexpression is reported in 6-35% of tumors including up to 42% of adenocarcinomas and correlates with poor prognosis (35-38). We detected no somatic HER2 focal amplifications or numerical CFA9 gains in five exome-sequenced cases (FIGS. 1B and 9) or two previously aCGH-profiled cell lines. However, four of these seven cases contained somatic, putatively activating HER2 SNVs. Given that HER2 amplification/overexpression and SNVs are typically mutually exclusive, it remains possible that our broader amplicon cohort contained undetected HER2 amplifications. We therefore utilized qRT-PCR and IHC studies to more broadly assess HER2 overexpression and did not find evidence for significant tumor-specific HER2 overexpression (FIGS. 20A-20B and FIGS. 6 and 17). Thus, it is unlikely that HER2 is frequently amplified in canine lung cancer.

**[0105]** Overall, though we observed a similar mutation spectrum in canine lung cancer relative to human never-smoker NSCLC, the notable exception is abundance of HER2 mutations and lack of EGFR mutations. EGFR mutations occur at low frequency in human smoker lung cancers (0-7%), but are enriched in human never-smokers (~45%). Canine HER2 shares normal and oncogenic roles with human HER2 based on sequence conservation (92.2% protein identity) and prior study of its role in canine cell signaling. HER2<sup>V659E</sup> occurs at a highly conserved residue (100% identity in the TMD from amino acids 654-674) and to the neu (rat HER2) variant identified in a rat glioblastoma cell line that originally led to discovery of HER2's oncogene status (39). HER2 has previously been implicated in canine cancers via overexpression by IHC and qRT-PCR in canine mammary tumors (40), through its utility as a vaccine target in canine osteosarcoma (41), and through downstream signaling activation in canine lung cancer (10). Thus, HER2 sequence and pathway biology is conserved, so the predominance of HER2 mutations as erbB signaling activators in lieu of EGFR mutations in cPAC may be the result of cell-of-origin and genetic background influences. Cell of origin determination in canine lung cancers is challenging because the pulmonary adenocarcinoma diagnosis includes tumors arising from primary, secondary and tertiary bronchioles and thus topographic origin can be difficult to determine. However, evidence supports that HER2 is broadly important for canine pulmonary epithelium. For example, neuregulin-stimulated HER2 increases proliferation in pulmonary epithelial cells by activation of the JAK-STAT pathway. Further, when HER2 activation is blocked via antibodies to neuregulin or HER2 in a scratch wound-healing assay of pulmonary epithelial cells, wound closure is significantly delayed, suggesting HER2 activation is necessary for epithelial proliferation (42).

**[0106]** We have also found that IHC of canine normal lung showed stronger HER2 staining of all bronchioalveolar regions when compared to EGFR staining of normal adult canine lung. These data suggest that HER2 may play a more central role than EGFR in canine alveolar and airway

epithelial cells during chronic lung injury and for general proliferative processes. Prolonged activation could lead to cellular transformation and neoplasia. Further, EGFR mutations have been associated with particular histotypes—i.e. they are frequent in lepidic and acinar patterns and infrequent in mucinous patterns in female Asian never-smoker PAC. In this population, the most frequent adenocarcinoma histotype was acinar (142 cases, 71.7%), followed by papillary (18 cases, 9.1%), solid (17 cases, 8.6%), lepidic (9 cases, 4.5%), and micropapillary (1 case, 0.5%). Interestingly, our canine cohort had predominantly papillary morphology (69%) with only 5% acinar (5%). Therefore, differences in cell of origin in both species could account for the differences in EGFR mutation frequencies. Background genetic context likely also plays a primary role in shaping enrichment for HER2 mutations in cPAC. This is also true in human lung cancer where EGFR mutation frequency varies by more than 3-fold between different human populations. The Asian population has a very high rate of EGFR mutation among the never-smoking population, up to 51.4% overall and as high as 64% in some populations such as the Kinh, versus about 20% in Caucasians (43-45). These differences in human populations suggest a sensitivity of EGFR mutations to genetic context. Conversely, HER2 mutations are found in all human populations at about the same frequency, suggesting that HER2 mutations in humans may not be as sensitive to genetic background.

**[0107]** We have additionally shown that HER2 hotspot mutations can be detected in the plasma of dogs bearing HER2 V659E cPACs even at early disease stages (FIG. 1E and FIGS. 16A-16C). In human NSCLC, ctDNA has been shown to be significantly enriched in plasma relative to controls with key genetic features identifiable via liquid biopsy. Associations have been found between ctDNA levels and tumor stage, grade, lymph node status, metastatic sites, response, and survival (46,47). The first FDA-approved liquid biopsy test was the cobas EGFR Mutation Test v2, a real-time PCR assay utilized in NSCLC for the detection of EGFR exon 18-21 mutations in tissue or plasma to guide EGFR inhibitor treatment assignment (48,49). Our proof-of-principle study supports that ctDNA is also detectable in primary canine lung cancer patient plasma. A non-invasive HER2 V659E assay will enable genotyping patients when tumor tissue is limited and may have a role in treatment monitoring or detection of minimal residual disease. This assay will also facilitate prospective analysis of HER2 V659E's diagnostic and prognostic value.

**[0108]** In human cancers, HER2 TMD mutations constitutively activate pro-survival HER2 signaling (33) and are associated with HER2 inhibitor responses (19). We have confirmed in this study that, similar to human HER2 TMD mutants, canine HER2 V659E cell lines constitutively activate downstream signaling through AKT and are selectively sensitive to the HER2 TKI inhibitors neratinib and lapatinib in vitro (FIGS. 2A-2B and FIG. 6). In order to further assess the role of dimerization in HER2 activation in cPAC, we also performed drug dose response studies for erlotinib and trastuzumab (FIGS. 21 and 22). One of two HER2-mutant cell lines showed erlotinib sensitivity. Trastuzumab responses were poor overall and did not correlate with HER2 status, although dose-response relationships were observed in three of five cell lines. Trastuzumab's human binding site is highly conserved in canine (only a single amino acid difference) and trastuzumab has been shown to

bind canine HER2 and inhibit proliferation of HER2-over-expressing canine cancer cell lines (50). However, even the human HER2-amplified cell line, BT474, did not show viability reduction below 50% in our hands. It is likely that the effects of trastuzumab on CellTiterGlo viability are broadly muted at the 72-hour timepoints we utilized. Overall, these studies indicate that HER2 V659E in cPAC is an activating event that stabilizes HER2 homo- and heterodimers, confers dependency on downstream signaling, and confers sensitivity to targeted HER2 tyrosine kinase inhibition. We have charted the genomic landscape of primary canine lung cancers including the NSCLC subtypes cPAC, cPASC, and cPSCC. We have identified recurrent HER2 mutations in these cancers and present, to our knowledge, the first complete suite of evidence supporting an oncogenic role for and dependency on constitutively activating mutations in HER2 in a canine cancer.

**[0109]** Further work is needed to exhaustively profile these tumors, particularly according to variation across breeds and through integration of additional data types including epigenomics, RNA sequencing, and proteomics. However, these data nonetheless offer significant immediate diagnostic and therapeutic opportunities for dogs with primary lung cancer and aid comparative understanding of never-smoker and HER2-mutant lung cancer. These findings set the stage for HER2 inhibitor toxicity, dose-finding, and efficacy studies in dogs that will guide utilization of HER2 inhibitors in the veterinary clinic.

**[0110]** It is to be understood that unless specifically stated otherwise, references to “a,” “an,” and/or “the” may include one or more than one and that reference to an item in the singular may also include the item in the plural. Reference to an element by the indefinite article “a,” “an” and/or “the” does not exclude the possibility that more than one of the elements are present, unless the context clearly requires that there is one and only one of the elements. As used herein, the term “comprise,” and conjugations or any other variation thereof, are used in its non-limiting sense to mean that items following the word are included, but items not specifically mentioned are not excluded.

**[0111]** While the invention has been described in connection with specific embodiments thereof, it will be understood that it is capable of further modifications and this application is intended to cover any variations, uses, or adaptations of the invention following, in general, the principles of the invention and including such departures from the present disclosure as come within known or customary practice within the art to which the invention pertains and as may be applied to the essential features hereinbefore set forth.

#### REFERENCES

- [0112]** 1. Wilson D W. Tumors of the Respiratory Tract. In: Meuten D J, editor. Tumors in domestic animals. 5th ed: John Wiley & Sons; 2017. p 467-98.
- [0113]** 2. Clement-Duchene C, Wakelee H. Lung Cancer Incidence in Never Smokers. *European Journal of Clinical & Medical Oncology* 2010; 2(2).
- [0114]** 3. Samet J M, Avila-Tang E, Boffetta P, Hannan L M, Olivo-Marston S, Thun M J, et al. Lung cancer in never smokers: clinical epidemiology and environmental risk factors. *Clin Cancer Res* 2009; 15(18):5626-45 doi 10.1158/1078-0432.CCR-09-0376.
- [0115]** 4. Govindan R, Ding L, Griffith M, Subramanian J, Dees N D, Kanchi K L, et al. Genomic landscape of

- non-small cell lung cancer in smokers and never-smokers. *Cell* 2012; 150(6):1121-34 doi 10.1016/j.cell.2012.08.024.
- [0116] 5. Hellmann M D, Ciuleanu T E, Pluzanski A, Lee J S, Otterson G A, Audigier-Valette C, et al. Nivolumab plus Ipilimumab in Lung Cancer with a High Tumor Mutational Burden. *N Engl J Med* 2018; 378(22):2093-104 doi 10.1056/NEJMoa1801946.
- [0117] 6. Hahn F F, Muggenburg B. A., Griffith W. C., editor. Primary lung cancer in the longevity study/control population of the ITRI beagle dog colony. Springfield, V A: National Technical Information Service; 1992. 133-6 p.
- [0118] 7. Griffey S M, Kraegel S A, Madewell B R. Rapid detection of K-ras gene mutations in canine lung cancer using single-strand conformational polymorphism analysis. *Carcinogenesis* 1998; 19(6):959-63.
- [0119] 8. Kraegel S A, Gumerlock P H, Dungworth D L, Oreffo V I, Madewell B R. K-ras activation in non-small cell lung cancer in the dog. *Cancer Research* 1992; 52(17):4724-7.
- [0120] 9. Tierney L A, Hahn F F, Lechner J F. p53, erbB-2 and K-ras gene alterations are rare in spontaneous and plutonium-239-induced canine lung neoplasia. *Radiation Research* 1996; 145(2): 181-7.
- [0121] 10. Mariotti E T, Premanandan C, Lorch G. Canine pulmonary adenocarcinoma tyrosine kinase receptor expression and phosphorylation. *BMC veterinary research* 2014; 10:19 doi 10.1186/1746-6148-10-19.
- [0122] 11. Forbes S A, Beare D, Boutselakis H, Bamford S, Bindal N, Tate J, et al. COSMIC: somatic cancer genetics at high-resolution. *Nucleic acids research* 2017; 45(D1):D777-D83 doi 10.1093/nar/gkw1121.
- [0123] 12. Alexandrov L B, Nik-Zainal S, Wedge D C, Aparicio S A, Behjati S, Biankin A V, et al. Signatures of mutational processes in human cancer. *Nature* 2013; 500(7463):415.
- [0124] 13. Gehring J S, Fischer B, Lawrence M, Huber W. SomaticSignatures: inferring mutational signatures from single-nucleotide variants. *Bioinformatics* 2015; 31(22): 3673-5 doi 10.1093/bioinformatics/btv408.
- [0125] 14. Sherry S T, Ward M-H, Kholodov M, Baker J, Phan L, Smigielski E M, et al. dbSNP: the NCBI database of genetic variation. 2001; 29(1):308-11.
- [0126] 15. Bai B, Zhao W-M, Tang B-X, Wang Y-Q, Wang L, Zhang Z, et al. DoGSD: the dog and wolf genome SNP database. 2014; 43(D1):D777-D83.
- [0127] 16. Liu C, Cui H, Gu D, Zhang M, Fang Y, Chen S, et al. Genetic polymorphisms and lung cancer risk: Evidence from meta-analyses and genome-wide association studies. 2017; 113:18-29.
- [0128] 17. Perdignes N, Murtaza M. Capturing tumor heterogeneity and clonal evolution in solid cancers using circulating tumor DNA analysis. *Pharmacol Ther* 2017; 174:22-6 doi 10.1016/j.pharmthera.2017.02.003.
- [0129] 18. Suzawa K, Toyooka S, Sakaguchi M, Morita M, Yamamoto H, Tomida S, et al. Antitumor effect of afatinib, as a human epidermal growth factor receptor 2-targeted therapy, in lung cancers harboring HER2 oncogene alterations. *Cancer Sci* 2016; 107(1):45-52 doi 10.1111/cas.12845.
- [0130] 19. Ou S I, Schrock A B, Bocharov E V, Klempner S J, Haddad C K, Steinecker G, et al. HER2 Transmembrane Domain (TMD) Mutations (V659/G660) That Stabilize Homo- and Heterodimerization Are Rare Oncogenic Drivers in Lung Adenocarcinoma That Respond to Afatinib. *J Thorac Oncol* 2017; 12(3):446-57 doi 10.1016/j.jtho.2016.11.2224.
- [0131] 20. Clemente-Vicario F, Alvarez C E, Rowell J L, Roy S, London C A, Kisseberth W C, et al. Human genetic relevance and potent antitumor activity of heat shock protein 90 inhibition in canine lung adenocarcinoma cell lines. *PLoS one* 2015; 10(11):e0142007.
- [0132] 21. Canonici A, Gijssen M, Mullooly M, Bennett R, Bouguern N, Pedersen K, et al. Neratinib overcomes trastuzumab resistance in HER2 amplified breast cancer. *Oncotarget* 2013; 4(10):1592.
- [0133] 22. Reif J S, Dunn K, Ogilvie G K, Harris C K. Passive smoking and canine lung cancer risk. *Am J Epidemiol* 1992; 135(3):234-9 doi 10.1093/oxfordjournals.aje.a116276.
- [0134] 23. Couraud S, Debieuvre D, Moreau L, Dumont P, Margery J, Quoix E, et al. No impact of passive smoke on the somatic profile of lung cancers in never-smokers. *Eur Respir J* 2015; 45(5):1415-25 doi 10.1183/09031936.00097314.
- [0135] 24. Bettini G, Morini M, Marconato L, Marcato P S, Zini EJTVJ. Association between environmental dust exposure and lung cancer in dogs. 2010; 186(3):364-9.
- [0136] 25. Campbell J D, Alexandrov A, Kim J, Wala J, Berger A H, Peadarallu C S, et al. Distinct patterns of somatic genome alterations in lung adenocarcinomas and squamous cell carcinomas. 2016; 48(6):607.
- [0137] 26. Nik-Zainal S, Wedge D C, Alexandrov L B, Petljak M, Butler A P, Bolli N, et al. Association of a germline copy number polymorphism of APOBEC3A and APOBEC3B with burden of putative APOBEC-dependent mutations in breast cancer. 2014; 46(5):487.
- [0138] 27. Errani C, Zhang L, Sung Y S, Hajdu M, Singer S, Maki R G, et al. A novel WWTR1-CAMTA1 gene fusion is a consistent abnormality in epithelioid heman-gioendothelioma of different anatomic sites. 2011; 50(8): 644-53.
- [0139] 28. Gao J, Aksoy B A, Dogrusoz U, Dresdner G, Gross B, Sumer S O, et al. Integrative analysis of complex cancer genomics and clinical profiles using the cBioPortal. 2013; 6(269):p11-pl.
- [0140] 29. Weinstein J N, Collisson E A, Mills G B, Shaw K R M, Ozenberger B A, Ellrott K, et al. The cancer genome atlas pan-cancer analysis project. 2013; 45(10): 1113.
- [0141] 30. Mazieres J, Peters S, Lepage B, Cortot A B, Barlesi F, Beau-Faller M, et al. Lung cancer that harbors an HER2 mutation: epidemiologic characteristics and therapeutic perspectives. *J Clin Oncol* 2013; 31(16):1997-2003 doi 10.1200/JCO.2012.45.6095.
- [0142] 31. Mazieres J, Barlesi F, Filleron T, Besse B, Monnet I, Beau-Faller M, et al. Lung cancer patients with HER2 mutations treated with chemotherapy and HER2-targeted drugs: results from the European EUHER2 cohort. *Ann Oncol* 2016; 27(2):281-6 doi 10.1093/annonc/mdv573.

- [0143] 32. Shigematsu H, Takahashi T, Nomura M, Majmudar K, Suzuki M, Lee H, et al. Somatic mutations of the HER2 kinase domain in lung adenocarcinomas. *Cancer Research* 2005; 65(5):1642-6.
- [0144] 33. Kanika Bajaj Pahuj a TTN, Bij ay S. Jaiswal, Kumar Prabhash, Tarjani M. Thaker, Kate Senger S C, Noelyn M. Kljavin, Aju Antony, Sameer Phalke, Prasanna Kumar, Marco Mravic, Eric W. Stawiski, Derek Vargas, Steffen Durinck, Ravi Gupta, Arati Khanna-Gupta, Sally E. Trabucco, Ethan S. Sokol, Ryan J. Hartmaier, Ashish Singh, Anuradha Chougule, Vaishakhi Trivedi, Amit Dutt, Vijay Patil, Amit Joshi, Vanita Noronha, James Ziai, Sripad D. Banavali, Vedam Ramprasad, William F. DeGrado, Raphael Bueno, Natalia Jura, and Somasekar Seshagiri. Actionable Activating Oncogenic ERBB2/HER2 Transmembrane and Juxtamembrane Domain Mutations. *Cancer Cell* 2018(34):15.
- [0145] 34. Takezawa K, Pirazzoli V, Arcila M E, Nebhan C A, Song X, de Stanchina E, et al. HER2 amplification: a potential mechanism of acquired resistance to EGFR inhibition in EGFR-mutant lung cancers that lack the second-site EGFR T790M mutation. *Cancer discovery* 2012.
- [0146] 35. Pellegrini C, Falleni M, Marchetti A, Cassani B, Miozzo M, Buttitta F, et al. HER-2/Neu alterations in non-small cell lung cancer: a comprehensive evaluation by real time reverse transcription-PCR, fluorescence in situ hybridization, and immunohistochemistry. *Clinical cancer research* 2003; 9(10):3645-52.
- [0147] 36. Rouquette I, Lauwers-Cances V, Allera C, Brouchet L, Milia J, Nicaise Y, et al. Characteristics of lung cancer in women: importance of hormonal and growth factors. *Lung Cancer* 2012; 76(3):280-5.
- [0148] 37. Langer C J, Stephenson P, Thor A, Vangel M, Johnson D H. Trastuzumab in the treatment of advanced non-small-cell lung cancer: is there a role? Focus on Eastern Cooperative Oncology Group study 2598. *Journal of clinical oncology* 2004; 22(7):1180-7.
- [0149] 38. Lara Jr P N, Laptalo L, Longmate J, Lau D H, Gandour-Edwards R, Gumerlock P H, et al. Trastuzumab plus Docetaxel in HER2/neu-Positive Non-Small-Cell Lung Cancer: A California Cancer Consortium Screening and Phase II Trial. *Clinical lung cancer* 2004; 5(4):231-6.
- [0150] 39. Bargmann C I, Hung M C, Weinberg R A. Multiple independent activations of the neu oncogene by a point mutation altering the transmembrane domain of p185. *Cell* 1986; 45(5):649-57.
- [0151] 40. Gama A, Alves A, Schmitt FJVA. Identification of molecular phenotypes in canine mammary carcinomas with clinical implications: application of the human classification. 2008; 453(2):123-32.
- [0152] 41. Mason N J, Gnanandarajah J S, Engiles J B, Gray F, Laughlin D, Gaumier-Hausser A, et al. Immunotherapy with a HER2-targeting listeria induces HER2-specific immunity and demonstrates potential therapeutic effects in a phase I trial in canine osteosarcoma. 2016; 22(17):4380-90.
- [0153] 42. Vermeer P D, Einwalter L A, Moninger T O, Rokhlina T, Kern J A, Zabner J, et al. Segregation of receptor and ligand regulates activation of epithelial growth factor receptor. *Nature* 2003; 422(6929):322-6 doi 10.1038/nature01440.
- [0154] 43. Yatabe Y, Kerr K M, Utomo A, Rajadurai P, Tran V K, Du X, et al. EGFR mutation testing practices within the Asia Pacific region: results of a multicenter diagnostic survey. *J Thorac Oncol* 2015; 10(3):438-45 doi 10.1097/JTO.0000000000000422.
- [0155] 44. Shigematsu H, Lin L, Takahashi T, Nomura M, Suzuki M, Wistuba, I I, et al. Clinical and biological features associated with epidermal growth factor receptor gene mutations in lung cancers. *J Natl Cancer Inst* 2005; 97(5):339-46 doi 10.1093/jnci/dji055.
- [0156] 45. Shi Y, Au J S, Thongprasert S, Srinivasan S, Tsai C M, Khoa M T, et al. A prospective, molecular epidemiology study of EGFR mutations in Asian patients with advanced non-small-cell lung cancer of adenocarcinoma histology (PIONEER). *J Thorac Oncol* 2014; 9(2): 154-62 doi 10.1097/JTO.0000000000000033.
- [0157] 46. Nie K, Jia Y, Zhang XJT. Cell-free circulating tumor DNA in plasma/serum of non-small cell lung cancer. 2015; 36(1):7-19.
- [0158] 47. Jiang T, Ren S, Zhou CJ. Role of circulating-tumor DNA analysis in non-small cell lung cancer. 2015; 90(2):128-34.
- [0159] 48. Kwapisz D JAotm. The first liquid biopsy test approved. Is it a new era of mutation testing for non-small cell lung cancer? 2017; 5(3).
- [0160] 49. Wu Y-L, Zhou C, Liam C-K, Wu G, Liu X, Zhong Z, et al. First-line erlotinib versus gemcitabine/cisplatin in patients with advanced EGFR mutation-positive non-small-cell lung cancer: analyses from the phase III, randomized, open-label, ENSURE study. 2015; 26(9): 1883-9.
- [0161] 50. Singer J, Weichselbaumer M, Stockner T, Mechtcheriakova D, Sobanov Y, Bajna E, et al. Comparative oncology: ErbB-1 and ErbB-2 homologues in canine cancer are susceptible to cetuximab and trastuzumab targeting. *Molecular immunology* 2012; 50(4):200-9.
- [0162] 51. Gordon I, Paoloni M, Mazcko C, Khanna C. The Comparative Oncology Trials Consortium: using spontaneously occurring cancers in dogs to inform the cancer drug development pathway. *PLoS medicine* 2009; 6(10):e1000161.
- [0163] 52. Murtaza M D S, Pogrebniak K, Rueda O M, Provenzano E, Grant J, Chin S F, Tsui D W, Marass F, Gale D, Ali H R, Shah P, Contente-Cuomo T, Farahani H, Shumansky K, Kingsbury Z, Humphray S, Bentley D, Shah S P, Wallis M, Rosenfeld N, Caldas C. Multifocal clonal evolution characterized using circulating tumour DNA in a case of metastatic breast cancer. *Nat Commun* 2015; 4(6):8760.
- [0164] 53. Li H, Handsaker B, Wysoker A, Fennell T, Ruan J, Homer N, et al. The Sequence Alignment/Map format and SAMtools. *Bioinformatics* 2009; 25(16): 2078-9 doi 10.1093/bioinformatics/btp352.
- [0165] 54. Hsu W L, Huang H M, Liao J W, Wong M L, Chang S C. Increased survival in dogs with malignant mammary tumours overexpressing HER-2 protein and detection of a silent single nucleotide polymorphism in the canine HER-2 gene. *Veterinary Journal* 2009; 180(1): 116-23 doi 10.1016/j.tvj.2007.10.013.



---

SEQUENCE LISTING

<160> NUMBER OF SEQ ID NOS: 7

<210> SEQ ID NO 1

<211> LENGTH: 16

<212> TYPE: DNA

<213> ORGANISM: Artificial Sequence

<220> FEATURE:

<223> OTHER INFORMATION: Primer

<400> SEQUENCE: 1

cccacgacca cagcca

16

<210> SEQ ID NO 2

<211> LENGTH: 21

<212> TYPE: DNA

<213> ORGANISM: Artificial Sequence

<220> FEATURE:

<223> OTHER INFORMATION: Primer

<400> SEQUENCE: 2

ccctgtgaca tccatcattg c

21

<210> SEQ ID NO 3

<211> LENGTH: 18

<212> TYPE: DNA

<213> ORGANISM: Artificial Sequence

<220> FEATURE:

<223> OTHER INFORMATION: Primer

<400> SEQUENCE: 3

cagaatgccc wccacagc

18

<210> SEQ ID NO 4

<211> LENGTH: 21

<212> TYPE: DNA

<213> ORGANISM: Artificial Sequence

<220> FEATURE:

<223> OTHER INFORMATION: Primer

<400> SEQUENCE: 4

catctgcacc attgatgtct a

21

<210> SEQ ID NO 5

<211> LENGTH: 20

<212> TYPE: DNA

<213> ORGANISM: Artificial Sequence

<220> FEATURE:

<223> OTHER INFORMATION: Primer

<400> SEQUENCE: 5

ggcccaagtc ttcattctga

20

<210> SEQ ID NO 6

<211> LENGTH: 20

<212> TYPE: DNA

<213> ORGANISM: Artificial Sequence

<220> FEATURE:

<223> OTHER INFORMATION: Primer

<400> SEQUENCE: 6

gcagccccag cgtcgtgatt

20

<210> SEQ ID NO 7

-continued

---

```
<211> LENGTH: 22
<212> TYPE: DNA
<213> ORGANISM: Artificial Sequence
<220> FEATURE:
<223> OTHER INFORMATION: Primer
```

```
<400> SEQUENCE: 7
```

```
catctcgagc aagccgctca gt
```

---

22

1. A method of treating lung cancer in a subject, comprising the steps of:

receiving a biological sample from the subject;  
analyzing the biological sample for a mutation in HER2, wherein the mutation in HER2 comprises V659E or an equivalent variant in a human orthologous gene; and  
treating the subject with an inhibitor of HER2 if the mutation is present.

2. The method of claim 1, wherein the HER2 inhibitor is selected from the group comprising trastuzumab, neratinib, lapatinib, erlotinib, and pertuzumab.

3. The method of claim 1, wherein the subject is a canine.

4. The method of claim 1, wherein the lung cancer is canine pulmonary adenocarcinoma.

5. The method of claim 1, wherein the biological sample is a tumor sample or a plasma sample.

6. The method of claim 1, wherein the analyzing step comprises subjecting the biological sample to amplification and exome sequencing.

7. A method of treating lung cancer in a subject, comprising the steps of:

receiving a biological sample from the subject;  
adding to a mixture comprising the biological sample a first primer consisting of SEQ ID NO: 1 and a second primer consisting of SEQ ID NO: 2;  
subjecting the mixture to conditions that allow nucleic acid amplification;  
detecting the presence of one or more markers selected from the group consisting of HER2 V659E, HER2 A664T, HER2 K676E, and equivalent variants thereof in a human orthologous gene by detecting the nucleic acid amplification; and  
treating the subject with an inhibitor of HER2 if one or more of the markers is present.

8. The method of claim 7, wherein the detecting step comprises sequencing a product of the nucleic acid amplification.

9. The method of claim 7, wherein the HER2 inhibitor is selected from the group comprising trastuzumab, neratinib, lapatinib, erlotinib, and pertuzumab.

10. The method of claim 7, further comprising adding to the mixture a probe consisting of SEQ ID NO: 3.

11. The method of claim 10, wherein the subject is a canine, and the lung cancer is canine pulmonary adenocarcinoma.

12. The method of claim 7, wherein the biological sample is a tumor sample or a plasma sample.

13. A method of treating lung cancer in a subject, comprising the steps of:

receiving a biological sample from the subject;  
analyzing the biological sample for one or more mutations selected from the group consisting of HER2 V659E, HER2 A664T, HER2 K676E, KRAS G12DN, SMAD4 D351Y/G, TP53 R239Q/G, and equivalent variants thereof in a human orthologous gene; and  
administering, if one or more of the mutations is present, a therapeutically effective amount of a pharmaceutical composition selected from the group consisting of trastuzumab, neratinib, lapatinib, erlotinib, and pertuzumab.

14. The method of claim 13, wherein the analyzing step comprises subjecting the biological sample to amplification and exome sequencing.

15. The method of claim 13, wherein the subject is a canine.

16. The method of claim 15, wherein the lung cancer is canine pulmonary adenocarcinoma.

17. The method of claim 13, wherein the biological sample is a tumor sample or a plasma sample.

18-20. (canceled)

21. The method of claim 1, wherein the subject is a human.

22. The method of claim 7, wherein the subject is a human.

23. The method of claim 13, wherein the subject is a human.

\* \* \* \* \*